

TAN
•Cl6
CER-89/90-14

ESSAYS ON RIVER MECHANICS

LIBRARIES
APR 20 1990
COLORADO STATE UNIVERSITY



Presented by the Graduate Students
in CE 717 River Mechanics (Spring 1990)

Instructor: P.Y. Julien

May 1990

CER89-90-PYJ-14

ESSAYS ON RIVER MECHANICS



Presented by the Graduate Students
in CE 717 River Mechanics (Spring 1990)

Instructor: P.Y. Julien

May 1990

CER89-90-PYJ-14

217⁴³²⁸⁰⁵ XL 570
11/00 38-000-00 GBC

FOREWORD

I am very pleased to honor the work of the graduate students in the class CE-717 River Mechanics with this report of their technical papers. Each student worked on a particular aspect of river engineering in order to meet the following objectives:

- 1) familiarize with the recent literature and new methodologies not available in textbooks;
- 2) compare various methods (new versus old) and discuss the advancement of engineering technology on a given topic;
- 3) develop skills to point out the key elements of recent technological developments;
- 4) share interesting findings with the other students through an oral presentation and a written paper.

The requirements for this project were:

- 1) select a topic relevant to river mechanics and sediment transport;
- 2) conduct a mini literature review including papers published in the past five years;
- 3) compare new methodologies with those detailed in textbooks on either a theoretical basis or through comparison with an appropriate data set;
- 4) write a 40 page report and discuss the major findings in a 30-45 minute oral presentation;
- 5) summarize the analysis and the results in a 12 page paper following the ASCE editorial standards (these papers are included herein).

Not only the students showed great enthusiasm in this class but the reader will certainly agree with me that the objectives were met with great success. I am personally very impressed with the overall quality of the reports presented and I can only compliment all of them for their effort.



Pierre Y. Julien
Assoc. Prof. of Civil Engineering

TABLE OF CONTENTS

Predicting Sediment Yield of a Watershed by Margaret Tauzer	1
Particle Entrainment by River Flows by Kathy Chase	13
Bed Forms and Resistance to Flow by Yasser Raslan	25
An Examination of the Dynamic Loop Rating Curve in Alluvial Rivers by Phil G. Combs	40
Scour Downstream of Hydraulic Structures by T.K. Burke	52
Distorted Physical Hydraulic Models, Theory and Practice by Fred L. Ogden	65
Life Expectancy of Reservoirs by T.G. Anthony Balan	77

Predicting Sediment Yield of A Watershed

by Margaret Tauzer

Abstract

The Universal Soil Loss Equation is the most widely used equation for the prediction of the sheet and rill soil losses in a watershed. The sediment yield can be calculated by multiplying the gross soil loss by the sediment delivery ratio. There are equations available for direct calculation of the sediment yield. Many studies have been done in an attempt to relate watershed parameters to the sediment yield at the catchment. Most of the equations developed are specific for the area and do not apply generally. There was a wide spread in the prediction of sediment yield, soil loss, and sediment delivery ratio when several of these relationships were applied to a small watershed of Central California.

Introduction

Land use changes often cause a change in sediment erosion. Streams may become deficient or overburdened with sediment, upsetting their fragile equilibrium. Changes can be drastic. A river may become braided where it was meandering, or it may begin eroding or depositing sediment in unwanted places. There may be detrimental effects caused by a simple change in a watershed. It is important to estimate the possible changes caused by a project before it is built.

A way to predict the effects of a change in a watershed is to estimate the change in the sediment yield delivered out of the watershed past a given point. The mechanism of soil loss over an entire watershed are not well understood. Although each physical process comprising soil erosion may be quantifiable, the combination of all the erosion sources acting together, as in a typical watershed, is more complex. There are general equations for determining sediment yield of a watershed. Most of the equations were developed for a specific area. The intention of this paper is to study a few of these equations and to consider their applicability to a small coastal watershed in Central California.

Methods to Predict Sediment Yield

There are four basic methods in use for the prediction of the sediment yield of a watershed. The four methods are 1. Suspended sediment load measurements, 2. Gross erosion - Sediment delivery ratio method, 3. Predictive equations, 4. Sediment Accumulation measurements. Each of these methods will be described. Where applicable, the method will be tested on a small watershed of California.

The most direct method for obtaining the sediment yield of a watershed is to measure the suspended sediment in the channel flowing out of the watershed. For an accurate prediction of the sediment yield, measurements of suspended load have to be taken at all representative flows of the stream. Factors such as storm intensity or pattern can cause a variation in the suspended sediment load with the same flow rate. A rating curve must be developed from the averaged values, giving tons of sediment per volume

of discharge. By multiplying the average daily discharges by the corresponding sediment rate and summing the values over a year, the average annual quantity of suspended sediment yielded from the watershed can be determined. The bedload is not included in the quantity. By taking field measurements of the stream bed material, bed load can be predicted by one of the many equations available such as Einstein or Meyer Peter and Muller formulas. The sum of the bedload and suspended loads gives a estimate of the total sediment yield of the watershed.

In practice, the percentage of total load attributed to bed load is often taken simply as a percentage of the measured suspended load. A table has been established to aid in determining what percentage to use. Table 1 is the table developed by Thomas Maddock, Jr., summarizing the classifications studied by Lane and Borland (1951).

Table 1 Maddock's Classification for Determining Bed Load (3)

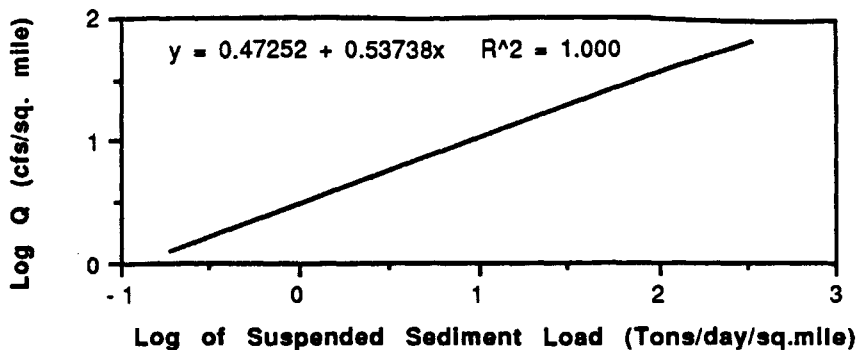
Concentration of Suspended Load, in parts per million	Type of Material Forming Channel of Stream	Texture of Suspended Material	Bed load Discharge, in terms of Suspended Sediment Discharge, as a percentage
Less than 1,000	Sand	Similar to bed material	25-150
Less than 1,000	Gravel, rock, or Consolidated Clay	Small amount of sand	5-12
1,000 - 7,500	Sand	Similar to bed material	10-35
1,000 - 7,500	Gravel, rock, or Consolidated Clay	25% sand or less	5-12
over 7,500	Sand	Similar to bed material	5-15
over 7,500	Gravel, rock, or Consolidated Clay	25% sand or less	2-8

Source: American Society of Civil Engineers, Manuals and Reports on Engineering Practice - no. 54, Sedimentation Engineering, 1975

The sediment rating curve usually requires many suspended load measurements and may take years to accumulate. The USGS has taken suspended sediment load measurements on numerous rivers. Statistical methods can be used to relate these measurements to ungaged rivers with similar characteristics. Knowing the annual average flows of the watershed, a sediment rating curve can be developed for the ungaged watershed.

The sediment yield has been calculated for the Apanolio watershed from suspended load measurements. Figure 1 shows the sediment rating curve developed. It was assumed that 5% of the total load is bed load from table 1. The total sediment load of a typical year and a high year were calculated to be 962 and 2036 tons per year, respectively. These values will be used for comparison to predictions from other methods developed.

Figure 1 Apanollo Rating Curve



Gross Erosion and the Sediment Delivery Ratio Method for Predicting Sediment Yield

Sheet and rill erosion are often the most important sources of erosion within a watershed. The Universal Soil Loss Equation (USLE) was developed to determine the sheet and rill soil loss from agricultural field plots. The MUSLE, a modified version of the USLE by Williams and Berndt (5), was developed for application to natural watersheds. Each of the factors was weighted by area, though the rainfall factor, R, may be assumed not to change over the area. The other factors should be modified as follows:

- $K = \sum(K_i * DA_i) / DA$ in which
- K = the soil erodibility factor for the watershed
- K_i = the soil erodibility factor for each soil type
- DA_i = the area covered by each soil type
- DA = the area of the entire watershed
- n = the number of different soils in the watershed

The term L in the USLE, the slope length, is the average overland flow length for the watershed. Considering a simple rectangular watershed with one channel extending the entire length of the watershed, the overland flow length is half of the width. The width is the area divided by the length. In this case:

- $L = 0.5 DA / LCH$
- L = the length of overland flow
- DA = Area of the watershed drainage area
- LCH = length of the channel

This has been found to be a realistic approximation for the slope length of more complex watersheds with LCH equal to the total length of channels within the watershed.

The slope term, S, can be approximated by:

$$S_i = [H(LC_j + LC_{j+1})/2 \cdot DA_i] \cdot 100\%$$

S_i = the average percent slope for area i between contours j and j+1 on a topographic map

H = the difference in elevation between the contours j and j+1

LC_j = the length of the contour j

DA_i = the area between contour j and j+1

The average watershed slope is computed by weighting the slopes computed for each contour interval according to their areas:

$$S = \text{sum}(S_i \cdot DA_i) / DA$$

The LS factor of the USLE can be estimated using the average slope and gradient as computed above. The equation used in the USLE for computing the LS factor is:

$$LS = 8.52 \cdot (L/72.6)^M \cdot (0.0076 + 0.0053 \cdot S + 0.00076 \cdot S^2)$$

in english units

M = a watershed constant dependent upon slope gradient, often taken as 0.5

The cropping management factor, C, is computed by weighting the C values for each crop and management type according to the area it covers.

$$C = \text{sum}(C_i \cdot DA_i) / DA \quad \text{in which } C = \text{the cropping management factor for crop } i$$

DA_i = the drainage area growing crop i of a certain management level

n = the number of crops grown multiplied by the number of management levels in the watershed.

The erosion control practice factor, P, for a watershed can be computed from:

$$P = (1.0 \cdot SR) + (0.3 \cdot SRWW) + P_t \cdot T \quad \text{in which}$$

SR = the portion of the watershed farmed with straight rows

SRWW = the portion of the watershed farmed with straight rows and grassed waterways.

P_t = the erosion control practice factor for terracing

T = the portion of the watershed that is terraced

The erosion control factor, P, will be taken as 1 for natural watersheds in which no erosion control is practiced.

A general iso-erodent map was used to determine the value of the erosivity factor, R, of the USLE (8). From the map the value should be greater than 50. The foothills of the Sacramento Valley show a value of 50 for the R factor on the map. The climate of the project area of this study is in a much more humid area with more intense storms. The range within the Sacramento Valley is between 20 and 50, therefore a value of 70 for the erosivity factor of this project area was chosen and considered constant over the project area.

Analysis of the suspended load of Apanolio Creek, made from field measurements by Hydrocomp Inc., showed 57% sand, 29% sand, and 9% clay. The soils of the watershed are derived from weathered granite. The transported material would be classified as sandy loam. It was assumed that the soils of the watershed were generally of the same composition. A value of 0.23 was selected for the value of the soil erodibility factor of the USLE (USDA-EPA, vol 1, 1975).

The LS factor of the USLE was determined as described for the modified USLE. A topography map of the area was divided into areas in 200 foot contour intervals. The area between contours was measured as was the length of the dividing contours. From these the effective slope of each area was determined. The weighted sum of the slopes by area was then divided by the total area to give and estimated of the average effective slope of the project area. In natural conditions, S was estimated at 43%. The effective channel length was determined to be over 2033 feet. These values for S and L were used as inputs to produce a value of 74 for the LS factor.

The cropping management factor, C, has been divided into three sub-factors by Wischmeier (5). Effects of canopy, effects of mulch or close growing vegetation, and effects of tillage and residual effects of the land use can be determined as subfactors. For the Apanolio watershed in natural conditions, the canopy was estimated as between 30% and 40% from field inspection. These values translate to cofactor of between .67-.75 (5). The cover by mulch or close growing vegetation was estimated at between 80%-90%, translating to a cofactor of .07 to .13. The residual effects, including root network and subsurface effects, was estimated as between 50% to 90% of the area. These values translate to cofactor values of 0.10 to 0.22. These three cofactors multiplied together give the estimate of the cropping management factor. The low estimate is .005 and the high value is .02. These values match Wischmeiers classification for unmanaged, medium stocked woodlands (5). The average value of 0.013 will be used to predict soil loss.

The erosion control management factor, P, was assumed to be one. A value of one for P is used for straight up and down row crops. There are no erosion control practices on the natural watershed of this study which, by definition, gives a value of near one for the P factor.

The factors of the MUSLE are multiplied together to produce the estimate of the sheet and rill erosion for the area as 9974 tons/year/square mile for a typical year. Using the high and low estimates for the cropping management factor, a maximum and typical value for soil loss was predicted as 15,345 and 3,836 tons/year/square mile, respectively.

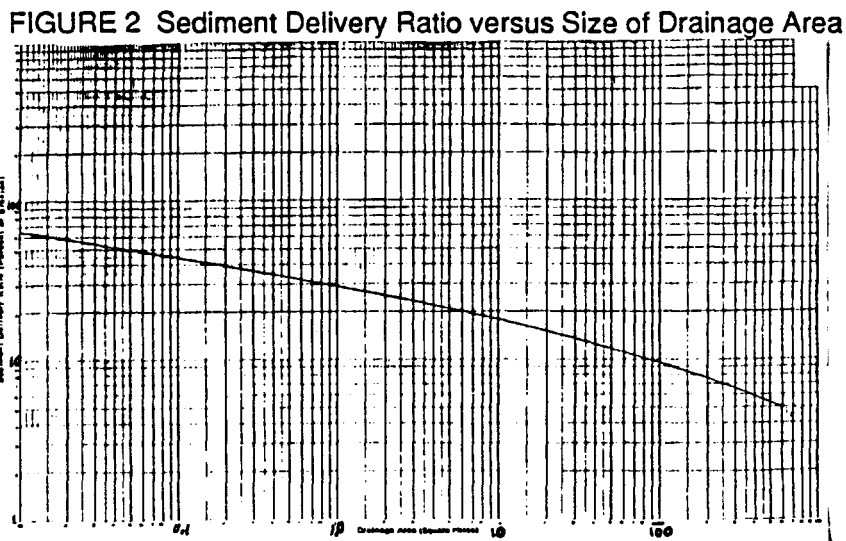
It was assumed that the gross erosion of the watershed could be estimated with the MUSLE. The ratio of the sediment yield predicted from the suspended load and the gross erosion gives and estimate of the sediment delivery ratio. The value was determined to be 10% for a typical year.

Predictive Methods for Determining the Sediment Yield of a Watershed

Many attempts to predict sediment yield of a watershed were made by correlating

parameters of the watershed with the measured sediment yield, and fitting a line by regression.

Graham Renfro of the SCS (1) has successfully related sediment delivery ratio to watershed area. Figure 2 was developed from widely scattered drainage areas. There is a correlation between sediment delivery ratio and the watershed area for watersheds throughout the country. The sediment delivery ratio varies inversely as the 0.2 power of the watershed area. Specific characteristics of a given watershed would have to be considered in applying the equation. If the watershed has high erosive factors, such as soils of silt or clay, the sediment delivery ratio would probably be higher than indicated by figure 2. Likewise, if the soil is coarse, the sediment delivery ratio would probably be lower. For the 1.4 square mile watershed of the Apanolio Canyon, a sediment delivery ratio of 28% is estimated from figure 2.



The area of a watershed is related to other watershed factors. The total length of all channels, channel density, relief, and area covered with alluvium all have a strong correlation with area. The total length of channels increases with size of watershed. The channel density is higher for small watersheds than larger ones. The total relief is higher for larger watershed areas. Large watersheds have more of their total area covered by alluvium than smaller watersheds. Therefore the relationship of sediment delivery ratio to the size of the watershed implicitly relates the sediment delivery ratio to the other parameters.

In another study by Renfro (1), an equation for the sediment delivery ratio was estimated by statistical analysis setting the relief-length ratio as the independent variable. In this study, 25 projects were compared and the following equation was developed:

$$\log(DRe) = 2.945259 - 0.82362 \log(r/L) \quad \text{where:}$$

DRe = the estimated sediment delivery rate in percent of the annual gross erosion
R/L = the relief-length ratio

The 25 projects used in this study were all within the same climatic region in Texas and Oklahoma. The coefficient of curvilinear correlation was determined to be .987. The Apanolio watershed has a relief length ratio of 0.115, which is high relative to the areas studied by Renfro. The sediment delivery ratio calculated by this equation is 148%. The results demonstrate the limited applicability of the correlation of watershed parameters in determining the sediment yield.

In a study by Elliot Flaxman (4), an equation was developed for general use in the west. Discharge was related to sediment yield. When the data was converted to logarithms and plotted it was determined that a straight line fit the data adequately. The equation is line is of the form:

$$Y = a X^m, \text{ Y is the sediment yield, X= the discharge, a= a coefficient, m= an exponent}$$

By plotting the discharge vs sediment yield of watersheds in the west, Flaxman determined that some trends to this equation exist. The coefficient a increases in more humid regions and decreases in the drier parts of the west. However, steepness of slope or low vegetative cover may also cause a high value of coefficient a. Sediment concentrations vary in the same manner as coefficient a. The value of m is equal to, or near, one for watersheds that have an increase in sediment discharge in direct proportion to an increase in discharge. These watersheds are called uniform. Watersheds with values of m less than one may be classified as a non-uniform watershed in which the sediment discharge increases at a rate less than the increase in the flow discharge. These watersheds have a high availability of sediment at low flows. The sources would probably be channels, gullies, or exposed slopes where water during low flows can erode. A value of m greater than one would be indicative of a watershed with a sediment discharge increasing at a rate larger than the increase in discharge. These watersheds tend to have a greater susceptibility to erosion during intense storms. Exponents higher than 1.5 have been classified in this type of non-uniform watershed. Watersheds with other predominant characteristics may not follow the equation well as a predictor of the sediment yield. These altering characteristics may be high amounts of snow or urbanization.

A straight line fit to the LOG-LOG plot of sediment load vs flow rate yields the following equation for Apanolio Creek:

$$Y = 0.11 Q^{1.88}$$

According to Flaxman's study (4), an exponent of 1.88 is considered high. Such a high exponent is considered indicative of low sediment concentrations during low and moderate flows relative to the concentrations at higher flows. Sediment discharge should be increasing at a rate faster than the increase in discharge. According to Flaxman, the Apanolio watershed is more susceptible to erosion during "periods of high climatic stress." This is consistent with the rainfall pattern of the area. Much of the 37 inches of rain come from drizzle and light rain, but some storms produce very intense rains during which most of the erosion could be expected to occur. A site investigation verified this phenomenon when over 8 inches of new sediment were deposited in the channel bottom after a 24 hour storm.

The value of the coefficient a, in the Flaxman study varies between 0.1 and 100,000. The value of a from the Apanolio study is 0.11. Low values of a are characteristic of watersheds in humid areas where vegetation becomes a major stabilization factor relative to arid climates.

Through another study by Flaxman in the Western United States (6), a relationship was determined for predicting sediment yield. Through the study of 28 different reservoirs in the Western United States, Flaxman came up with the following equation for estimating sediment yield by multiple regression analysis:

$$\text{Log}(Y+100)=6.21301-2.19113 \log(x1+100) + 0.06034 \log(x2+100) - 0.01644 \log(x3+100) + 0.04250 \log(x4+100)$$

Y= the sediment yield

x1= represents the effect of climate. It is the P/T ratio, the average annual precipitation divided by the average annual temperature. For every 1000 feet of change in elevation from the weather station, temperatures were increased or decreased 3° depending on increased or decreased elevation respectively. The x1 factor is intended to represent the vegetation response to climate. High values of x1 indicate a high amount of vegetative cover assuming natural conditions. An area that has been altered by urbanization or other stripping of the natural vegetation would receive a value of zero for x1 even though the P/T ratio may be high. Flaxman reduced some values of x1 based on the vegetation not being in its natural conditions.

x2 represents watershed slope. It is the weighted average slope of the watershed, as a percentage. To find this value, U.S.G.S. topographic maps were used. Areas between every fifth contour line was measured along with the length of the contour. The area divided by the length gives the average width of the interval. The average width divided by the contour interval is the average slope of the interval. By multiplying the area of the interval by the percent slope, an average weighted slope is obtained.

x3 is the percent of soil particles coarser than 1 mm in the top two inches of the soil profile. This variable is intended to account for the effect of armoring and the resistance of transport of the larger particles.

x4 is an indicator of the aggregation or dispersion characteristics of clay size particles ($<2.0 \cdot 10^{-6}$ m) in the top two inches of the soil profile. The small particles may either work to stabilize the soil or be highly erosive depending on the soil type. In general, soils with pH of more than seven are considered more erodible. These soils are associated with low precipitation, thus less vegetation and less organic matter in the soil. These soils are usually less aggregated and more erodible. Soils with low pH values are usually associated with high precipitation, high vegetative cover, and are more aggregated. There are exceptions to this classification. Soils derived from limestone may have a high calcium carbonate content, thus a high pH level, but are usually well aggregated. Field inspection should be done of each soil type. In addition to the pH levels, the amount of clay effects the soils ability for aggregation or dispersion. In order to quantify these different soil effects the following rules were used: When a pH of greater than 7 is found for the soil, a positive value is given to the percent finer than 2 micrometers. For soils with pH less than or equal to 7, a negative value is given to the percent finer than 2 micrometers. When the soil is found to have more than 25% of particles greater than 1 mm the value for x4 was set to zero. The theory behind this is that the effects of the

larger particles on the erosiveness of the soil will dominate the erosion characteristics of the soil regardless of the tendencies of the particles less than 2 micrometers.

The units of the sediment yield are acre-feet per square mile per year. The equation was developed for sediment yield predictions of rangelands in the western states. The equation was found to give negative values for watersheds whose yields were measured as less than 0.2 acre-ft per square mile per year. The sediment yield calculated by this equation excludes the erosions caused by gully formations and channel erosion within the watershed. The sediment yield expected from these sources would have to be added to the value from the equation. From this study, Flaxman deduced that the sediment yield of a watershed can be described adequately by a few variables regardless of the great variety of climates, topography, soils, geology and land conditions.

Average temperatures for the Apanolio watershed is 55° F, average precipitation is 36 inches. The effective slope as determined for the USLE, is 43%. As a broad assumption, values for soil aggregation and percent silt were used from three watersheds from similar climates used by Flaxman. With these values in the equation, the predicted sediment yield for the Apanolio watershed is between 100 and 130 tons per year per square mile.

Dendy and Bolton, 1976 (11) derived a sediment yield equation having widespread capability. They used data from deposits in about 800 reservoirs and related drainage area. The watersheds of their study ranged from one to 30,000 square miles. Runoff ranged from near zero to 50 inches per year. For areas with runoff greater than two inches per year, they derived the following equation to predict sediment yield:

$$S = 1958 e^{-0.055Q} (1.43 - 0.26 \log A)$$

S= the sediment yield in tons per square mile per year
Q= the mean annual runoff (inches)
A= the area in square miles

The Apanolio watershed has an average annual runoff of 11.9 inches per year. The predicted sediment yield is 1413 tons/square mile/year. Considerably higher than the previous estimates. The recommended use for this equation is on a regional basis rather than for a specific watershed.

Williams (1975) developed an equation to predict sediment yield of individual the storms. The equation, $Y = 11.8 (Q q_p)^{0.56} K L S P C$ predicts sediment yield in metric tons using the storm runoff volume, and the peak runoff rate, q_p .

Data for individual storms is not available for the Apanolio Watershed. Because of the large fluctuation of runoff for the area, predicting sediment yield by rainfall is much more reasonable.

Sediment Yield Estimates Based on Sediment Accumulation Method

Reservoirs catch and accumulate sediment that is washed out of the watershed. The amount that is accumulated within a known time period is an indication of the sediment

yield of the watershed. However, some of the sediment remains in suspension as it passes through the reservoir. For this reason the measured accumulated sediment must be divided by the trap efficiency of the reservoir to obtain an estimate of the total yield of the watershed.

The Soil Conservation Service has established that the sediment yield of one watershed can be estimated from a watershed with similar characteristics of topography, soil type, and with the same land use (7). Where the watershed of interest is no less than half or no more than twice the size of the measured watershed linear extrapolation is used to estimate the sediment yield of the unmeasured watershed to that of the measured watershed. Beyond these limits the SCS uses the following equation to estimate annual sediment yield: $Y_e = Y_m (A_e/A_m)^{0.8}$ where

Y_e = the sediment yield of the unmeasured watershed in tons per year, Y_m = the sediment yield of the measured watershed in tons per year, A_e = drainage area of the unmeasured watershed, A_m = drainage area of the measured watershed. This equation was developed for humid areas east of the rockies (7).

Results

The variation of the predicted sediment yield, gross erosion, and sediment delivery ratio resulting from the assumptions of annual flow rates and in the estimation of the cropping management factor are shown in table 2.

Table 2

	Column 1	Column 2	Column 3	Column 4
	Sediment Yield (tons/sq mi/yr)	C Factor Estimate	Gross Erosion (tons/sq mi/yr)	Sediment Delivery Ratio column 1/column 2
Typical Flow Year	962	0.005	15345	6%
		0.013	9974	10
		0.02	3836	25
High Flow Year	2036	0.005	15345	13
		0.013	9974	20
		0.02	3836	53

The difference of soil loss predicted during a high flow year and a low flow year is over 1000 tons per year. The same type of variation may result from different types of storms of varying frequency, timing, or location on the watershed. The linear assumption of the sediment rating curve of the log-log plot of the measured suspended sediment load and the flow rate ignores such variations.

The typical year was used for comparison of the sediment yield as calculated by other methods. The average value of the cropping management factor was also used to calculate the sheet and rill erosion, and the resulting sediment delivery ratio. Table 3 shows the comparison of predicted values by the methods discussed for the Apanolio watershed.

TABLE 3

	Sheet and Rill Erosion (tons/sq mi/year)	Sediment Yield (tons/sq mi/yr)	Sed. Del ratio
A. Measured Suspended Load plus Bed Load		962	
B. MUSLE (Williams/Berndt)	9974		
SDR (A/B) SDR (FIGURE 2) Williams (1976)		160	10% 2.8%
Dendy/Bulton		1413	
Flaxman (1972)		100-130	

The sediment yield calculated by the various methods show nearly the same variation as the gross erosion caused by the uncertainty in the C factor. The closest value to the measured sediment yield was by the Dendy and Bolton equation. This equation was intended for use on a regional basis. The sediment delivery ratio from figure 2 is significantly larger than the predicted one from suspended sediment measurements and the MUSLE. According to Flaxman an even higher value should be used from figure 2 since the area is in a humid region of high precipitation.

The equation used by Flaxman (4), relating sediment yield to flowrate can be used. Knowledge of the value of the exponent and the coefficient of the equation is helpful in cases as this report, where there is only limited data available for developing a sediment rating curve. In this case the few points were plotted, and the equation of a straight line approximation through these points was observed. The values of the coefficient and the exponent were compared to the generalizations that Flaxman determined. The trend of the measured line was found to be consistent with his conclusions. However, this study was done in the Western U.S. and is probably only applicable in that area.

A landfill is proposed for the Apanolio Canyon. The possible effects of the added material on the sediment yield of the watershed is of interest. The MUSLE was used to predict such changes. The area was measured on a topographic map. The expected slopes of the landfill area were used to adjust the effective slope of the watershed area. The cropping management factor was altered. Denuded land has a C factor value of near 1.0. A value of 0.8 was used for the landfill area. Terraces are planned for part of the landfill so the P factor was adjusted accordingly. The resulting values are shown in table 4.

TABLE 4

Watershed Condition	Tons/sq mi/year
Natural Conditions	9974
Landfill in Initial Condition	11840
Landfill in Final Condition	8547

As expected, the gross erosion was increased by adding the landfill. Though the factors used in the MUSLE were rough estimates, the calculations demonstrate the use of the

MUSLE for predictions of effect of land use changes. For comparison studies, only the factors that are expected to change need be estimated.

Conclusions

The Universal Soil Loss Equation involves factors that are hard to measure. The determination of the values are subjective. The usefulness of the equation seems to be in predicting relative changes within a watershed caused by a land use change. When used for such comparisons only the changing factors need be determined for each situation. When the gross erosion is multiplied by the sediment delivery ratio, the resulting sediment yield must be considered only a rough approximation.

Climatic variations in a location make the prediction of sediment yield unreliable. Only generalized information can be predicted such as an increase or decrease. An estimation within an order of magnitude seems appropriate for sediment yield prediction. Extensive site information is required to apply the generalized equations developed.

6.0 References

1. Graham W. Renfro, *Use of Erosion Equations and Sediment-Delivery Ratios for Predicting Sediment Yield*, p 33, Agricultural Research Service, U.S. Dept of Agriculture, report ARS-S-40, June 1975 *Present and Prospective Technology for Predicting Sediment Yields and Sources*
2. John Holeman, *Procedures Used in the Soil Conservation Service to Estimate Sediment Yield*, p5, Agricultural Research Service, U.S. Dept of Agriculture, report ARS-S-40, June 1975 *Present and Prospective Technology for Predicting Sediment Yields and Sources*
3. American Society of Civil Engineers, *Manuals and Reports on Engineering Practice - no. 54, Sedimentation Engineering*, 1975
4. Elliot Flaxman, *The Use Of Suspended-Sediment Load Measurements and Equations for the Evaluation of Sediment Yield in the West*, pp. 46-56, Agricultural Research Service, U.S. Dept of Agriculture, report ARS-S-40, June 1975 *Present and Prospective Technology for Predicting Sediment Yields and Sources*
5. Jimmy R. Williams and Harold D. Berndt, *Sediment Yield Computed with Universal Equation*, Journal of the Hydraulics Division, Proceedings of the American Society of Civil Engineers, December 1972, pp.2087-2098.
6. Elliot Flaxman, *Predicting Sediment Yield in the Western United States*, Journal of the Hydraulics Division, Proceedings of the American Society of Civil Engineers, December 1972, pp.2073-2085.
7. Soil Conservation Service, United States Department of Agriculture, *National Engineering Handbook, Section 3, Sedimentation*, ch.3, 1983
8. Soil Conservation Service, United States Department of Agriculture, *National Engineering Handbook, Section 3, Sedimentation*, ch.6, 1983
9. W.H. Wischmeier, *Estimating the Soil Loss Equation's Cover and Management Factor For Undisturbed Areas*, p118, Agricultural Research Service, U.S. Dept of Agriculture, report ARS-S-40, June 1975 *Present and Prospective Technology for Predicting Sediment Yields and Sources*
10. Hyrocomp Inc., *Report on the Hydrology of the Apanolio Canyon*, January 1990
11. ASAE, *Proceedings of the National Symposium on Soil Erosion and Sedimentation by Water*, December 12-13, 1977, Palmer House, Chicago, Illinois
12. John W. Roehl, *Sediment Source Areas, Delivery Ratios and Influencing Morphological Factors*, International Association of Scientific Hydrology, publication 60-62

PARTICLE ENTRAINMENT BY RIVER FLOWS by Kathy Chase

INTRODUCTION

This report focuses on the ability of rivers to entrain particles in their beds. A river's forces can be related to its flow velocities or to the shear stresses it exerts on its bed. A rock of a particular size will sit on the river bed until the velocity, or shear, is high enough to dislodge it. This mobilizing velocity or shear is referred to as "critical".

REVIEW OF EXISTING FORMULAS

CRITICAL VELOCITY

SIXTH-POWER LAW

The Sixth Power Law, as described by Rubey, is:

$$R = (3/4) (\theta/\tan(\phi)) (\Omega/\Omega_s - \Omega) v_b^2/g \quad (1)$$

Where
R=radius of particle
 v_b =flow velocity against the stone
 θ =empirical variable describing the proportion of the particle exposed to the current and the proportion of the current's force that is actually expended on the particle
 ϕ =particle angle of repose
 Ω =water density
 Ω_s =sediment density
g=acceleration of gravity

R varies as the square of the critical velocity, and thus the volume or weight of the largest particle moved is proportional to the velocity raised to the sixth power.

RUBEY, 1937

William W. Rubey studied several experiments to establish a general coefficient to replace the parameter $\{3/4[\theta/\tan(\phi)]\}$ in the Sixth Power Law equation. He then related the velocity against the stone to the average flow velocity using experimental data and logarithmic velocity profile relationships developed by Prandtl. His equation is as follows:

$$R = 0.22 \{ \log(r/R_m) + 2.96 \} \frac{\Omega}{(\Omega_s - \Omega)} \frac{v_m \sqrt{(rs)}}{\sqrt{g}} \quad (2)$$

Where
 R_m = the median radius of the bed material
s = slope = $\tan\beta$
P = wetted perimeter of the channel

r = hydraulic radius of the channel cross section,
 $r = A/P$
 v_m = mean flow velocity

Rubey cautioned, however, that more data was required to establish the generality of equation (2).

HJULSTROM, 1935

Hjulstrom developed a relationship of particle diameter to average velocity, v_m , at which sedimentation, transportation, and erosion will occur based on data for loose, homogeneous bed material, (see Figure 1).

FAHNESTOCK, 1963

Fahnestock also developed a $v_{el} - v_s - d$ curve from his extensive data on sediment transportation at White River, Mount Rainier, WA. His observations, however, were made on rocks already in motion, and therefore incipient motion velocities could be expected to be higher. (See Figure 2). Where possible, Fahnestock measured the velocity at $0.8 \times$ flow depth to obtain a "bottom velocity". At times, he calculated v_b from float velocities.

HELLEY, 1969

Helley derived an equation for the critical velocity at $0.6 \times A$, where A is the short axis of the particle. In the graph in Figure 3, Helley plotted his equation, which has the form of the "Sixth Power Law", for the range of particle shapes encountered at his Klamath, CA site. By observing brightly colored floats which popped up when rocks moved, he obtained critical bed velocity measurements. These are also plotted on Figure 3. In Figure 4, one can observe how his calculations compare with the findings of Hjulstrom and Fahnestock.

CRITICAL SHEAR STRESS

SHIELDS, 1936

Shields developed the well known "Shield's Diagram", a curve relating the "dimensionless shear stress", $\tau / [(s_p - s) d]$, to the flow Reynolds number, Re , from existing data. When dealing with large particles, usually $Re > 1000$, and the following relationship results:

$$\frac{(\tau)_{cr}}{(s_p - s) d} = 0.047 * \quad (3)$$

Where τ = shear stress = force exerted by moving water on a river's bed and walls, $\tau = s_p \cdot r \cdot s$
 $(\tau)_{cr}$ = critical shear stress

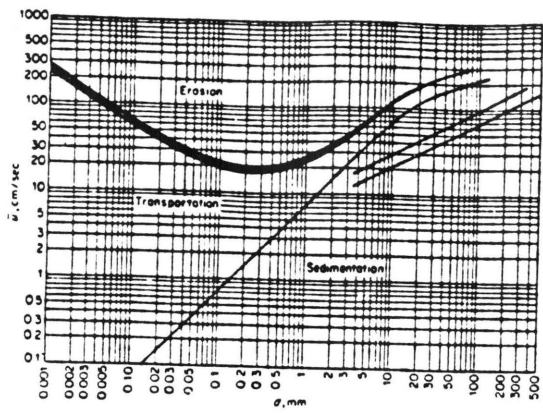


Fig. 1 Erosion-deposition criteria for uniform particles. [After HULLSTRUM (1935), (From Graf (1984)).]

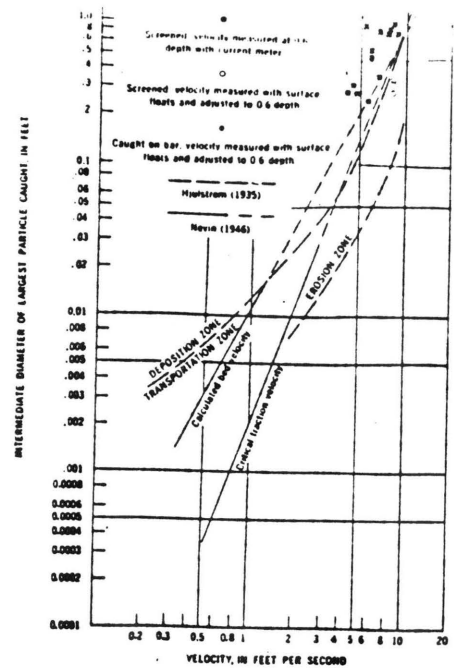


FIGURE 2.—Relation of particle size to velocity. From FANNING (1963).

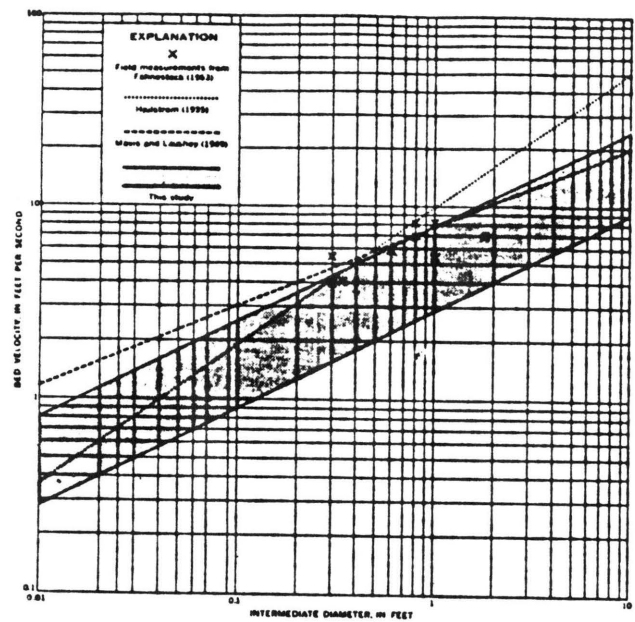


Fig. 4—Relation between bed velocity at incipient motion & particle size. From HELLEY (1969).

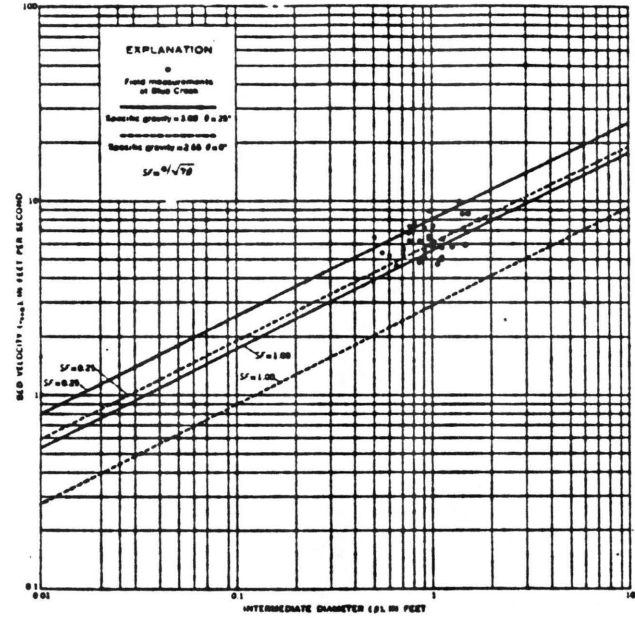


FIGURE 3.—Relation between bed velocity at incipient motion and intermediate particle diameter for the range in specific gravity, G , and β found in the test reach at Blue Creek as calculated from equation 2. From HELLEY (1969).

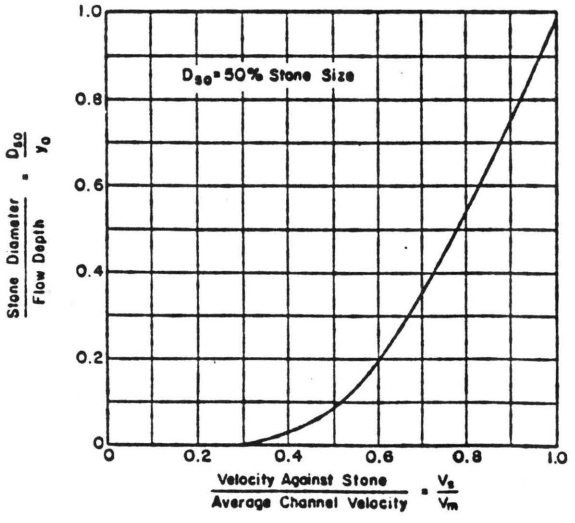


Fig. 10 Velocity against stone on channel bottom (From MEC 11, U. S. DOT, 1967). From *Highways in the River Environment*, by Richardson, Simons and Julian for US Dept of Transp., 1977.

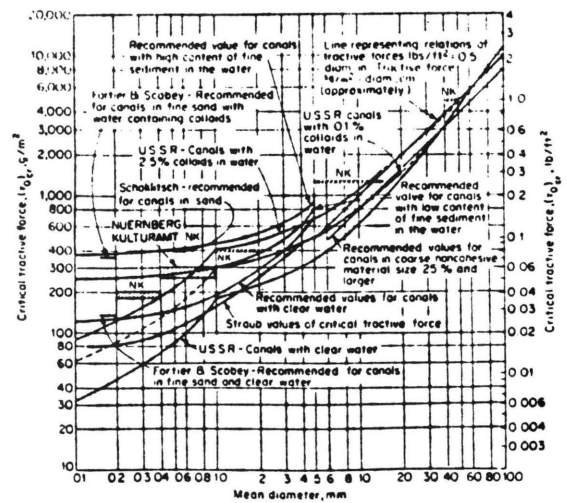


Fig. 5 Critical shear stress as function of grain diameter. [After LANE (1953), From Graf (1984)].

sp=specific gravity of water
 sp_s=specific gravity of sediment

(* Different researchers report different values for the right-hand of equation (3). Values range from 0.03 to 0.06).

EGIAZAROFF, 1965

Ippen (1962) found that the Shield's diagram does not adequately describe sediment movement over heterogeneous beds. For this more common situation, Egiazaroff proposed the equation:

$$\frac{(\tau)_{cr}}{(sp_s - sp) d} = \frac{0.1}{[\log_{19} (d/d_m)]^2} \quad (4)$$

Where d_m = average diameter for particles on the bed and in the bed load

LANE, 1953

Lane used extensive field data to establish the limiting tractive force diagram in Figure 5.

KALINSKE, 1947

Kalinske considers the velocity fluctuations that may occur in turbulent flow. By studying experimental data, he determined that actual bed velocities in rivers can vary up to 1.75 times the mean bed velocity. Since the shear stress is proportional to the square of the velocity, the maximum shear stress, (τ_{max}) , equals $(1.75)^3 * \tau_{ave}$, or

$$\tau_{max} = 3 * \tau_{ave} \quad (5)$$

Where τ_{ave} = average shear stress

WIBERG AND SMITH, 1987

P.L. Wiberg and J.D. Smith developed theoretical equations for critical shear stress on uniform and heterogeneous sediments. Their general equation for critical shear is as follows :

$$\tau * cr = \frac{2}{(C_D)_{cr}} \frac{1}{a [f^2 \langle z/z_0 \rangle]} \frac{(\tan \phi \cos \beta - \sin \beta)}{[1 + F_L/F_D \tan \phi]} \quad (6)$$

where $(C_D)_{cr}$ = drag coefficient at critical shear stress,
 a function of the particle Reynolds number, $Re = vd/\nu$
 a describes the grain geometry, $a = 1.5$ for spheres
 z = flow depth
 z₀ = the zero level of the bed, taken to be the mean level of the centers of the grains

comprising the bed surface, or $z_0 = k_s/30$, where k_s is the scale length for bed roughness. Wiberg and Smith took k_s as d_{65} of the bed material in their calculations, therefore, $z_0 = d_{65}/30$

$f^2 \langle z/z_0 \rangle$ = the square of the velocity profile function. For $Re > 1000$, $f^2 \langle z/z_0 \rangle = K^{-1} \ln(z/z_0)$
 ϕ = angle of repose, Wiberg and Smith said ϕ varies between 50° and 60° for uniform sediments

Wiberg and Smith used equation (8) to derive the τ -vs- Re graphs in Figure 6. One curve depicts $\phi = 50^\circ$, the other, $\phi = 60^\circ$. The authors use a roughness Reynolds number, $Re = vk_s/\nu$, (ν = water's kinematic viscosity), for all of their curves.

For heterogeneous sediments, the ratio of the particle size to the roughness scale of the bed becomes important, as can be seen in Figure 7. The value of ϕ in equation (6) is inversely proportional to the relative roughness, d/k_s . If $d/k_s > .5$:

$$\phi = \cos^{-1} \left[\frac{d/k_s + z_*}{d/k_s + 1} \right] \quad (7)$$

z_* is the average level of the bottom of the almost moving grains. Wiberg and Smith used $z_* = -.02$ for their calculations.

In Figure 8, the nondimensionalized critical shear, defined as $\tau_{*cr} = \tau_{cr}/[(\Omega_s - \Omega)d]$, is plotted against the critical roughness Reynolds number, R_{*cr} . To determine which particle sizes are likely to move first, the authors nondimensionalized τ_{cr} by $k_s(\Omega_s - \Omega)$ instead of using the particle diameter, d . In Figure 9, river beds with a scale size of sands fall in the range $1 < R_{*cr} < 60$ and gravels, $60 < R_{*cr} < 1500$. From this graph, it is evident that critical shear stress does not vary greatly for any size fraction on a given bed. Wiberg and Smith found that this "equal mobility" condition was indeed satisfied by analysis on data collected from a gravel bed river in California. Their results are consistent with studies on other gravel bed rivers by Parker and Klingeman, (1982) and Andrews, (1983).

Wiberg and Smith caution that their plots stop at roughness Reynolds numbers corresponding to $k_s = 5$ cm, and that their equations were derived for "tranquil flow", or Froude numbers less than one, ($Fr = v/\sqrt{gh}$).

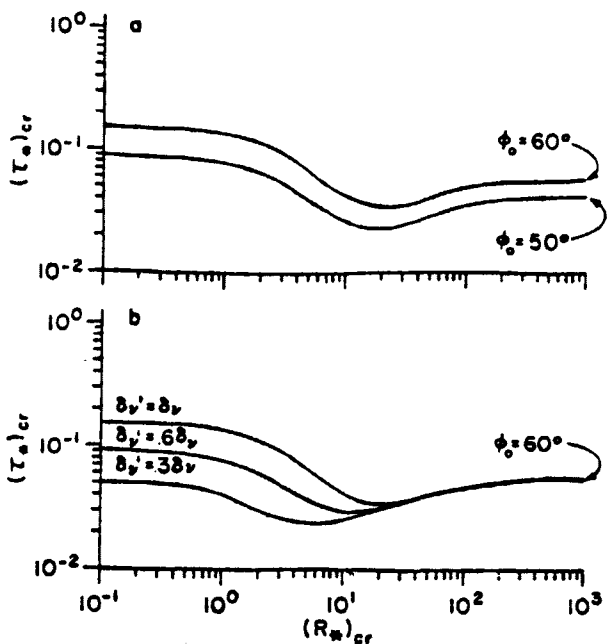


Fig. 6 (a) Theoretical initial motion curves for nondimensional critical shear stress $(\tau_{cr})_{cr} = \tau_{cr} / [(\rho_s - \rho)gD]$ as a function of critical roughness Reynolds number $(R_{*})_{cr} = (u_{*})_{cr} k_s / \nu$, calculated for $k_s = D$ (uniform sediment) using (8) with particle angles of repose $\phi_0 = 50^\circ$ and 60° . Shields' relationship for initial motion, indicated by the stippled band, is given for comparison; the width of the band indicates the scatter of data used by Shields. (b) Theoretical initial motion curves for particle angle of repose, $\phi_0 = 60^\circ$, with the viscous sublayer height δ_v , suppressed by 33% and 60% ($\delta_v' = 0.33\delta_v$, and $\delta_v' = 0.6\delta_v$, respectively), as well as at its full height. From Wiberg & Smith.

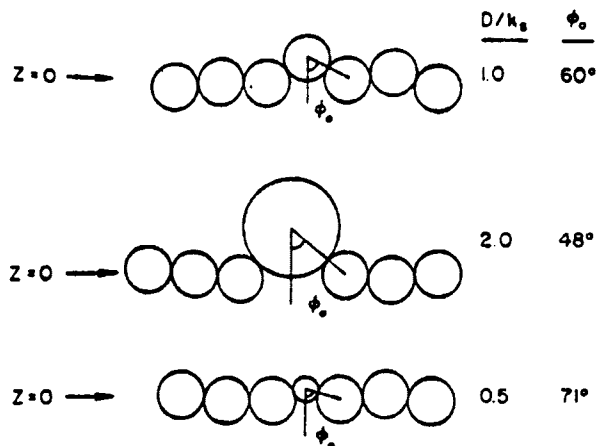


Fig. 7 Relationship between the particle angle of repose, ϕ_0 , and the ratio of particle size to bed roughness scale, D/k_s , as used to rationalize the nearshore sand data of Miller and Byrne [1966]. In this schematic, two-dimensional representation the bottoms of the almost moving grains are at the assumed zero level of the bed, indicated by the arrows at $z = 0$. From Wiberg & Smith (1977).

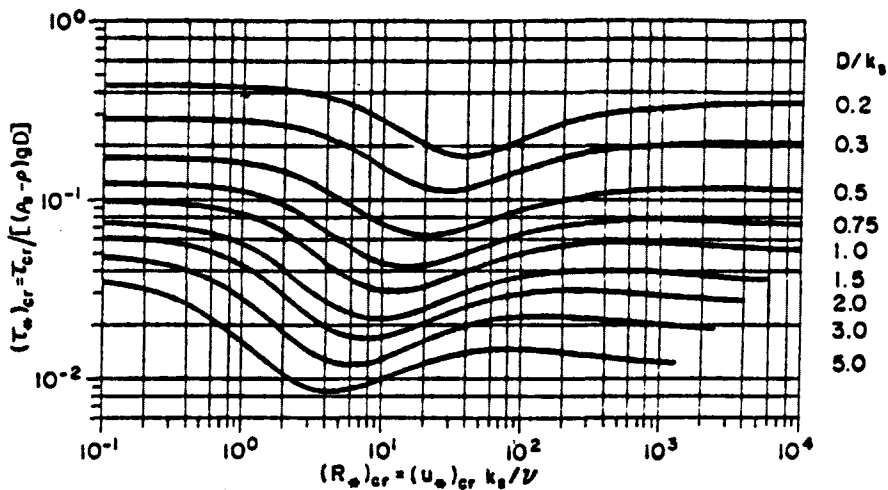


Fig. 8 Calculated nondimensional critical shear stress $(\tau_{cr})_{cr}$ as a function of critical roughness Reynolds number $(R_{*})_{cr}$ for values of particle diameter to bed roughness scale, D/k_s , from 0.2 to 5.0. From Wiberg & Smith (1977).

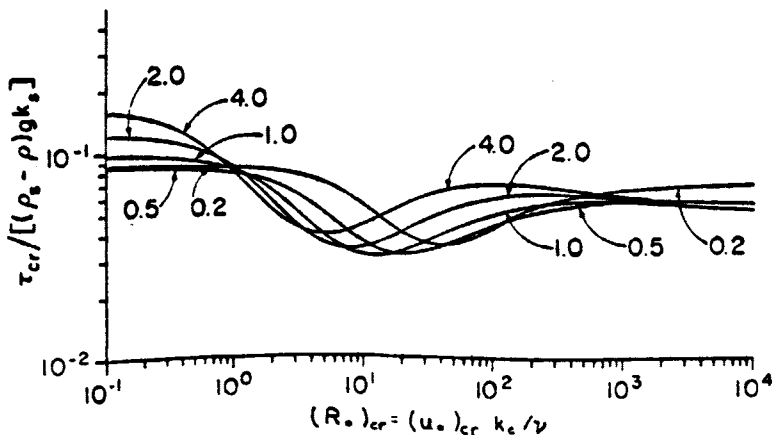


Fig. 9 Calculated shear stress nondimensionalized by bed roughness, k_s , rather than D . From Wiberg & Smith (1977).

DATA ANALYSIS

MUSSETTER, 1989

Bob Mussetter collected extensive data on hydraulic characteristics and sediment transport capacity of steep mountain streams in Southern Colorado. Important assumptions in Mussetter's study were:

- (a) the observed moving particles were set in motion under conditions similar to those where channel characteristics were measured, and
- (b) Since larger material was available in the stream beds, the sizes in motion were the largest that the streams had the capacity to move.

Thirteen sets of data were selected from six of Mussetter's sites. The actual critical velocities and shear stresses were calculated for the largest material in motion at each site. The following parameters were used to calculate critical velocities and shear stresses by the predictive equations discussed earlier: the median of the bed material, (d_{50} of the bed), the largest rocks observed in motion, (d_{100} moving), the energy slope, s , and the hydraulic radius, r . The results are summarized in Tables 1 and 2, and Figures 11 through 14.

The actual mean velocity, (V_m) and velocity against the stone, (V_b), observed at each site are plotted versus the largest particles observed moving in Figure 11. Mean velocities were calculated by dividing Mussetter's reported flow, (Q), by the cross sectional area, (A). The velocity against the stone, (V_b) was determined using the graph in Figure 10. The ratio of moving particle size to D_{50} of the bed material, (D_{moving}/D_{50} bed), is identified for each point on the graph. According to the theory behind Wiberge and Smith's equations, the stones with the lower D_{100} moving/ D_{50} bed ratios should move at higher critical velocities. This seems to happen for the 0.07 and the 0.17-foot diameter particles.

In Figure 12, the velocities against the stone for different stone sizes are compared to those calculated by the 6th Power Law and those read from Helley's chart. The theoretical methods in this figure tend to overestimate the velocity required to move sediment sizes in the 0.07 to 0.2 foot range. Neither of these methods considers the ratio of the size of the particle in motion to the bed material size.

Figure 13 compares actual mean velocities to the mean velocities calculated from Rubey and read from graphs by Hjolstrom and Fahnestock. Hjolstrom and Fahnestock both disregard the ratio D_{100} moving/ D_{50} bed, and both tend to overestimate the critical velocity for the sizes studied.

ENTRAINMENT VELOCITIES								
MUSSETER DATA		ACTUAL		6th POWER	RUBEY	HJULSTROM	HELLEY	FAHNESTOCK
SITE/DATE	BED D50 (mm)	MOVING D100 (mm)	Calc from Data		U _{bc} (req)	trans/eros		U _m
			U _b /U _m (ft/sec)	U _{bc} (req) (ft/sec)	U _m (ft/sec)	U _b (ft/sec)	U _m (ft/sec)	
47D2/ 6-10	200	29	0.38/0.8	1.53	1.16	4.6/6.9	2	3.5
47E1/ 5-23	100	40	1.1/2.0	1.80	3.44	5.2/8.2	2.2	3.9
	100	20	1.4/3.1	1.27	1.46	3.9/5.9	1.5	3
1B / 6-21	55	50	1.3/2.0	2.01	0.21	5.9/8.5	2.8	5.8
/ 7-7	55	30	1.2/2.0	1.56	5.35	4.9/6.9	2	3.6
1E / 7-7	75	62	1.2/1.9	2.24	8.61	6.6/9.2	3	6
/ 6-8	75	50	1.3/2.3	2.01	6.17	5.9/8.5	2.8	5.8
/ 5-25	75	40	0.8/1.3	1.80	6.25	5.2/8.2	2.2	3.9
47G / 5-31	40	50	1.5/2.3	2.01	11.90	5.9/8.5	2.8	5.8
/ 7-11	40	40	1.7/3.2	1.80	7.04	5.2/8.2	2.2	3.9
/ 8-5	40	20	1.3/2.7	1.27	3.62	3.9/5.9	1.5	3
7.8 / 6-30	40	50	0.9/1.7	2.01	2.58	5.9/8.5	2.8	5.8
/ 8-13	40	24	0.9/1.9	1.40	1.43	4.2/6.6	1.5	3.5

TABLE 1

CRITICAL SHEAR										
MUSSETER DATA		Calc from		EGIAZARROF		LANE		KALINSKE WIBERG&SMI		
SITE/DATE	BED D50 (mm)	MOVING D100 (mm)	Data		TAUreq		TAUreq		TAUreq	
			TAUact (N/m ²)	SHIELDS (N/m ²)	TAUreq (N/m ²)					
47D2/ 6-10	200	29	463.56	20.82	1504.52	23.94	116	149.10		
47E1/ 5-23	100	40	116.79	27.62	207.19	33.52	160	117.52		
/ 6-10	100	20	135.62	13.01	574.39	14.36	80	102.83		
1B / 6-21	55	50	37.05	34.52	69.50	40.70	200	36.73		
/ 7-7	55	30	29.51	20.71	115.03	23.94	120	44.07		
1E / 7-7	75	62	50.23	42.80	104.22	43.09	240	72.86		
/ 6-8	75	50	50.60	34.52	129.24	40.70	200	66.11		
/ 5-25	75	40	30.27	27.62	161.55	33.52	160	50.76		
47G / 5-31	40	50	17.64	34.52	36.76	40.70	200	29.38		
/ 7-11	40	40	27.81	27.62	45.95	33.52	160	29.38		
/ 8-5	40	20	23.62	13.01	91.90	14.36	80	29.38		
7.8 / 6-30	40	50	314.04	34.52	36.76	40.70	200	29.38		
/ 8-13	40	24	219.22	16.57	76.50	19.15	96	31.73		

TABLE 2

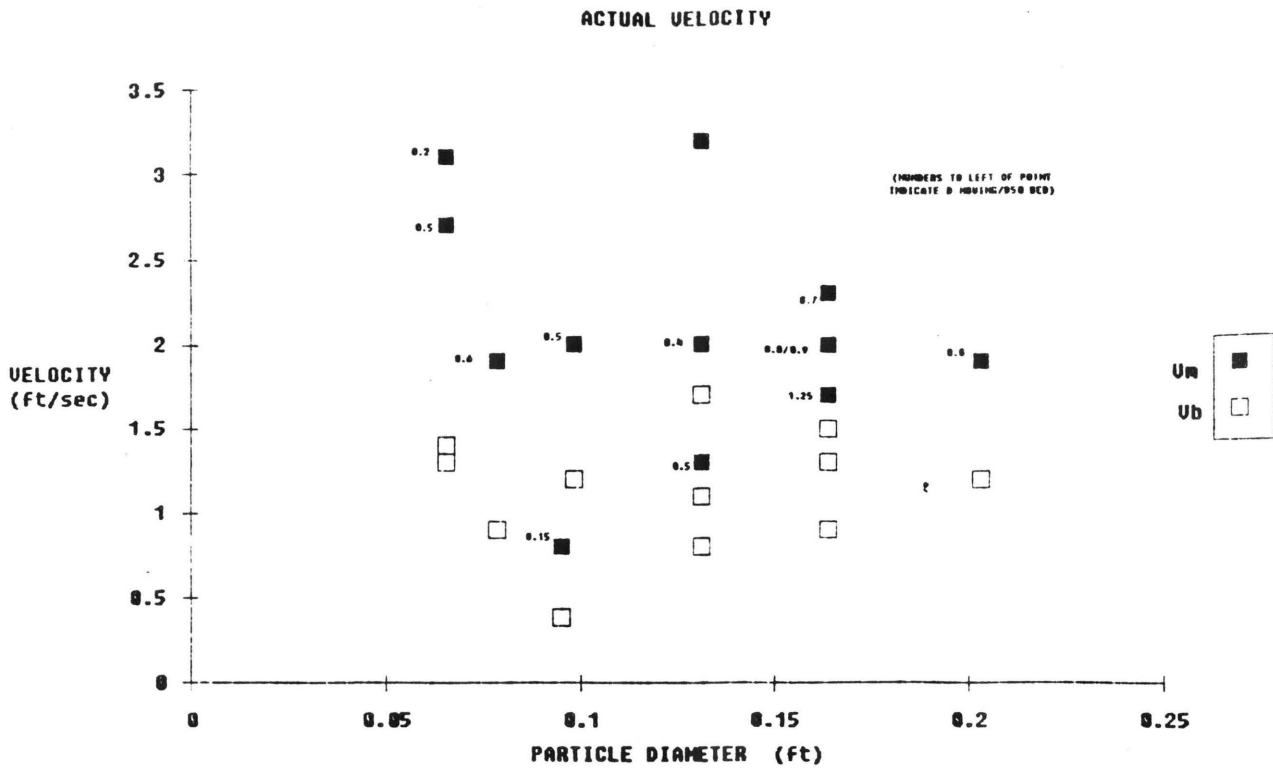


FIGURE 11

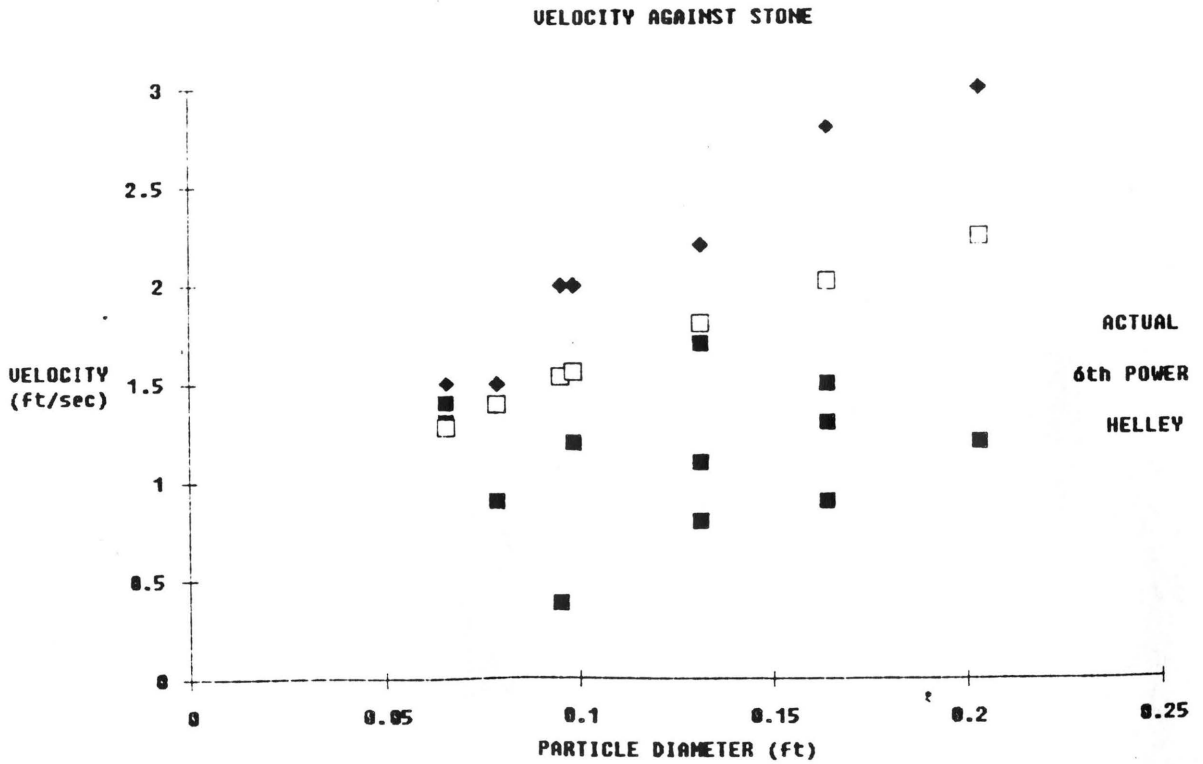


FIGURE 12

CRITICAL MEAN VELOCITY

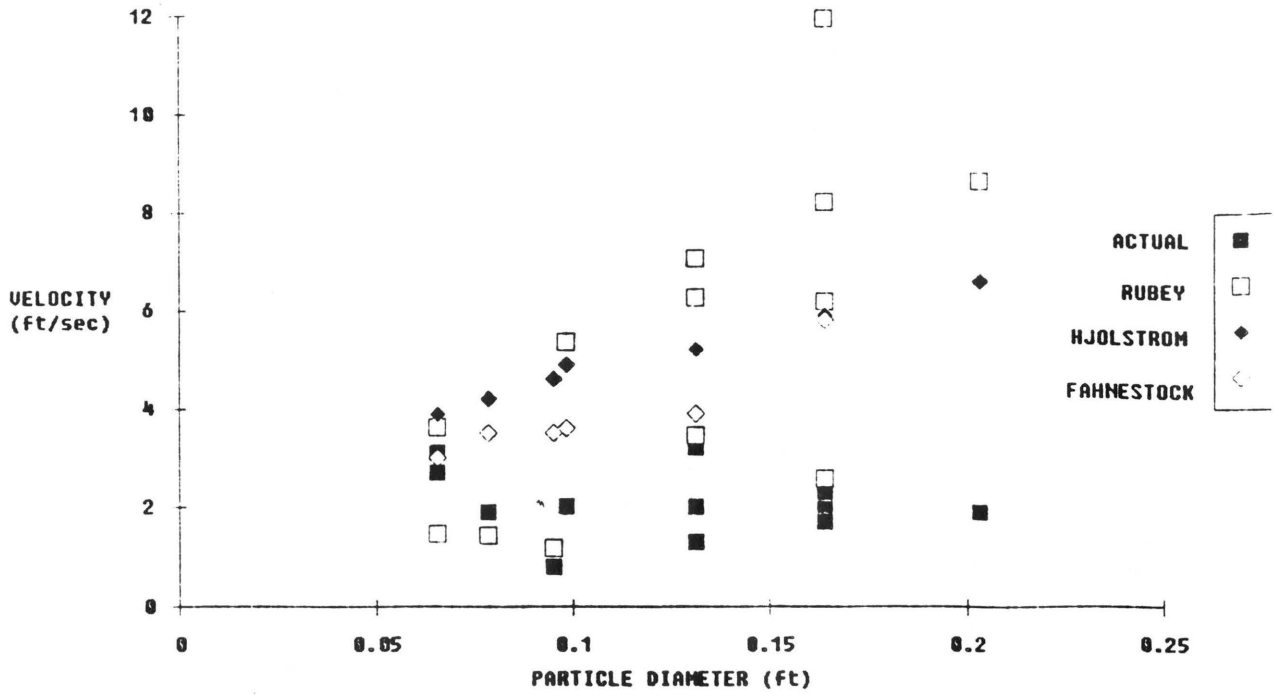


FIGURE 13

CRITICAL SHEAR

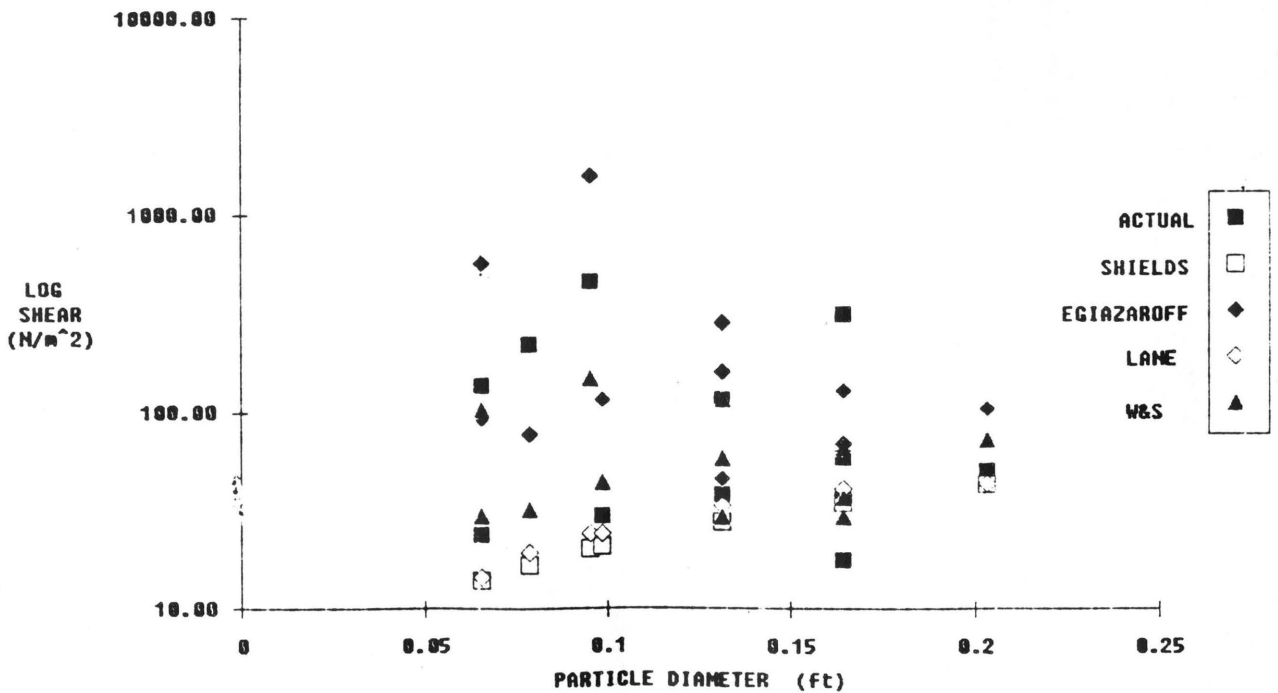


FIGURE 14

Rubey's method does consider particle size, (see Equation 2). In this case, Rubey's method consistently overestimates critical velocities.

Figure 14 is more elucidating. Actual critical shear stresses are plotted along with the stresses calculated using the theories discussed earlier. Shields' and Lane's methods, neither of which take D_{100} moving/ D_{50} bed into account, both underestimate critical shear stress. This underestimation by the formulas developed for uniform, homogeneous material could be expected. Most of the Mussetter's data results from smaller particles moving over a larger bed, and, according to the "equal mobility" concept, these particles would be more difficult to move than the same particles on a uniform bed. Egiazaroff's equation, (equation 4), does look at the bed material sizes as well as the moving particles. In most cases, application of equation 4 results in shear values considerably higher than those observed. Wiberg and Smith's equations seem to fit Mussetter's data the best, though critical shears are sometimes over- or under-estimated by more than an order of magnitude.

CONCLUSION

Though incipient motion has been studied for over fifty years, no one can predict precisely at what flow velocity or tractive force a particle will move. This is mostly due to the variations in natural conditions such as river turbulence and particle shape and orientation. Several workers have derived predictive equations for a particle's critical velocity. However, determining the location of this velocity and actually measuring it are difficult tasks. Shear stress, on the other hand, is a function of hydraulic radius and bed slope, variables that are relatively easy to measure directly.

A small particle on a riverbed composed of larger rocks will require larger critical flows than that same stone on a bed of smaller rocks. A gravel on a sand bed will move more easily than if it were resting on gravel. Therefore, equations like those of Wiberg and Smith, which consider the ratio of moving particle diameter to bed material size, should be used when studying natural rivers.

REFERENCES

- Bradley, W.C. and A.I. Mears, (1979). "Calculations of Flows Needed to Transport Coarse Fraction of Boulder Creek Alluvium at Boulder, Colorado", in Geological Society of America Bulletin, Part 11, vol. 91, p. 1057-1090.
- Egiazaroff, J.V., (1965). "Calculation of Nonuniform Sediment Concentrations", in Proceedings of the American Society of Civil Engineers, Vol. 91, No. HY4.
- Fahnestock, Robert K., (1963). "Morphology and Hydrology of a Glacial Stream- White River, Mount Rainier, Washington", Geological Survey Professional Paper 422-A.
- Graf, W.H., (1984), Hydraulics of Sediment Transport, Water Resources Publications, Littleton, CO.
- Helley, E.J., (1969). "Field Measurements of the Initiation of Large Bed Particle Motion in Blue Creek Near Klamath, CA", USGS Professional Paper 562-G.
- Hjulstrom, F. (1935). "The Morphological Activity of Rivers as Illustrated by Rivers Fyris, Bulletin of the Geological Institute in Uppsala, vol. 25, chapter III.
- Ippen, A.T. and P.A. Drinker, (1962). "Boundary Shear Stresses in Curved Trapezoidal Channels", in Journal of the Hydraulics Division, American Society of Civil Engineers, vol. 85, no. HY5
- Lane, G. (1953). Progress Report on Studies on the Design of Stable Channels of the Bureau of Reclamation, Proceedings of the American Society of Civil Engineers, vol. 79.
- Kalinske, A.A., (1947). "Movement of Sediment as Bed-Load in Rivers," Transactions of the American Geophysical Union, vol. 23, part 2.
- Mussetter, R.A., (1989). Dynamics of Mountain Streams, Ph.D. Dissertation, Colorado State University.
- Richardson, E.V., Simons, D.B. and Julien, P.Y., (1988). Highways in the River Environment. Prepared for U.S Department of Public Transportation, Federal Highway Administration.
- Rubey, W.W., (1938), "The Force Required to Move Particles on a Stream Bed," USGS Professional Paper 189-E.
- Schall, J.D., (1979), "Spatial and Time Distribution of Shear Stress in Open Channel Flows", Masters Thesis, Colorado State University.
- Vanoni, V.A., (1975), Sedimentation Engineering, American Society of Civil Engineers, ASCE Manuals and Reports on Engineering Practice- No. 54.
- Wiberg, Patricia L. and J.D. Smith, (1987). "Calculations of the Critical Shear Stress for Motion of Uniform and Heterogeneous Sediments", in Water Resources Research, vol. 23, No. 8, p. 1471-1480, August 1987.

BED FORMS AND RESISTANCE TO FLOW

Yasser Raslan

ABSTRACT: A summary for some of the different methods for the resistance to flow is presented. Some analysis for the data by Williams (1970) were done to figure out the relation between the bedforms geometry and the hydraulic elements of a small flume. Studying bedform in this report is restricted to dune bed only using very course sand.

INTRODUCTION

Fredsoe (4) developed a mathematical model to calculate the shape of the dunes by using the continuity equation of sediment. He expressed the shape of the dunes at large shear stress as follows:

$$\left(\frac{h}{\omega} \right)^{2/3} = \frac{\tau^* - \theta_c}{\theta_{top}^* - \theta_c} \quad (1)$$

At large shear stress the suspended sediment has an influence on the dune height and length. The expression for dune height is given as follows:

$$\frac{\frac{H}{D}}{\left(1 - \frac{H}{2D} \right)} = \frac{\phi_b}{2\phi \left(\frac{d\theta_b}{d\theta} + \frac{d\phi_s}{d\tau} \right)} \quad (2)$$

The length is given by:

$$L = \frac{[16Hq_b + (16H + \delta)q_s]}{(q_b + q_s)} \quad (3)$$

Fredsoe concluded that the dune height and the dune steepness decreases at large shear stress. Also, the amount of suspended load does not depend only on the skin friction, but also the other parameters such as fall velocity, shear velocity and grain size.

Van Rijn (9) derived by analyzing flume and field data a relationship for the dune height and length.

The bed form height was related to the other parameters as follows:

$$\frac{h}{D} = F \left[\frac{d_{50}}{D}, d_*, T \right] \quad (4)$$

Where,

$$T = \text{Transport stage parameter} = \frac{u_*'^2 - u_{*cr}^2}{u_{*cr}^2}$$

Similarly, the bed form steepness can be expressed as follows:

$$\frac{h}{L} = F \left[\frac{d_{50}}{d}, d_*, T \right] \quad (5)$$

By using the field and flume data in fitting the curves the following relationships were obtained by regression analysis:

$$\frac{h}{d} = 0.11 \left[\frac{d_{50}}{D_{50}} \right]^{0.3} (1 - e^{-0.5T}) (25 - T) \quad (6)$$

$$\frac{h}{L} = 0.015 \left(\frac{d_{50}}{D_{50}} \right) (1 - e^{-0.5T}) (25 - T) \quad (7)$$

Where, $T < 25$, water temperature was considered = 25 C as it was not available from the data.

From Eq. 6 and Eq. 7, the following relationship was obtained after eliminating the side wall effect of the flume using the method of Vanoni-Brooks (8):

$$L = 7.3 D \quad (8)$$

Eq. 8 is similar to the one which was derived by Yalin (1964):

$$L = 2\pi D \quad (9)$$

Einstein's Approach, 1950

Einstein proposed this relation for the resistance due to skin

$$\frac{u}{u_*'} = 5.75 \log \left[12.27 \frac{R'}{k_s} x \right] \quad (10)$$

Where, x is a correction factor which compensates for rough conditions and depends on the value of

$$\frac{k_s}{\delta} \quad \text{and} \quad \delta = \frac{11.6 \nu}{u_*'}$$

The following functional relationship was suggested for the form roughness

$$\frac{u}{u_*''} = F(\psi') \quad (11)$$

Where ψ' is the intensity of shear versus representative particles and

$$\psi' = \frac{\gamma_s'}{\gamma} \frac{D_{35}}{SR'} \quad (12)$$

The functional relationship in Eq. 11 was developed based on field data.

Simons and Richardson's Approach (1966):

The authors have suggested a particular formula for each type of bed form.

- 1) For a plane bed with sediment transport:

$$\frac{c}{\sqrt{g}} = 5.9 \log \frac{D}{D_{85}} + 5.44 \quad (13)$$

- 2) For a plane bed with sediment transport:

$$\frac{c}{\sqrt{g}} = 7.4 \log \frac{D}{D_{85}} \quad (14)$$

- 3) For ripples:

$$\frac{c}{\sqrt{g}} = \left[7.66 - \frac{0.3}{u_*} \right] \log D + \frac{0.13}{u_*} + 11 \quad (15)$$

- 4) For dunes and antidunes:

$$\frac{c}{\sqrt{g}} = 7.4 \log \frac{d}{D_{85}} \sqrt{1 - \frac{\Delta RS}{RS}} \quad (16)$$

where the terms ΔRS is an adjustment for RS to compensate for the form roughness. ΔRS is a function of RS for dunes. For antidunes, the term $\sqrt{1 - \frac{\Delta RS}{RS}}$ is a function of sand size, shear stress and depth.

Engelund and Hansen's Approach (1966)

In the case of a dune bed, a part of the total loss of the mechanical energy is due to the flow expansions after each crest

and another part is due to friction. The magnitude of the expansion head loss can be estimated from Carnot's formula

$$\Delta H'' = \alpha \frac{(u_1 - u_2)^2}{2g} \quad (17)$$

where α is a non-dimensional coefficient depending on the flow geometry

$$\text{and } u_1 = \frac{q}{D - 1/2 H}, \quad u_2 = \frac{q}{D + 1/2 H}$$

Engelund derived this equation after some mathematical procedure

$$\frac{\gamma RS}{(\gamma_s - \gamma)d} = \frac{\gamma RS'}{(\gamma_s - \gamma)d} + \frac{\alpha}{2} \frac{\gamma h^2}{(\gamma_s - \gamma)Ld} F^2$$

$$\text{i.e., } \theta_* = \theta_*' + \theta_*'' \quad (23)$$

where θ_* and θ_*' are the dimensionless total shear, shear stress due to grain roughness and shear stress due to bed form roughness, respectively.

Brownlie's Approach (1983)

Brownlie described the flow resistance as a function of unit discharge, channel slope, and sediment properties, i.e.,

$$\frac{R_s}{d} = \frac{(\rho_s - \rho)}{\rho} \tau_* = F \left[\frac{q}{(gd^3)^{1/2}}, S, \sigma_g \right] \quad (24)$$

By using data in determining multiple regression analysis, Brownlie got the following two equations.

For lower regime

$$\frac{R}{d} = 0.3724 (q_*)^{0.6539} S^{-0.2542} (\sigma_s)^{0.105} \quad (25)$$

For upper regime

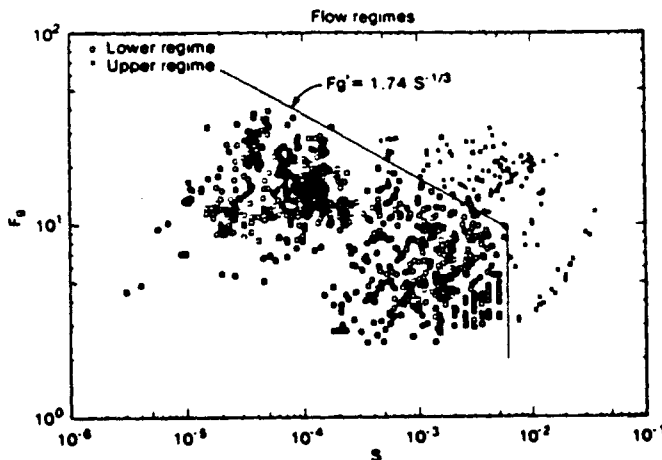
$$\frac{R}{d} = 0.2836 (q_*)^{0.6248} S^{-0.2877} (\sigma g)^{0.08013} \quad (26)$$

For every set of independent variables, there are two possible depths: one for the lower regime and the other for the upper regime.

The grain Froude number is an indication of the flow regime

$$F_g = \frac{u_*'}{[(\rho_s - \rho)gd]^{1/2}}$$

The variable u_*' is the shear velocity which occurs on the upper flow regime when no dunes occur. Figure (1) shows the value of S which divides the flow regime



Determination of flow regimes: grain Froude number F_g plotted against slope S (Brownlie, 1963).

where F' is equal to F along the line.

The transition region for the upper limit of the lower flow regime is expressed by

$$\log \frac{F_g}{F_g'} = -0.2026 + 0.07026 \log \frac{d}{\delta} + 0.933 \left(\log \frac{d}{\delta} \right)^2 \quad \text{for } \frac{d}{\delta} < 2$$

$$\log \frac{F_g}{F_{g'}} = \log 0.8 \quad \text{For } \frac{d}{\delta} \geq 2$$

For lower limit of the upper flow regime

$$\log \frac{F_g}{F_{g'}} = -0.02469 + 0.1517 \log \frac{d}{\delta} + 0.8381 \left(\log \frac{d}{\delta} \right) \quad \text{for } \frac{d}{\delta} < 2$$

$$\log \frac{F_g}{F_{g'}} = \log 1.25 \quad \text{For } \frac{d}{\delta} \geq 2$$

This method is well accepted because it is based on a large data base.

PRESENTATION OF DATA

The data which were used in this project were collected by Garnett P. Williams in 1970. Williams used a non-recirculating flume with 52 ft. length for the experiments. The flume could be tilted from horizontal to maximum slope of about 0.035 ft. per foot. The maximum width was 3.9 ft. The controlled variables in the experiment were sediment transport rates, grain size, water depth and channel width. The dependent variables were water discharge, mean velocity, slope (energy gradient) and bed form characteristics. Grain size was uniform (particles with a 1.35 mm diameter for all runs).

The feed sediment enters the flume was controlled upstream. Williams measured the mean velocity, the surface velocity, water temperature, units of sediment, transport rate and the bed forms characteristics.

Summary of Runs

<u>No. of Run</u>	<u>Width in feet</u>	<u>Depth in feet</u>	<u>Grain size</u>
48	0.25	0.1, 0.3, 0.5, 0.7	1.349 mm
46	0.5	0.1, 0.3, 0.5, 0.7	1.349 mm
53	1.0	0.1, 0.3, 0.5, 0.7	1.349 mm
25	2.0	0.1, 0.3, 0.5, 0.7	1.349 mm
5	3.0	0.7	1.349 mm

TABLE 1.0

 FLOW WIDTH = 7.5 CM.

BED MATERIAL SIZE = 1.35 MM.

<u>DISCH</u> <u>L/S</u>	<u>DEPTH</u> <u>M</u>	<u>SLOPE</u> <u>S*1000</u>	<u>TYPE</u>	<u>BED FORM</u> <u>HEIGHT</u> <u>CM</u>	<u>LENGTH</u> <u>CM</u>	<u>V_s</u> <u>CM/SEC</u>	<u>q</u> <u>KG/SEC/M</u>
3.256	0.092	2.58	DUNE	0.4	185	0.047	0.001
3.455	0.091	2.95	DUNE	0.4	169	0.14	0.002
3.37	0.09	3.1	DUNE	0.6	134	0.098	0.003
3.823	0.093	3.71	DUNE	0.6	82	0.15	0.007
4.134	0.092	4.35	DUNE	0.8	81	0.2	0.009
4.587	0.083	5.95	DUNE	1	65	0.51	0.021
6.088	0.155	2.71	DUNE	1	204	0.042	0.002
6.484	0.153	2.88	DUNE	1	109	0.12	0.004
6.824	0.152	2.63	DUNE	1.6	114	0.084	0.007
7.532	0.153	4.85	DUNE	1.8	103	0.14	0.015
8.551	0.153	6.51	DUNE	1.8	69	0.43	0.03
9.146	0.153	7.63	DUNE	2	64	0.6	0.048
10.76	0.154	10.4	DUNE	2.4	98	0.87	0.101
9.854	0.218	3	DUNE	1.6	117	0.062	0.006
12.176	0.221	5.39	DUNE	3.2	101	0.23	0.029
15.715	0.217	7.93	DUNE	3	91	0.93	0.085
17.472	0.214	10.1	DUNE	3.8	78	1.01	0.132

DISCUSSION OF RESULTS

The geometrical properties of the dune were plotted versus the different hydraulic parameters for one sediment size which is 1.349 mm and flume width = 7.5 cm. The following relationships were obtained.

Figure 2 shows regression analysis for the relationship between the dune steepness H/L and the relative height. The relationships indicated that the dune geometry is dependent on the flow depth. Which agree with the work of Van Rijn (9).

From figure 3 it can be seen that the dune height increases with the increase of the discharge.

Figure 4 shows the relationship between the velocity of the downstream movement of dunes and the mean velocity of the flow. It can be seen from this figure that the velocity of dunes increases with the increase of mean velocity.

Figure 5 shows that the dune steepness depends on the slope of energy gradient for the dunes, i.e., dune steepness increases with the increase of the slope.

Figure 8 shows that the relative height of the dunes (H/D) increases with the increase of the slope of energy gradient.

Figure 7 shows that the dune height increases with the increase of the unit transport rate of the sediment.

Figure 6 shows that the Froude number increases with the increase in dune steepness.

The examination of the proposed formula for dune length by Yalin (1964) ($L = 2\pi D$) and Van Rijn's (1986) ($L = 7.3D$) did not show an agreement with the measure data. Although Van Rijn used

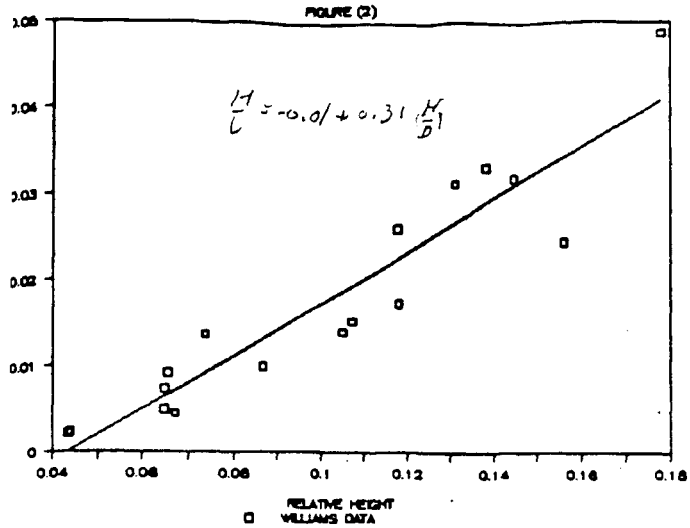
this data as a part of his data set in deriving his formula, (Figures 9, 10.)

CONCLUSIONS

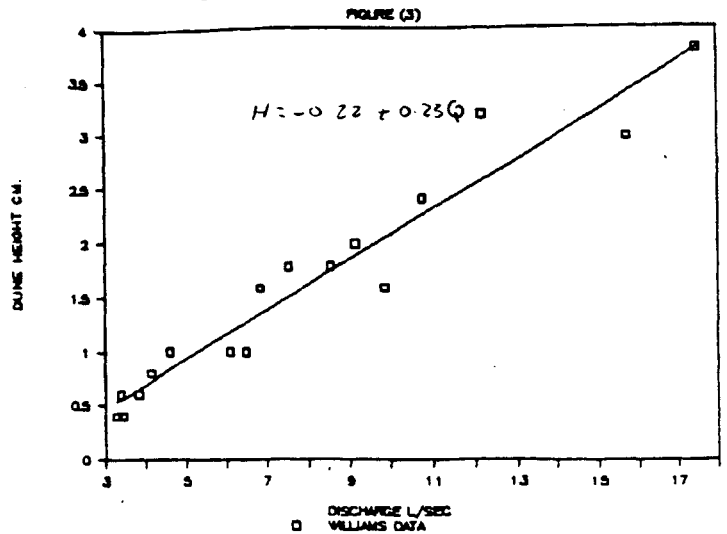
This study showed that for sediment size 1.349 mm:

- 1) Dune steepness $(H/L) \propto$ relative height of dunes (H/D)
- 2) Dune height is related to the discharge.
- 3) Both dune steepness and relative height of dunes depend on the slope of the energy gradient.
- 4) There is a relationship between the speed of the downstream movement of dunes and the mean velocity.
- 5) Dune height is proportional to unit transport rate of sediment.
- 6) Dune steepness increases with the increase of Froude number.
- 7) Small flumes give good results, although no correction has been made to include the side wall effect.

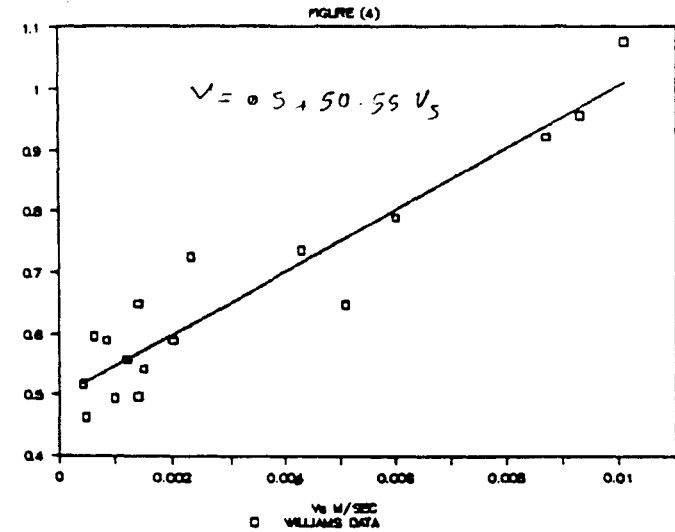
DUNE STEEPNESS Vs RELATIVE HEIGHT



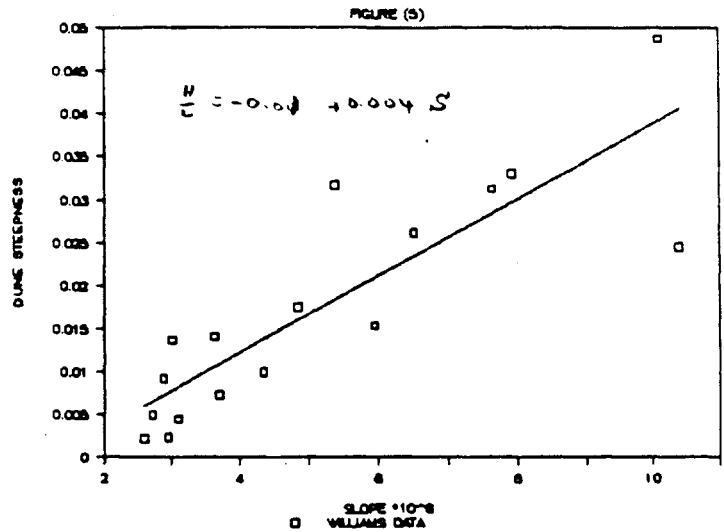
DUNE HEIGHT Vs DISCHARGE



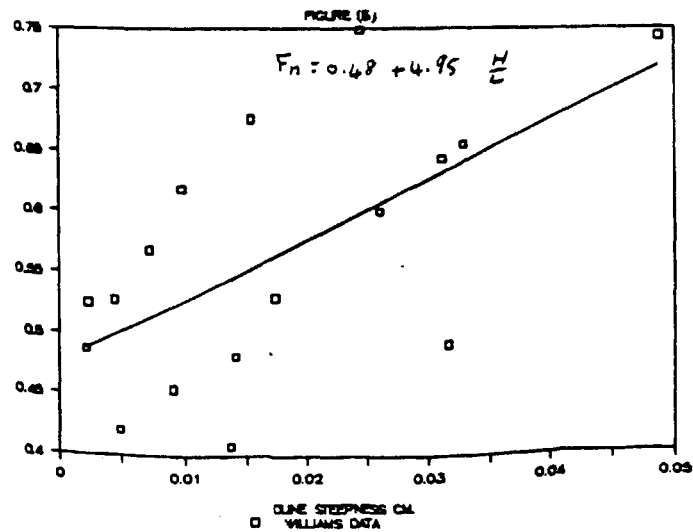
V Vs V_s



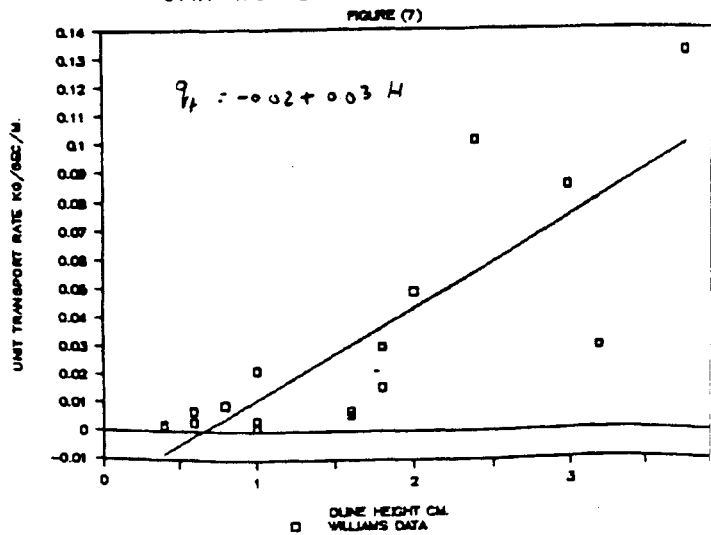
DUNE STEEPNESS Vs SLOPE



FROUDE NU. Vs DUNE STEEPNESS

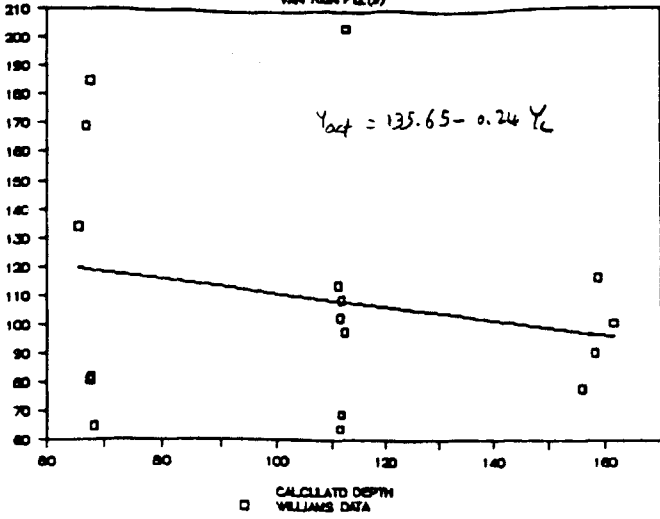


UNIT TRANSPORT Vs DUNE HEIGHT



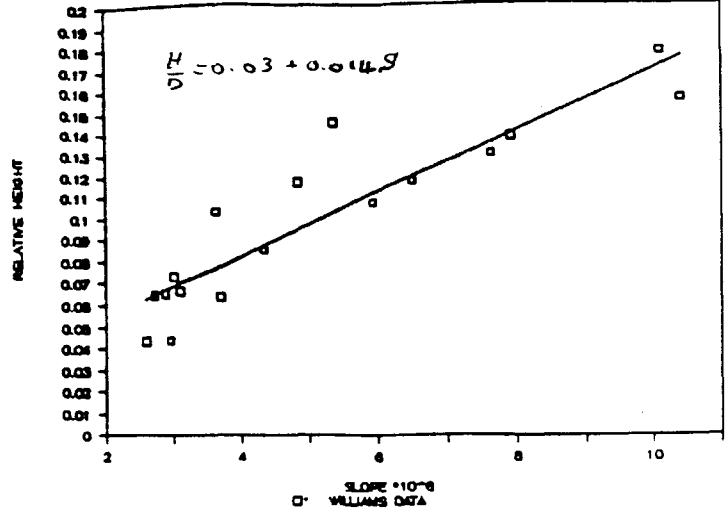
ACTUAL DEPTH Vs CALCULATED DEPTH

VAN PELJN FIG.(9)



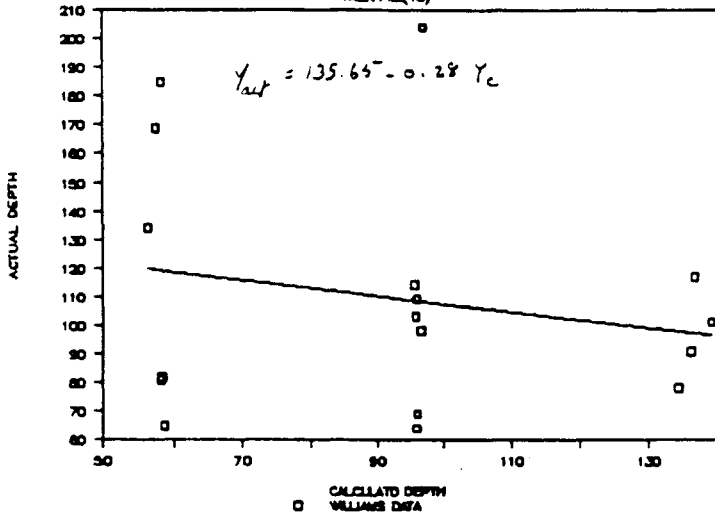
RELATIVE HEIGHT Vs SLOPE

FIGURE (8)



ACTUAL DEPTH Vs CALCULATED DEPTH

YALIN FIG.(10)



APPENDIX I - REFERENCES

- 1) Brownlie, W. R., 1983, Flow depth in sand bed channels, Journal of Hydraulic Engineer., ASCE, vol. 109, no. 7, pp. 671-706.
- 2) Chang, 1988, Fluvial process in river engineering, Pub. John Wiley & Sons.
- 3) Engelund and Hansen, 1967, A monograph on sediment transport in alluvial streams, Copenhagen.
- 4) Fredsoe, J., 1982, Shape and dimension of stationary dunes in rivers, Journal of the Hydraulic Division, ASCE, vol. 108, No. HY8, pp. 932-947.
- 5) Guy, Simons and Richardson, 1966, Summary of alluvial channel data from flume experiments, 1956-1961. U.S. Geological Survey Professional Paper, 462-I.
- 6) Simons and Richardson, 1966, Resistance to flow in alluvial channels. U.S. Geological Survey Professional Paper, 422-J.
- 7) Simons and Senturk, 1977, Sediment transport technology, Water Resources Publications, Fort Collins, CO 80522.
- 8) Vanoni and Brooks, 1957, Laboratory studies of the roughness and suspended load of alluvial streams, sedimentation laboratory, California Institute of Technology, Pasadena, California, Report No. E-68.
- 9) Van Rijn, L. C., 1984, Sediment transport, Part III: bed forms and alluvial roughness, Journal of the Hydraulic Division, ASCE, vol. 110, no. 12, pp. 1733-1754.
- 10) Williams, G. P., 1970, Flume width and water depth effects in sediment-transport experiments, U.S. Geological Survey Professional Paper, 462-H.

APPENDIX II - LIST OF SYMBOLS

u	mean velocity
u_*	shear velocity
u_{*cr}	critical bed-shear velocity for initiation of motion
u_*'	u related to skin friction
R'	R related to skin friction
K_s	Equivalent sand grain roughness
x	Einstein's correction factor
u_*''	u related to bed forms
ψ^1	Dimensionless parameter defined by Einstein
τ_o	Shear stress at bed
γ^s	Specific weight of sediment
d_{50}	Particle size for which 50% of sediment mixture is finer
c	Chez's roughness coefficient
g	Gravitational acceleration
d_{85}	The particle size for which 85% of sediment is finer
D	Flow depth
ΔR	Correction to hydraulic radius
R	Hydraulic radius
q	Unit discharge discharge per unit width
H	Bed form height
L	Bed form length
S	Slope of energy line
S'	Friction of the energy slope required to overcome surface drag.
$\Delta H''$	Friction loss due to bed forms
τ'	Shear stress due to surface drag
τ''	Shear stress due to form drag
T	Specific weight of water
α	Coefficient dependent on flow geometry
ρ	Density of sediment
σg	Geometric standard deviation
d	Median size of sediment

q^+	$q / (gd^3)^{1/2}$
F_g	Grain Froude number
ν	Kinematic viscosity
δ	Laminar sublayer
τ^*	Local dimensionless shear stress
ϑ_c	Critical dimensionless shear stress
ϑ_{top}^*	Dimensionless shear stress at top
ω	Fall velocity of suspended sediment
ϕ_b	Dimensionless bed load transport
ϕ_s	Dimensionless suspended sediment transport
q_b	Bed load sediment transport
q_s	Suspended sediment transport
d_*	Particle parameter
T	Transport stage parameter
v_s	Bed form's travel velocity

AN EXAMINATION OF THE DYNAMIC
LOOP RATING CURVE IN ALLUVIAL RIVERS
By Phil G. Combs

ABSTRACT

The relationship between stage and discharge is one of the most important hydraulic characteristics which is used by engineers, planners, designers, farmers and the general public. The stage-discharge curve relates to the user the stage that corresponds to a particular flow event. The farmer may be interested in the required stage for a specific flow needed to irrigate his fields, the planner may be interested in the stage which corresponds to the 100 year frequency discharge for flood plain management purposes or the engineer may be interested in the stage discharge relationship for a variety of reasons relating to engineering design and analysis. Some engineering considerations for use of rating curves are for providing flood forecasting for the river basins, determining levee heights for flood control studies and conducting studies analyzing the channel changes which are reflected in the stage-discharge rating curve. As is clearly seen the stage-discharge relationship is a very important part of our technical understanding of river channels.

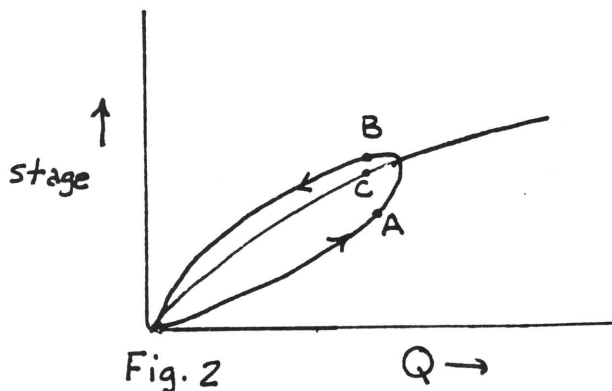
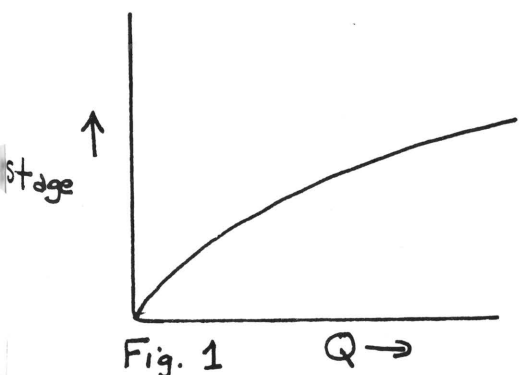
There are several different kinds of stage-discharge rating curves which can be experienced in open channel flow; (1) unique single valued curve, (2) discontinuous and (3) loop rating curve.

This paper is an investigation of the loop rating curve in alluvial channels. The paper presents the findings of an extensive literature review and then an analysis of observed data gathered from two large alluvial rivers (Mississippi and Red Rivers).

INTRODUCTION

The relationship between stage and discharge is one of the most important hydraulic characteristics which is used by engineers, planners, designers, farmers and the general public. This paper will focus upon the engineering application and interpretation of the stage-discharge rating curve. The conceptual rating curve presented in Fig. 1 represents the idealized relationship between stage and discharge- a single valued unique curve. The rating curve may be viewed as a snapshot of the channel reach, hopefully a representative snapshot. It reflects the required stage to pass a particular flow through the channel which implicitly reflects the channel conveyance of the channel reach.

However, in alluvial channels the curve depicted in Fig. 1 is generally not representative. More common to the alluvial channels is the loop or hysteresis curve, which is the subject of this paper.



The loop rating curve depicted in Fig. 2 represents the more common rating curve experienced in alluvial channels. No complete analysis has been found in the literature which has been conducted to determine the causative factors and influences which generate the loop rating curve. This paper will seek to improve the state of the knowledge of the dynamic loop rating by reviewing the previous applicable literature and then analyzing data from the Mississippi and Red Rivers which give significant insight into the loop rating curve.

LITERATURE REVIEW

In evaluating the causative factors of the loop rating curve in alluvial channels it becomes readily apparent that there are four principal factors which must be addressed; (1) dynamic effects, (2) bedform changes and Manning's 'n' changes, (3) temperature effects, and (4) aggradation and degradation of the channel.

Even though temperature is known to affect the stage discharge relationship by changing the kinematic viscosity it will not be specifically addressed in this paper.

Henderson, Jensen, Cunge and others have attributed the loop rating curve to be the result of the dynamic effects of a flood hydrograph. However, none of these writers has included flume or field data to evaluate the completeness of the assumptions for the dynamic control of the rating curve. These three writers utilize the dynamic terms within the St. Venant equation to explain the loop effect. An order of magnitude analysis of the terms of the St. Venant equation revealed that the flatter the bed slope the more impact the dynamic terms will have on the friction slope and correspondingly the more influence it will have on the loop rating curve. This paper is addressing the Red and Mississippi Rivers which have bed slopes flat enough to allow the dynamic terms to be dominant. By considering only the dynamic terms in a rigid boundary channel there are three different depths which can occur in a channel, for a given flow, rising limb depth, falling limb depth and uniform flow depth. This is demonstrated in Fig. 2 by points A, B, and C.

Figure 3 represents observed rating curves for the Mississippi River at Vicksburg, Miss. These observed curves clearly show that the conceptual curve considered by Henderson, Jensen and Cunge is much more simplistic than the rating curves which occur in nature. The observed curves imply that there are more factors to be considered than just the dynamic effects.

Combs and Flowers conducted extensive studies in 1975-1977 evaluating the loop rating curve on the Mississippi River with a fully dynamic wave numerical model (Combs and Flowers, 1977, and U.S. Corps of Engineers, 1977). These studies were conducted to determine whether the loop effect could be simulated numerically. These studies found that the Manning's 'n' value decreased as the stage increased, decreasing from .028 to .016. As the 1973 hydrograph was routed through the numerical model it computed a rating curve at Vicksburg which reproduced the observed rating curve on the rising limb of the hydrograph but fell below the observed rating curve on the recession of the hydrograph, as demonstrated on Fig. 4. In order to reproduce the rising and falling limbs of the hydrograph two sets of 'n' values had to be used, Figs. 5-6. It should be noted that the loop rating curve produced by using the rising limb 'n' values was generally about one half the size of the observed loop (computed loop was about 1.0-1.2 ft. and the observed loop was about 2.0-2.5 ft.). Thus in addition to the dynamic effects which were fully reproduced, there were other factors influencing the loop effect. The higher 'n' values on the recession limb of the hydrograph implied that the greater roughness was due to a combination of

increased roughness due to bed forms and/or channel geometry changes. Combs and Flowers did not attempt to identify the causative factors influencing the loop rating curve besides the dynamic effects.

We will now consider the effect of the resistance to flow on the loop rating curve in alluvial channels. Several writers (Brooks, Vanoni and Brooks, Einstein and Ning Chien and Simons and Richardson) have investigated the grain and form roughness of alluvial channels and the relationship of velocity, depth, and slope to the form of roughness. We will turn our attention to the findings of Simons and Richardson(1960,1961), Simons, Richardson and Haushild(1962), Colby(1960) and Dawdy(1961). These works are representative of the state of the knowledge of the relationship of the stage-discharge curve to resistance to flow.

The form of bed roughness in alluvial channels is a function of the sediment characteristics and the flow characteristics. The bed configuration can be changed by altering either the discharge(which affects the depth), slope, temperature or the bed material size distribution. (Simons and Richardson, 1960)

In considering the case of a hysteresis effect reflected in the stage-discharge curve Simons and Richardson, 1961 stated that "... the magnitude of resistance to flow lags the actual discharge, that is, the change of bed roughness lags the change of discharge. This results in a smaller resistance to flow and smaller depth than would normally occur for equilibrium flow. The reverse occurs on the falling stage."

It has been shown with documented evidence for gentle bed sloped alluvial channels that the loop rating curve is significantly influenced by the dynamic terms in the St. Venant equation and by the bed forms and channel roughness. Unfortunately the only known dynamic studies on a natural channel is the work of Combs and Flowers. Similarly there is not an extensive amount of information or published literature on alluvial channel bed forms and channel roughness.

Another important factor influencing the loop rating curve is the change in channel geometry throughout a hydrograph. There is no known literature which addresses specifically the aggradation and degradation which occurs throughout a channel reach within a hydrograph. However, it is known that generally the bends scour in high flow and the crossings aggrade, while in low flow this trend is reversed. The data which follows from the Red River provides definitive evidence that the aggradation/degradation processes are more complex than the broad generalization.

DATA COLLECTION AND ANALYSIS

Analysis of stream gaging data collected on the Red River was conducted to aid in evaluating the causative factors of the loop rating curve. The study reach of the Red River is located in central Louisiana in the vicinity of Alexandria, La., realigned miles 43-90. Discharge and suspended sediment samples are collected on a regular basis at Alexandria, La.

The 1989 flow on the Red River was high which was reason to intensify the stream gaging data collection. During the high flow periods discharge was measured on a daily basis in order to accurately determine the flow rate, (see Table 1).

Additionally, during 1989 longitudinal thalweg profiles were obtained for reaches along the Red River from Alexandria downstream to Lock and Dam 1, approx. 47 miles. These profiles were conducted from a moving boat profiling the thalweg continuously along the reach. The profiles reflect depth of flow and by inspection and interpretation the type and magnitude of bed forms present throughout the reach may be determined. The boat

profiles are uncontrolled surveys, but location can be determined relatively accurately by markings made on the profile scrolls by the technicians indicating land markings or river mile markers. The profiles represent thalweg surveys and since the same operators and technicians obtained all the data it is reasonable to assume the surveys were obtained in a consistent manner.

Rating Curve Analysis

The 1989 flow hydrograph, Fig. 7 and Table 1, was quite unusual in that there were three highwater events experienced at Alexandria, La all of which closely approximated the 10 year frequency flow, 145,000 cfs. Note that the first event occurred in February, while the second event occurred at the end of May and the third event occurred at the beginning of July. The second event was clearly independent of the first while the third event occurred before the river had returned to base flow from the second event.

Figure 8 represents the rating curve reflecting the 1989 flow conditions. The lower loop represents the first flood event, while the second and third flood events are represented by the two higher loops respectively. The first rise had a loop of approximately 1.5 ft. while the second and third flood events had loops of 1.6 and 3.0 ft. respectively. These three loops in the rating curve are reason to be alarmed that the channel is changing conveyance. Each of the successive flood events is higher than the previous loop rating curve. As seen from analysis of Fig. 8 the second flood event peaked 3.5 ft. above the first peak and the third peak occurred 4.0 ft. above the second peak or a total of 7.5 ft. above the first peak. None of the literature has ever addressed this phenomenon but an analysis of the stream gaging data will be conducted in order to gain insight into the channel processes. The dynamic and bedform roughness changes appear to be producing the three individual loops.

It has been shown that the dynamic effects and the bed form roughness changes influence the magnitude of the loop rating curve. It would require development of a dynamic routing model to clearly identify the portion of the loop effects experienced at Alexandria, La in 1989 and to make judgments on the change in the bed form roughness. However, considerable insight will be gained by analysis of the stream gaging, sediment and longitudinal profile data gathered throughout the highwater period on the Red River.

Area vs. Discharge

Evaluation of the discharge and the corresponding cross sectional area for each measurement provides evidence whether there is a constant or variable relationship between the two variables. Fig. 9 gives a clear indication that the Q vs. Area relationship remains virtually constant throughout the hydrograph, while the Q vs. Stage varies as much as 7.5 feet. This data implies that if the Q vs. Area is constant and the Q vs. Stage is rising that the channel must be aggrading to compensate for the rise in stage.

Bed Elevation vs. Q

An analysis was then conducted to determine how the bed elevation varied with discharge. The analyses consisted of evaluating the bed elevation derived from the gaging station at Alexandria and evaluation of the longitudinal profiles. Both data sets indicated a similar relationship. There is a clear indication that the bed is higher for each successive flood event. Figures 10-12 reflect the change in bed elevation

corresponding discharge values.

The longitudinal profiles were begun on 26 May 1989 and continued throughout the remainder of 1989. The typical reach selected is located at river miles 55-59.5, realigned mileage. This reach was selected since it has a gage located on the Moncla Bridge at the upper end of the reach, and water surface elevation and slope could be easily be determined. Additionally, the reach is considered to be a typical reach of the lower Red River. Figs. 13-17 are copies of the longitudinal profiles in the general vicinity of the typical reach. From review of the profiles for the same dates it becomes obvious that the boat traversed the reach at different speeds. This was due primarily to the channel velocity.

Examination of the profiles indicates the following:

Date of Survey	Representative Bed Elevation, NGVD
26 May 1989	18
7 July 1989	29
22 July 1989	27
25 Sep 1989	20
10 Oct 1989	21

The representative bed elevation was determined by visually recognizing an elevation which represents the reach. No attempt was made to average or to develop a regression analysis to determine the representative bed elevation. For the purposes of this analysis the visual method was adequate to reflect trends of aggradation and degradation. As clearly obvious these profiles reflect the same aggradation trends as seen in Figs. 13-17. The bed aggrades approximately 11 feet from the second flood event to the third event and thereafter degrades back to an elevation of about 20 feet NGVD. Therefore, the data derived from the cross sections at the gaging station were representative of the channel reach. This conclusion verifies one of the assumptions in the introduction that the rating curve is representative of the channel reach.

Bed Forms

These profiles may also be used to study the channel bed forms. Review of Fig. 13, which is the longitudinal profile for 26 May, reveals that the bed is composed of small dunes in the range of 2-4 feet in height. Whereas, Fig. 14, representing 7 July, indicates dunes ranging in height from 5-8 feet and similarly for 22 July, Fig. 15, indicates dunes varying in height from 3-10 feet. The vast majority of the latter dunes are more than 5 feet in height. Then on Fig. 16 the profile indicates dunes or ripples about 2-3 feet in height. Finally, Fig. 17 for 10 Oct shows ripples or dunes being about 2-2.5 feet in height. It is difficult to discern whether the latter two profiles indicate ripples, dunes or a combination. The general height of the dunes tends to correlate with the discharge, Table 1. It is noteworthy that the bed forms do not diminish in magnitude with increasing flow, as found by Simons and Richardson in alluvial channels and some channels which have steeper slopes than the Red River. At this time it is difficult to determine what influence the bed forms had on the rating curve. Additional study would be necessary with a numerical model to differentiate the effects caused by the bed form changes.

Shields Parameter and Unit Stream Power

An analysis was conducted of the typical reach data and the discharge measurements to evaluate the Shields parameter and to compute the unit

stream power. Table 2 is a compilation of data derived from the discharge measurements and the longitudinal profiles. The grain Reynolds number, R^* , and the Shields parameter, τ_* , were computed to determine whether the hydraulic conditions could be classified laminar, transition or fully turbulent. The corresponding theoretical bed forms for these three hydraulic conditions are ripples, transitional ripples/dunes or dunes, respectively. Note that all the data indicate a R^* less than 15 which is all within the transition zone between ripples and dunes. These computations were made using a constant slope of 0.00009 ft./ft. Even though it is known that the slope was not constant throughout the hydrograph, it would not have materially changed the R^* values.

Five different bed form predictors were used to determine suitability predicting bed forms in the Red River. Tables 1 and 2 contain the data and variables used for the bed form predictors. None of the bed form predictors accurately predicted the observed bed forms. The Simons and Chardson method predicted antidunes and the Albertson method predicted transition between dunes and antidunes. The values of the variables for other predictors fell off the scales and could not make a prediction of the bed forms.

It is obvious that in the large rivers such as the Red River significant research needs to be performed to develop a dependable bed form predictor. These bed form predictors would greatly enhance the capability to estimate the channel roughness values throughout a hydrograph.

SUMMARY

It has been shown that the loop rating curve for the alluvial channels considered in this paper is sensitive to the dynamic effects of the hydrograph, the bed form and grain roughness changes and also to the aggradation/degradation changes in the channel bed. As a result it is more appropriate to refer to the loop rating curve as the dynamic loop rating curve. This more closely identifies that it is dynamic in nature.

There is no known literature that has identified the aggradational processes which have been shown to occur on the Red River. This data set not only provides insight into the hydraulic and sediment transport processes, but will serve as a means for improving our analysis of stream rating data.

RECOMMENDATIONS

The following are recommendations based upon the studies and findings of the research conducted for this paper:

- 1. Develop a 1-D unsteady flow model with an uncoupled sediment transport capability, allowing for aggradation and/or degradation.
- 2. Conduct studies to allow development of dependable bed form predictors for the large alluvial rivers such as Red and Mississippi Rivers.
- 3. In analyzing rating curves and developing specific gage records for rivers similar to the Red River a more thorough understanding of the channel processes and the interrelationship with the hydrographs should be obtained.
- 4. Research should be conducted on other large alluvial rivers to ascertain whether the findings of this paper are representative. Such research could result in general methods or data analysis techniques to provide insight into channel processes to aid in flood forecasting or similar activities.

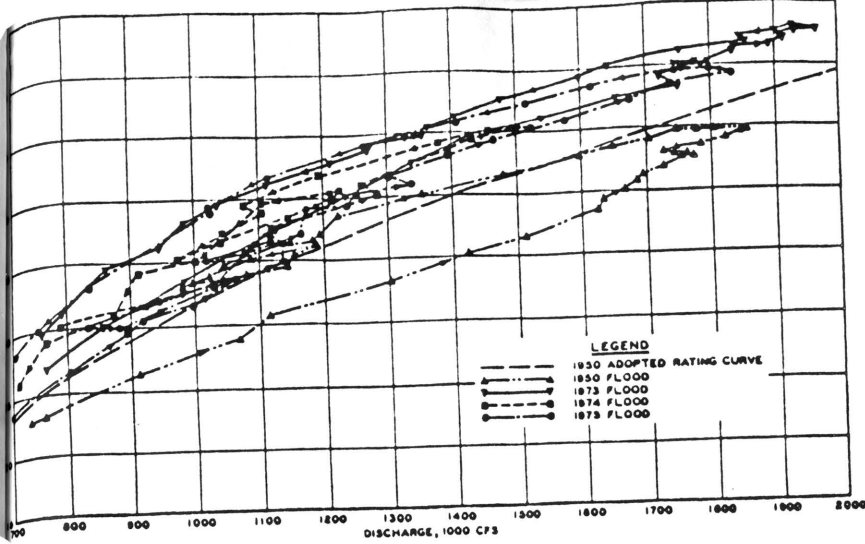


Figure 3

DYNAMIC LOOP EFFECT
VICKSBURG-RECENT FLOODS
MEASURED RATING CURVES

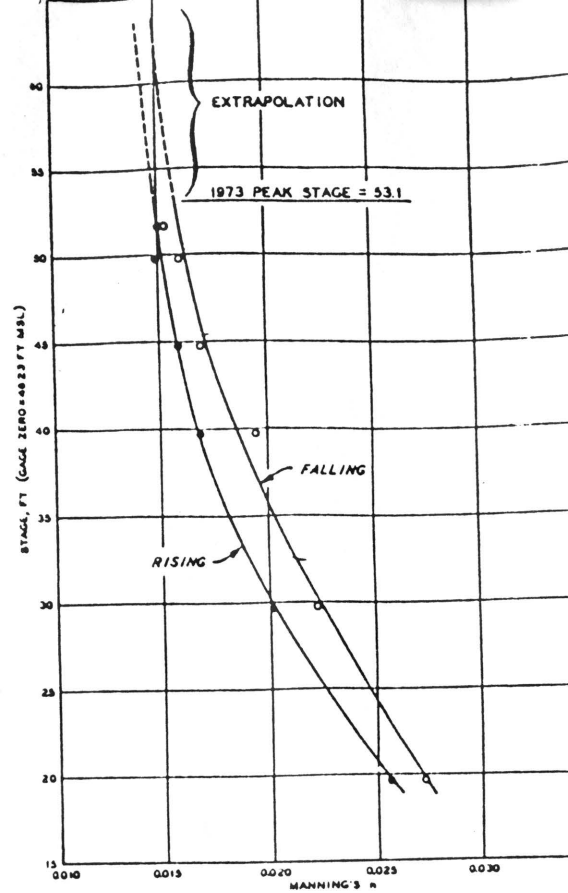


Figure 6

DYNAMIC LOOP EFFECT
VICKSBURG - 1973 FLOOD
EXTRAPOLATION OF
CHANNEL ROUGHNESS

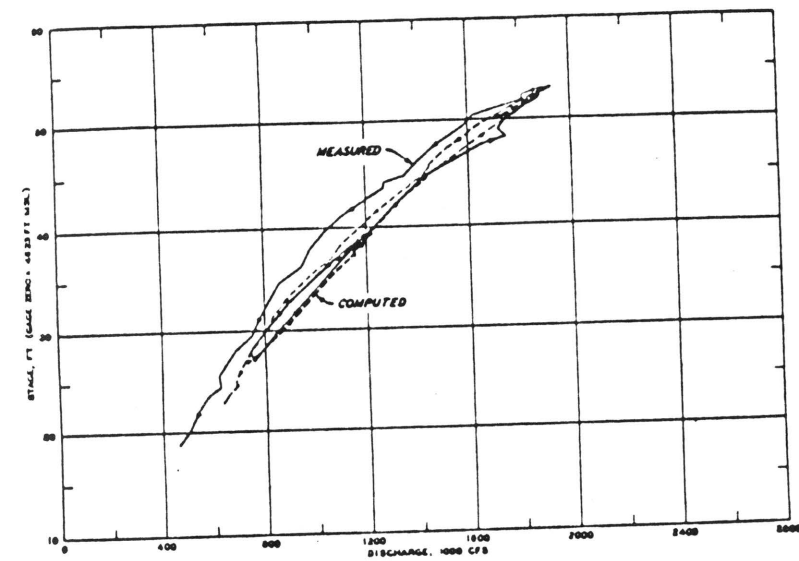


Figure 4

DYNAMIC LOOP EFFECT
VICKSBURG - 1973 FLOOD
COMPUTED RATING CURVE
USING SINGLE VALUED
MANNING'S n IN MODEL

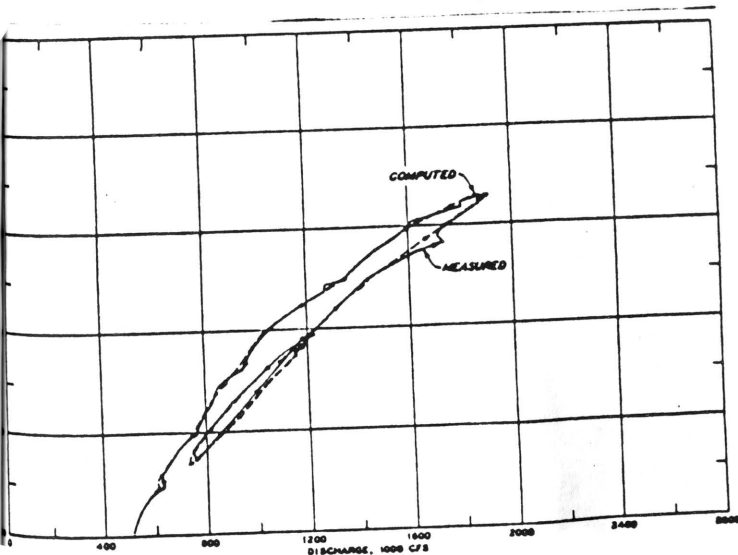


Figure 5

DYNAMIC LOOP EFFECT
VICKSBURG - 1973 FLOOD
COMPUTED RATING CURVE
USING DOUBLE VALUED
MANNING'S n IN MODEL

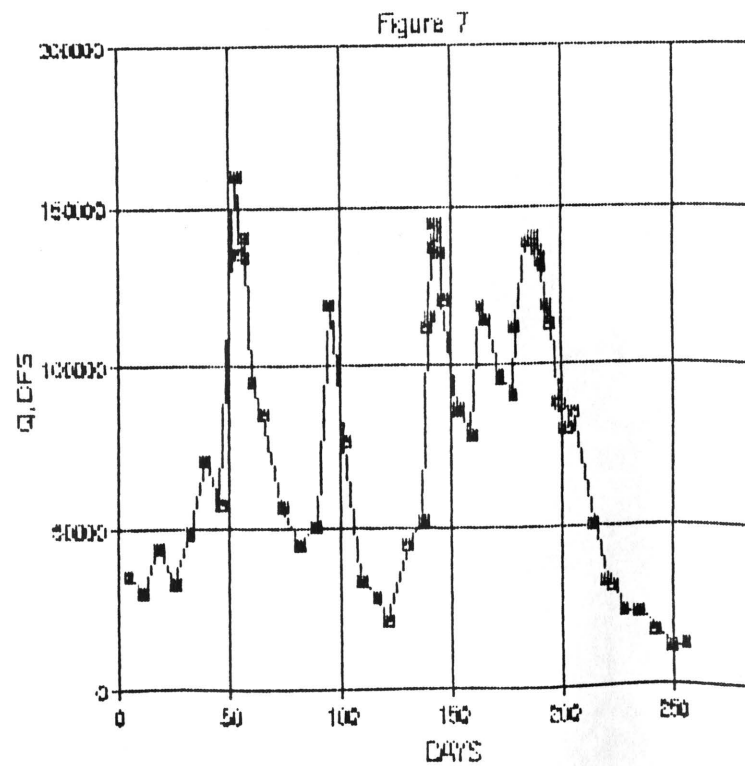


Figure 7

Figure 8

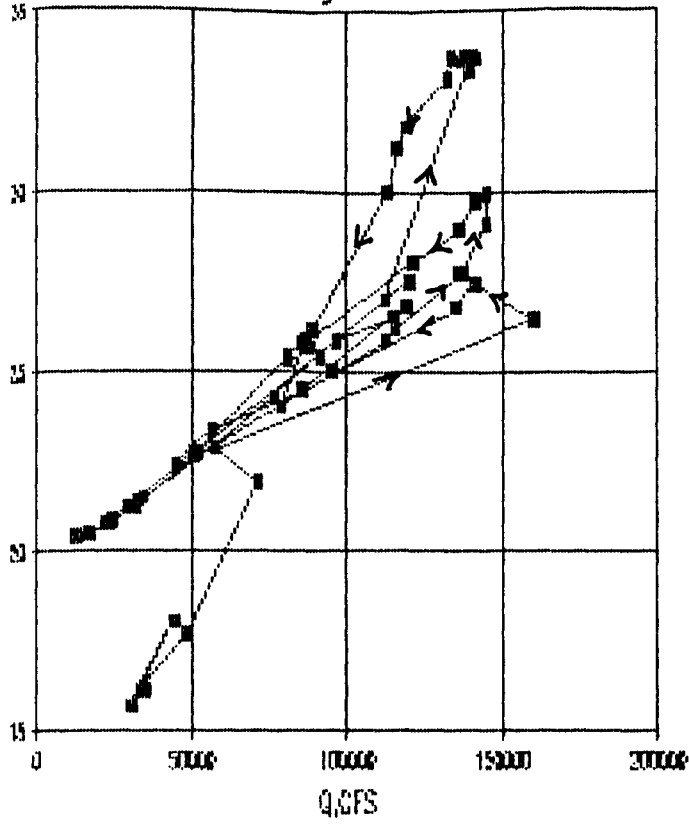


Figure 9

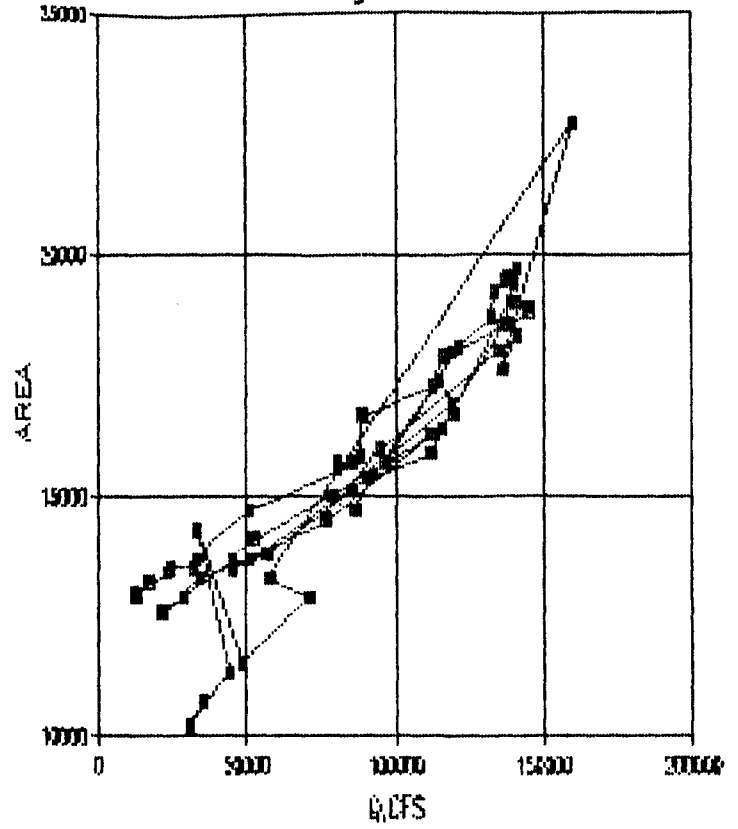


Figure 10

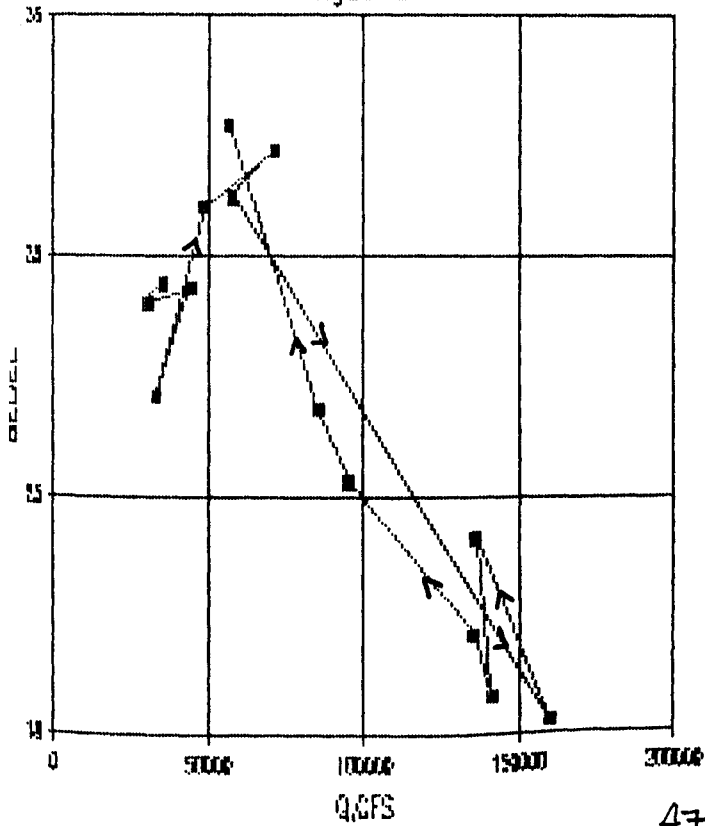


Figure 11

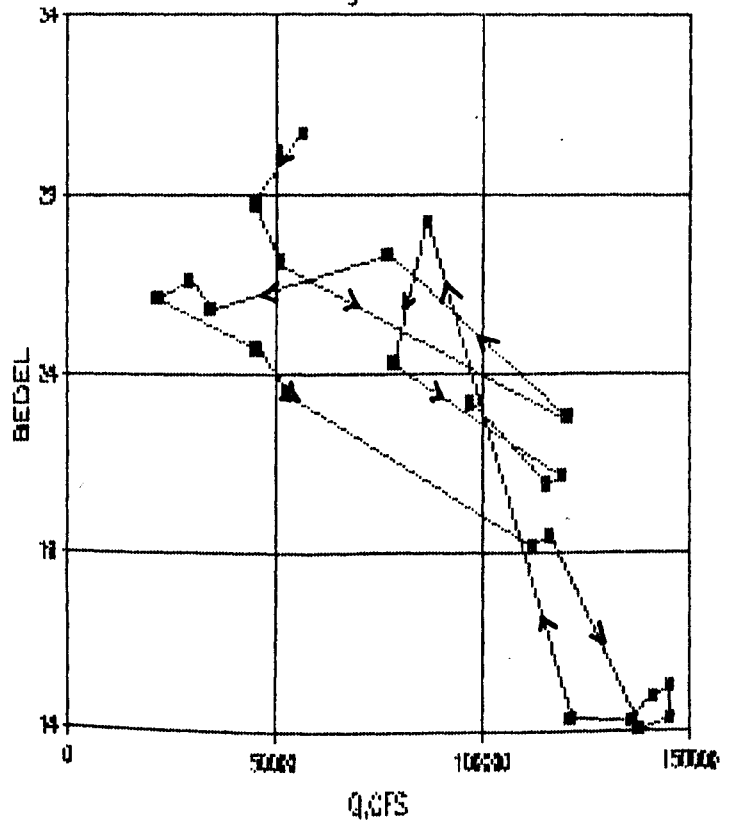


Figure 12

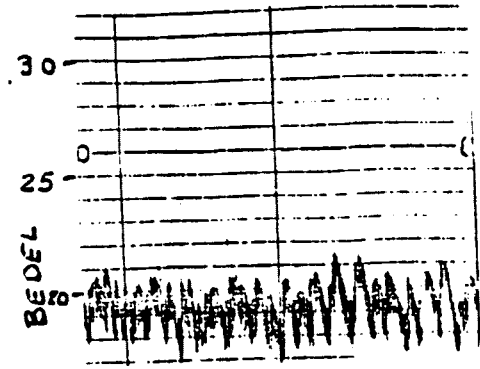
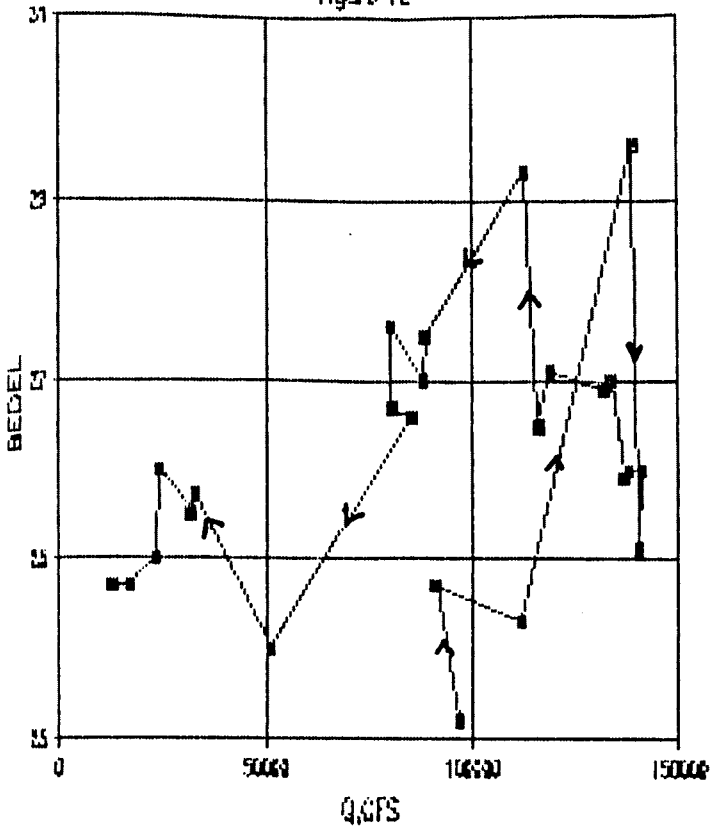


Figure 13 26 May 1989

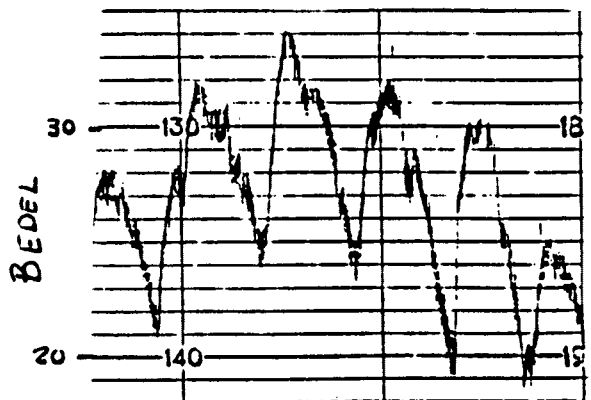


Figure 14 7 July 1989

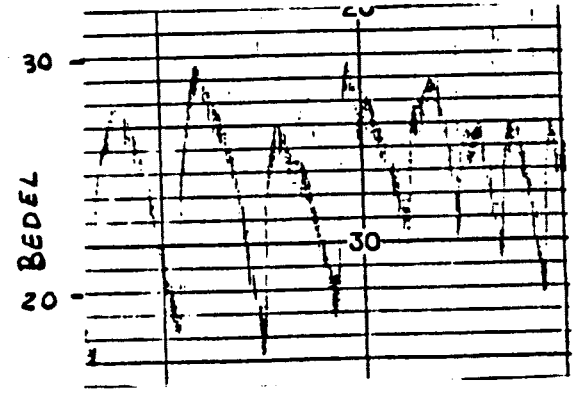


Figure 15 22 July 1989

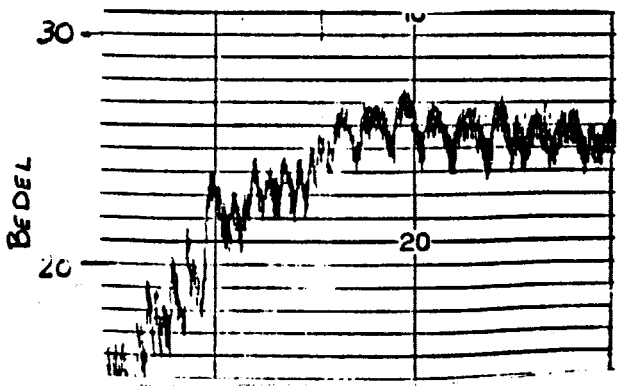


Figure 16 25 Sep. 1989

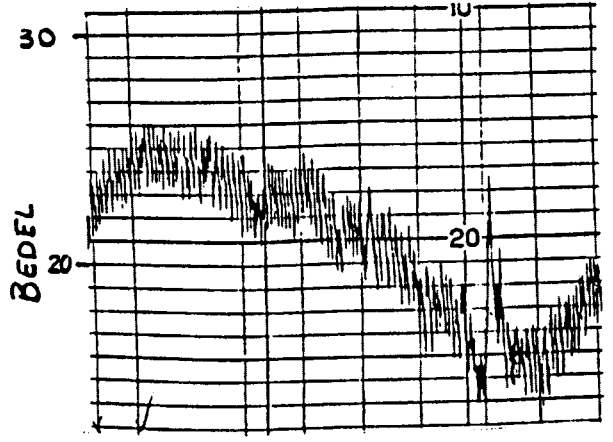


Figure 17 10 Oct. 1989

DATE	STAGE	Q,CFS	AREA	BEDEL	AVG. VEL	WIDTH	DEPTH	FROUDE	SHR.STR.	POWER
4JAN	16.1	35400	10700	27.4	3.31	437	24.5	.12	.14	.46
11JAN	15.7	30600	10200	27	3	434	23.5	.11	.13	.39
18JAN	18.03	44300	11300	27.3	3.92	438	25.8	.14	.14	.55
25JAN	16.1	33100	14300	25.1	2.31	508	28.1	.08	.16	.37
1FEB	17.7	48700	11500	29	4.23	440	26.1	.15	.15	.63
8FEB	21.9	71200	12900	30.2	5.52	450	28.7	.18	.16	.88
15FEB	22.88	57800	13300	29.2	4.32	452	29.4	.14	.17	.73
22FEB	26.46	160000	22700	18.3	7.05	565	40.2	.2	.23	1.62
24FEB	27.76	136000	17600	22.1	7.73	514	34.2	.23	.19	1.47
25FEB	27.45	141000	18300	18.8	7.7	511	35.8	.23	.2	1.54
26FEB	26.8	135000	18000	20.1	7.5	514	35	.22	.2	1.5
1MAR	25	95100	16000	23.3	5.94	505	31.7	.19	.18	1.07
6MAR	24.49	85300	15100	24.8	5.65	488	30.9	.18	.17	.96
15MAR	23.36	56700	13800	30.7	4.18	452	30.5	.13	.17	.71
22MAR	22.4	45000	13500	28.7	3.41	451	29.9	.11	.17	.58
30MAR	22.8	50800	13700	27.1	3.71	482	28.4	.12	.16	.59
5APR	27.53	120000	16700	22.8	7.19	499	33.5	.22	.19	1.37
12APR	24.27	76700	14500	27.3	5.29	485	29.9	.17	.17	.9
19APR	21.52	34100	13300	25.8	2.56	441	30.2	.08	.17	.44
26APR	21.29	29000	12900	26.6	2.25	440	29.3	.07	.16	.36
1MAY	20.8	21500	12600	26.1	1.71	439	28.7	.06	.16	.27
10MAY	22.36	45200	13700	24.7	3.3	442	31	.1	.17	.56
17MAY	22.73	52400	14100	23.5	3.72	476	29.6	.12	.17	.63
19MAY	25.9	112000	16300	19.2	6.8	484	33.7	.21	.19	1.29
20MAY	26.2	115700	16400	19.5	7.05	486	33.7	.21	.19	1.34
21MAY	27.75	137500	18550	14.1	7.41	491	37.8	.21	.21	1.56
22MAY	29.1	145000	18800	14.4	7.71	492	38.2	.22	.21	1.62
23MAY	29.95	145000	18900	15.3	7.67	494	38.3	.22	.22	1.69
24MAY	29.71	141200	19000	15	7.43	504	37.7	.21	.21	1.56
25MAY	28.95	136000	18500	14.3	7.34	491	37.7	.21	.21	1.54
26MAY	28.05	121000	18070	14.4	6.7	490	36.9	.19	.21	1.41
2JUN	25.87	86500	14700	28.2	5.88	448	32.8	.18	.18	1.06
8JUN	24.01	78400	15000	24.3	5.23	446	33.6	.16	.19	.99
12JUN	26.85	119000	16900	21.2	7.04	453	37.3	.2	.21	1.48
15JUN	26.56	115000	17400	20.9	6.61	503	34.6	.2	.19	1.26
21JUN	25.86	96600	15700	23.2	6.15	449	35	.18	.2	1.23
27JUN	25.41	91000	15400	24.7	5.9	448	34.4	.18	.19	1.12
28JUN	27.01	112000	15900	24.3	7.04	449	35.4	.21	.2	1.41
3JUL	33.33	139000	19000	29.6	7.32	528	36	.22	.2	1.46
5JUL	33.75	140200	19400	25.1	7.23	555	35	.22	.2	1.45
6JUL	33.66	141000	19700	26	7.16	555	35.5	.22	.2	1.43
7JUL	33.7	137900	19500	26	7.07	555	35.1	.21	.2	1.41
8JUL	33.59	136800	19450	25.9	6.99	555	35	.21	.2	1.4
9JUL	33.69	133600	19200	27	6.96	555	34.6	.21	.19	1.32
10JUL	33.08	132000	18700	26.9	7.06	522	35.8	.21	.2	1.41
12JUL	31.78	119000	18000	27.1	6.61	535	33.6	.2	.19	1.26
13JUL	31.23	116000	17900	26.5	6.48	513	34.9	.19	.2	1.3
14JUL	30	112800	17300	29.3	6.52	525	33	.2	.19	1.24
17JUL	26.15	88600	16650	27.5	5.32	521	32	.17	.18	.96
18JUL	25.65	88100	15800	27	5.58	515	30.7	.18	.17	.95
19JUL	25.3	80400	15600	27.6	5.15	515	30.3	.16	.17	.88
21JUL	25.38	80600	15700	26.7	5.13	515	30.5	.16	.17	.87
24JUL	25.78	85500	15700	26.6	5.45	505	31.1	.17	.17	.93
2AUG	22.66	50900	14700	24	3.46	485	30.3	.11	.17	.59
8AUG	21.43	32900	13700	25.7	2.4	472	29	.08	.16	.38
11AUG	21.22	31800	13500	25.5	2.36	470	28.7	.08	.16	.38
16AUG	20.87	24300	13500	26	1.8	469	28.8	.06	.16	.29
23AUG	20.74	23400	13400	25	1.75	470	28.8	.06	.16	.28
30AUG	20.49	17100	13200	24.7	1.3	463	28.8	.04	.16	.21
6SEP	20.39	12300	13000	24.7	.95	470	28.8	.03	.16	.15
13SEP	20.39	12800	12900	24.7	.99	469	28.8	.03	.16	.16

0
0

Table 2
RED RIVER BED FORM ANALYSIS 1989 FLOW CONDITIONS

DATE	Q, CFS	BEDFORM	HEIGHT	DEPTH	KINVIS	R*	TAU*
26MAY	121000	DUNES	2,4		42 .0000109	10.51	6.98
7JUL	143000	DUNES	5,8		44 .0000093	12.59	7.32
11JUL	138000	DUNES	3,7	43.9	.0000091	12.86	7.3
14JUL	130000	DUNES	3,7	41.4	.0000091	12.48	6.88
15JUL	127000	DUNES	3,7	41.3	.0000091	12.47	6.87
16JUL	108000	DUNES	2,5	39.8	.0000091	12.24	6.62
17JUL	98800	DUNES	2,5	38.6	.0000091	12.06	6.42
18JUL	94700	DUNES	2,5	36.2	.0000091	11.67	6.02
19JUL	94000	DUNES	2,5	36.2	.0000091	11.67	6.02
22JUL	91800	DUNES	3,10	36.6	.0000091	11.74	6.09
23JUL	91500	DUNES	3,5	37	.0000091	11.8	6.15
24JUL	91000	DUNES	3,8	37.7	.0000093	11.66	6.27
25JUL	94000	DUNES	4,7	38	.0000105	10.4	6.32
26JUL	97100	DUNES	2,7	38.6	.0000104	10.6	6.42
28JUL	89500	DUNES	2,6	38.7	.0000101	10.86	6.44
31JUL	59600	DUNES	2,5	36.7	.0000101	10.58	6.1
2AUG	62000	DUNES	2,5	35.5	.0000101	10.41	5.9
3AUG	54800	DUNES	2,4	35.7	.0000101	10.44	5.94
4AUG	49600	RIP/DUN	2,4	35.3	.0000093	11.28	5.87
7AUG	36600	RIP/DUN	2,3	33.9	.0000101	10.22	5.64
14AUG	27000	RIP/DUN	2,3	31	.0000093	10.57	5.16
28AUG	24700	RIP/DUN	2,3	29.1	.0000092	10.35	4.84
11SEP	12000	RIP/DUN	2,3	26.8	.0000093	9.83	4.46
25SEP	13000	RIP/DUN	2,3	26.8	.0000108	8.5	4.46
10OCT	14300	RIP/DUN	2,2.5	26.9	.0000104	8.77	4.47

REFERENCES

- ks, Norman H.(1955), 'Mechanics of Streams with Movable Beds of Fine', with discussion, Transactions of the American Society of Civil Engineers, vol.123, 1958, p. 526-594.
- y, Bruce R.(1960), 'Discontinuous Rating Curves, for Pigeon Roost and Tawa Creeks, Mississippi, U.S. Dept. Agriculture, Agriculture Research Service 41-36,p.31.
- s, Phil G. and Flowers, Don(1977), 'A Study of the Dynamic Rating Curves of the Mississippi River', Proceedings of the Mississippi Water Resources Conference, Mississippi Water Resource Research Institute, Mississippi, Miss.
- e, Jean A.(1975), 'Applied Mathematical Modeling of Open Channel Flow', in Mahmood,K. and Yevjevich,V.(Ed.), Unsteady Flow in Open Channels, Ch. 10, Water Resource Publications, Ft. Collins,Co.
- y, David R.(1961), 'Depth-Discharge Relations of Alluvial Streams - Discontinuous Rating Curves', U.S. Geological Survey Water Supply Paper 1450-C,p.16.
- erson, F.M.(1966), 'Open Channel Flow',p.391-394, Macmillan Company, New York.
- en,P.Ph., Bendegom, L.van, Berg,J.vanden, deVries, M., and van, A.(Ed.)(1979), 'Principles of River Engineering, the non-tidal river', Pittman Publishing, London.
- ons,D.B., and Richardson,E.V.(1961), 'Forms of Bed Roughness in Alluvial Channels', Journal of Hyd Div, American Society of Civil Engineers, No. HY5, May1961, p.87-105.
- ons,D.B., and Richardson,E.V.(1960), 'Resistance to Flow in Alluvial Channels', Journal of Hyd Div, American Society of Civil Engineers, HY5, May1960, p.73-99.
- ons,D.B., Richardson,E.V. and Haushild,W.L.(1962), 'Depth-Discharge Relations in Alluvial Channels', Journal of Hyd Div, American Society of Civil Engineers, HY5, Sep1962, p.57-73.
- . Army Corps of Engineers, Vicksburg District(1977), 'Dynamic Loop Method'.
- oni, Vito A. and Brooks, Norman H.(1957), 'Laboratory Studies of the Bed Roughness and Suspended Load of Alluvial Streams', Report No.E-68, Hydraulics Laboratory California Institute of Technology.

Scour Downstream of Hydraulic Structures

(Historical Perspective and Analytic Critique)

By T. K. Burke¹

Abstract: This paper presents an overview of some of the more important derivations of scour depth that have been proposed over the last seventy years. Some of the factors that have gone into these equations are discussed, and their limitations are analyzed. Three of these equations are then compared with a theoretical equation proposed by Bormann. All of these equations are compared to measured model data taken by Bormann during exhaustive testing program.

Introduction

Scour occurring downstream of hydraulic structures has traditionally been a problem to all hydraulic engineers trying to control the flow depth, grade, or alignment of rivers and streams. A good definition of scour has been defined by Emmett Laursen as "...the enlargement of a flow section by the removal of material composing the boundary through the action of the fluid in motion." This definition is particularly applicable to scour downstream of a hydraulic structure because a scour hole downstream of a structure is often quite well defined. The potential for scour is inherent in hydraulic structure design by the very nature of the structure modifying the flow path of the water. The proper analysis and determination of the potential scour depth is extremely important in order to ensure the stability of the structure, downstream facilities, and preserve human life. In addition to the normal scour which may be caused by the tractive force of the prevailing flow, additional scour downstream of a structure is often caused by the turbulence resulting from the accelerating and changing flow path of the water. A total understanding of the nature of scour downstream of structures still eludes engineers, but through careful model studies along with an increased understanding of turbulence and sediment transport we have been able to propose several empirical equations to predict scour and compensate for its devastating consequences. These equations although accurate for the structure and geological conditions represented by that particular model, are not easily transferable to other structures or locations. Recently though, researchers have been concentrating not on modeling a particular structure, but on modeling the physics of scour in general. It is hoped that the results of these studies are general enough to be transferred to other structures and geological conditions. It is the purpose of this paper to follow some of the more important developments in scour analysis, and make a comparative analysis of the equations developed from these studies.

General Analysis

Typically flow is accelerated as it flows over a control structure. This accelerated flow can separate from the structure forming a free jet, or the flow can remain attached to the floor

¹Member ASCE; Fellow, Center for Excellence in the Geosciences, Colorado State University, Fort Collins Colorado 80521.

of the structure and is referred to as a wall jet. Figure 1 and 2 show examples of these different types of jets.

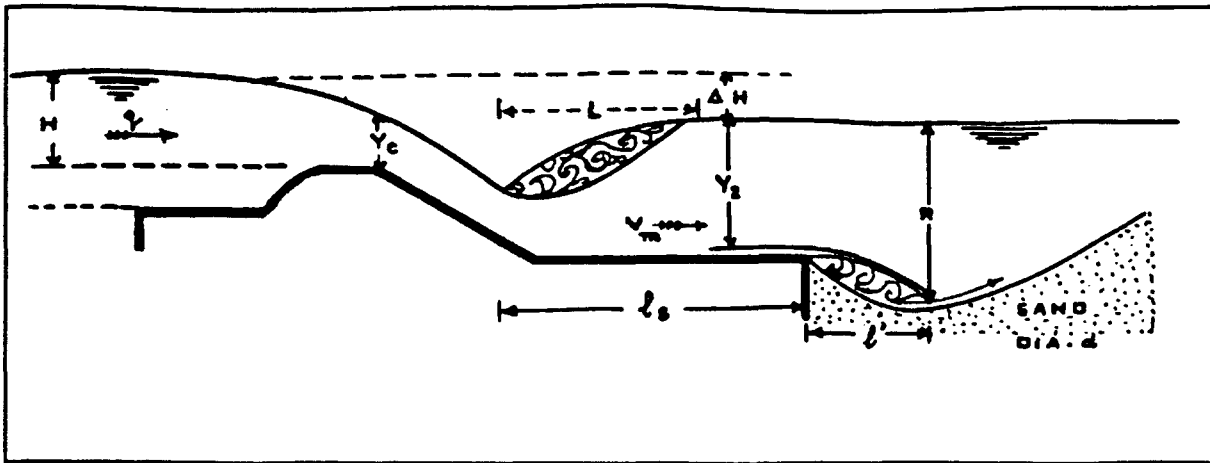


Figure 1 Attached Wall Jet

In the case of the free jet, scour is formed by the impinging jet on the surface of the unprotected bed material. For a free jet to occur, the underside of the nappe must be at atmospheric pressure. If the jet does not separate from the face of the structure or if the nape of the jet is not at atmospheric pressure, the jet is deemed a wall jet. In a wall jet the path of the jet is effected by the vortex under the nape. This vortex tends to pull the jet down towards the face of the structure. A third significant case to be studied is that of flow coming off an apron after a hydraulic jump. In this case scour is initiated by the highly turbulent flow coming out of the jump and inversion of the velocity profile along the bed. It has been observed that flows exiting from a hydraulic jump tend to have higher velocities near the bed and lower velocities near the surface.

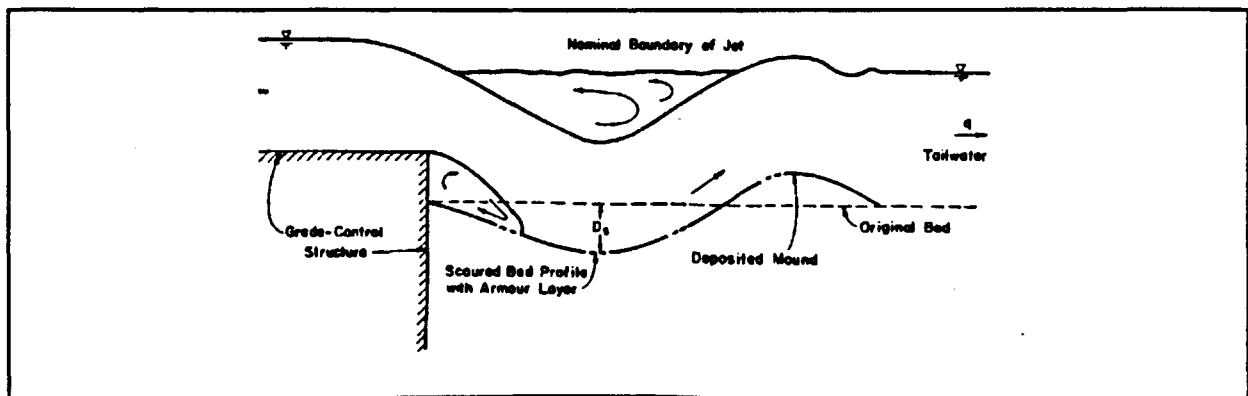


Figure 2 Free Overfall Jet

The erosion process in a scour hole continues until the hydrodynamic forces in the jet are diffused to the point that particle motion can no longer be maintained. The bed material that is scoured is carried down stream and deposited on the existing bed where the sediment transport capacity can no longer support the eroded material. This often leads to a graded deposition of material downstream of the scour hole. The larger material is deposited first

with the finer material carried downstream until it falls out. That process can be observed in figure 2.

In the analysis of scour downstream of hydraulic structures Bormann identified 4 separate processes that are significant to the problem.

1. The path of the jet in the tailwater,
2. The determination of the jet diffusion so as to allow computation of the velocity on the surface of the bed.
3. Relate the velocity at the bed to the initiation of motion of the bed material in the scour hole,
4. Analysis of the particle stability in the scour hole so as to determine the maximum scour hole depth.

Many of the scour studies for the analysis of prototypes under particular conditions specific one location tend to only answer 1, and 4 from above, and even though only for that particular model and prototype. It has only been recently that studies into the nature of jet impingement and the resulting velocity along the bed boundary have been investigated. Figure 2 taken from Bormann, shows a schematic of a free overfall jet. As the flow leaves the crest of the drop structure, it forms a free jet. As this free jet enters the water shear along the surface of the jet generates turbulence in the edge of the jet and in the surrounding water. The turbulent eddies penetrate into the jet as the distance from the crest increases. As the turbulence penetrates the jet it causes the jet to diffuse. As the turbulence reaches the center of the jet it begins to reduce the maximum velocity of the jet. This distance is referred to as the flow establishment distance S_0 and can be seen in figure 3. The jet continues to diffuse until it approaches the bed boundary. When it nears the boundary the pressure begins to increase as the flow is forced to deflect parallel to the bed surface. The pressure increase which is related to the impingement velocity can be quantified by the equation of motion. The flow is accelerated after the jet impinges on the boundary. This accelerated flow is the discharge which causes the bed to scour. The shear stress on the bed resulting from this accelerated flow, if greater than the critical shear stress, will cause displacement of the bed material. This bed scour rate decreases with time in a logarithmic fashion until equilibrium of critical shear stress for the particles and applied shear stress of the fluid are equal. This equilibrium can be reached either by a deepening of the scour hole which allows the jet velocity to be diffused below the critical value, or armoring of the scour hole by larger bed particles.

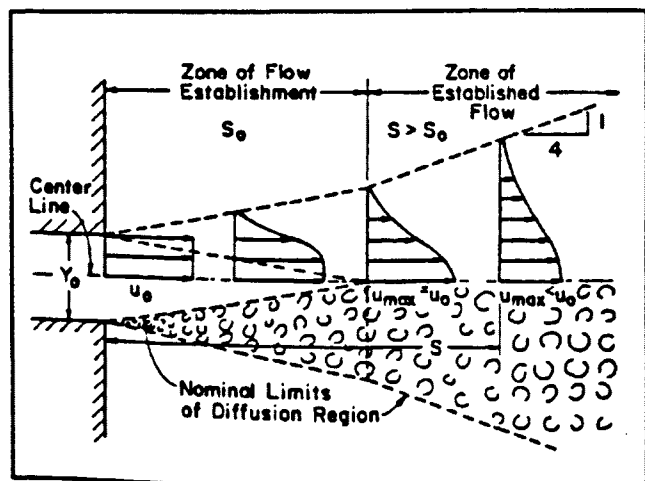


Figure 3 Jet Diffusion

Bed material can be removed from the

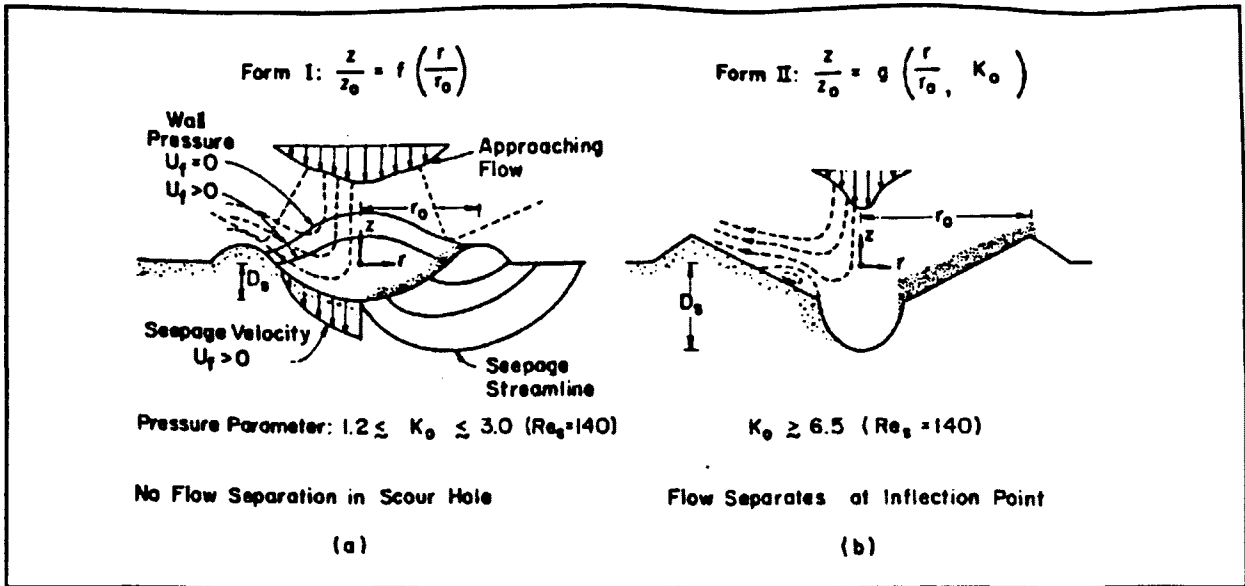


Figure 4 Forms of scour holes Bormann

scour hole as either suspended load or as bed load. A vertically impinging jet generally moves bed material by suspension. In this type of scour bed material will continue to be removed until the vertical component of the deflected jet velocity is equal to or greater than the fall velocity of the bed material. For jet impingement angles other than vertical the scour is a result of suspended load and bed load. Figure 4 shows a comparison of the scour profiles of a jet primarily removing material by suspended load to that of a jet removing material by bed load. As can be seen in figure 4a in a condition where the particles are being removed by bed load the jet must stay attached to the wall of the scour hole for motion to exist. In figure 4b the scour hole has progressed more quickly in the center than on the sides. This will cause the jet to separate from the sides of the scour hole and the material must also be removed as suspended load. Although in case b the bed material must be removed as suspended load if it comes out of suspension before it is displaced past the sloping sides to keep it from falling back in.

Historical analysis of Erosion downstream of Hydraulic Structures

Some of the earliest examples of attempts to understand and control scour downstream were in the 1800's. In these studies and reports, attempts were made to prevent scour from occurring rather than to understand the physical process of erosion that was causing the scour to occur. Many attempts were made to design stilling basins and outlet aprons that would allow a hydraulic jump to occur thus changing the flow regime immediately downstream of a structure from supercritical to subcritical. Equation 1, The Belanger formula, was developed early in the design of hydraulic structures to describe the transition from supercritical to subcritical flow.

$$\frac{y_2}{y_1} = \frac{1}{2} [\sqrt{1+8F_1^2} - 1] \quad (1)$$

The realization that this transformation from one flow regime to another was necessary to reduce the flow velocity was an important step in the development of stable structures, but it did little to increase our knowledge of the physics of scour.

One of the earliest investigations into the nature of scour in an attempt to understand the physics of the process was DuBoys who in 1879 presented the idea of tractive force. In which the sediment discharge is a function of the applied shear stress minus the critical shear stress required for motion ($\tau_o - \tau_c$). This concept although now viewed as controversial was at least a first step in trying to understand sediment transport from a physical point of view. It wasn't until the 1930's and 1940's that significant contributions to the nature of scour was introduced. One of the earliest studies was by Schoklitsch in 1932. This equation for a free overfall related the maximum scour depth to the unit discharge, d_{90} of the sediment size, and the head difference upstream and downstream of the structure.

$$D_s = 0.521 \left[\frac{H_t^{0.2} q^{0.57}}{d_{90}^{0.32}} \right] \quad (2)$$

This equation is reportedly to be good for large values of H_t and d_{90} . This equation was developed for large hydraulic structures with an impingement angle near 90 degrees for the overflow jet.

In the 1950's much attention was placed on the long term nature of scouring action. An early study by Rouse(1940) proposed that over a long period of time scour will continue to occur regardless of the bed material or the discharge. This scour will continue at an ever decreasing rate but would be asymptotic to no set value. Laursen presented a study in 1952 which shows a limiting value to scour depth based not on the ability for the jet to move material within the scour hole but on the ability of the jet to carry it out of the hole. This study was conducted with a highly submerged horizontal jet on 3 different bed material types with d_{90} ranging from 0.28 to 1.12. In his experiment he used a submerged horizontal jet of a thickness of 0.025 ft. with a submergence of 2.0 ft. He found that at the beginning of flow most of the scour was transported as bed load. As the upstream face of the scour hole approached the natural angle of repose the transport mechanism changed to suspension. The results of his work were similar to that of Ahmad(1953) in that the scour profiles were similar for all discharges and sand grain sizes in the range of d_{50} from 0.35 mm to 1.08 mm. Tarapore (1956) verified Laursen's conclusion of a limiting scour depth by conducting several long term experiments.

An additional study was conducted by Hartung (1959) which had similar results to the previous two studies, but with slightly different values for head and discharge. This equation is shown below:

$$D_s = 1.40 \left[\frac{H_t^{0.36} q^{0.64}}{d_{85}^{0.32}} \right] \quad (3)$$

The previous equations have not been dimensionally homogeneous. Many of the equations of this form accounted for grain size, and some of them stated that the grain size was a minor term. This is not what would normally be expected in a scour problem. Mason and Arumugam conducted an exhaustive research of many of the early equations and proposed an equation that they feel would better represent the conditions that would produce scour. They also report that this equation would be representative of the model and prototype conditions.

$$D_s + Y_t = (6.42 - 3.1 H_t^{0.10}) \left[\frac{q^{0.6 - \frac{H_t}{300}} H_t^{0.15 - \frac{H_t}{200}} Y_t^{0.15}}{g^{0.3} \left(\frac{d_{50}}{1000}\right)^{0.10}} \right] \quad (4)$$

The authors do not discuss the angle of the jet in relation to the original bed floor in their formulation. A contribution to scour analysis by Akashi and Saitou (1986) was in terms of the effects caused by tailwater on the scour depth. They were able to determine that the tailwater depth effects the shape of the mound of removed material which is deposited downstream of the scour hole. The mound in turn effects the depth of the scour hole. One of the first empirical studies conducted on scour by a submerged jet was conducted by Albertson et al. as described by Bormann. Albertson went into a great deal of detail to describe the diffusion of a submerged jet. Albertson defined the distance required to establish a diffused flow as S_o , and developed an equation to predict S_o as:

$$\frac{S_o}{Y_o} = 5.2 \quad (6)$$

$$\frac{U_m}{U_o} = 2.28 \left(\frac{Y_o}{S}\right)^{\frac{1}{2}} \quad (5)$$

The diffusion process is shown graphically in Figure 3. The distance required to establish a diffused flow is defined as that distance required for the turbulent eddies created at the boundary of the jet to penetrate into the center of the jet. Beltaos and Rajaratnam continued upon the work of Albertson and studied the case of a vertical jet impinging on a horizontal bed. Beltaos subdivided the jet into two sections, the free jet region and the impingement region. Figure 5 shows a schematic of the analysis by Beltaos and Rajaratnam. For the maximum velocity in the free jet region the following equation was derived.

$$U_m = 2.4 \left(\frac{Y_o}{S}\right)^{\frac{1}{2}} U_o \quad (7)$$

$$U_{mi} = 2.7 \left(\frac{Y_o}{D_p}\right)^{\frac{1}{2}} \quad (8)$$

Beltaos found that the maximum velocity in the impingement region U_{mi} was described by: and evaluated the maximum bed shear in the impingement region of the jet to be defined by

$$\tau_{oi} = 0.03 U_o^2 \rho \frac{Y_o}{D_p} \quad (9)$$

This set of equations yields similar results to that of Albertson, Equation 5.

During the 1970's several significant contributions were made to the theory of sediment transport and the hydrodynamics of jets. Bogardi's text in 1974 increased our knowledge on the critical velocity for particle motion under turbulent flow. Beltaos(1976) investigated the impingement of jets other than that of a 90° impingement angle. His investigation found that the maximum shear stress was a function of the impingement geometry and not the impingement angle.

Yuen(1984) has proposed one of the more physically based analysis of a free jet. Yuen has considered the fundamental dynamics of jet diffusion and impingement on a moveable boundary. Three different impingement angles were investigated

Ali Uyumaz(1988) performed a study on the scour effects of discharge over and under a sluice gate. From his experiments he determined that for simultaneous flow over and under the sluice gate the minimum amount of downstream scour was found.

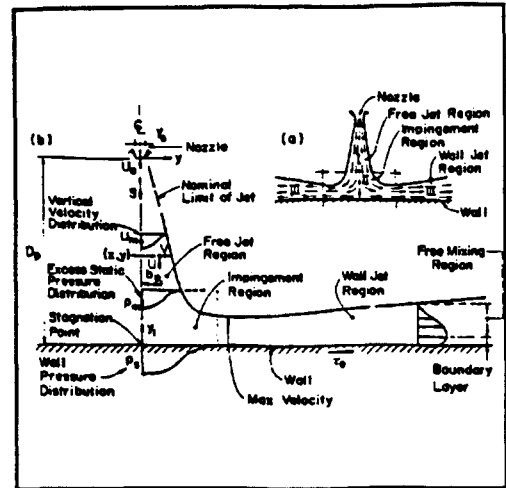


Figure 5 Submerged Plane Jet Beltaos(1973)

Present Analytical Techniques

One of the most recent analysis of scour formation was done by Bormann (1988). In this formulation Bormann attempted to create a full physically based analysis of equilibrium scour depth. His study which was based on analyzing grade control structures with vertical and sloping downstream faces is one of the most detailed analyses that the author has found. The end result of his analysis was to develop a stability factor for bed material which was used to determine the maximum depth of the scour hole. To this end he incorporated the results of Stevens and Simons(1971) work on particle motion on a sloped bed.

He took into account the diffusion of the jet below the tailwater, the deflection of the jet under submerged conditions, the tailwater depth and the entrance angle of the entering jet. Using the Von Karman-Prandtl logarithmic velocity profile over a hydrodynamically rough surface he was able to develop a scour stability parameter χ .

$$\chi = \frac{\rho U_o^2 Y_o}{(\gamma_s - \gamma) d_s S_c} \quad (10)$$

This can be considered as a ratio of the forces causing scour to the gravitational forces resisting scour. From these basic assumptions he developed 3 equations for computing the equilibrium scour depth D_s , the most physically based equation is shown below:

$$D_{sa} = \left[\left(\frac{\tan \phi}{\cos \hat{\beta} (\tan \phi + \tan \hat{\beta})} \frac{0.426 \rho}{(\gamma_s - \gamma)} \right)^{0.796} \frac{C_d^2 U_o^{1.59} Y_o^{0.59}}{d_s^{0.387}} \right] \sin \hat{\beta} D_p \quad (11)$$

Breusers (1975) presents an interesting development for the computation of the velocity profiles in scour holes. In his analysis he transformed the Navier-Stokes equations in two dimensions into a diffusive equation and solved the diffusion equation by finite difference techniques. Although his analysis holds promise he fails to relate this computed velocity profile to sediment transport or any other scour calculations.

Barfuss (1988) presented a development based on the work of Kotoulas for the prediction of scour depth below flip buckets and overfall spillways. This research is similar to many of the early studies except for the fact that Barfuss accounted for the energy loss in the flow due to friction along the flip bucket chute. Figure 6 is a schematic of his analysis.

A regression equation based on model results by the author is used to formulate an equation for the computation of maximum scour depth.

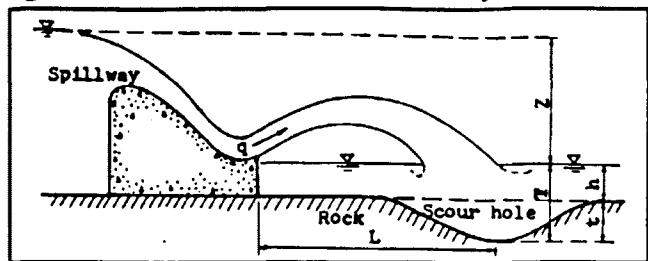


Figure 6 Flip Bucket Profile

$$D_s = 2.44 (K_r h_k^{0.89} z^{0.11}) - T_w \quad (12)$$

Shixia also presented an equation for predicting scour depth downstream of a flip bucket. His analysis was conducted using prototype data from varied data sets. The unit discharge values ranged from 2.63 to 180 m³/s, and a drop height ranging from 6 meters to 166 meters. The equation for this study differs from that of other studies in that the jet was impinging on rock.

$$D_s = 2.432 \frac{q^{0.66} E_j^{0.33}}{(g d_{90}^{0.32})} \quad (13)$$

Figure 7 shows the correlation of shixia's equation to 50 data sets of prototype scour measurements. From an analysis of variance it has been shown that the standard error of the estimate of T/K_r is equal to 1.94 meters

Comparison of Predictive Techniques

For a comparison of the relative magnitude of the scour depth predicted by several of these formulas I have evaluated four of the maximum scour depth prediction equations and plotted up the results for a comparative analysis. The equations that I have chosen

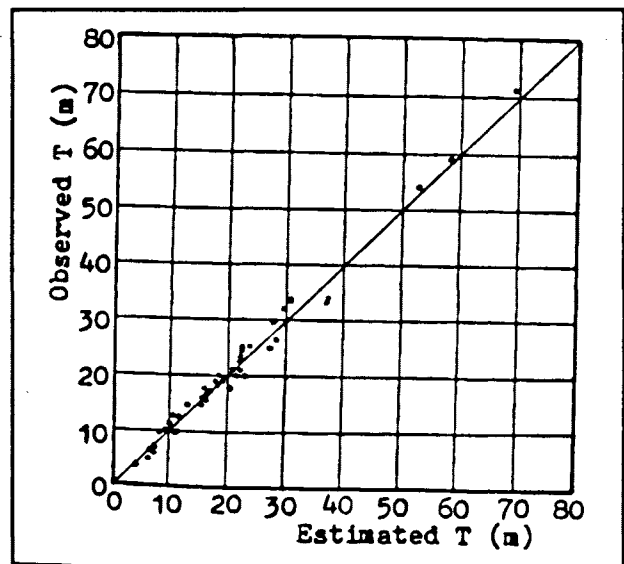


Figure 7 A comparison between the T observed and the T estimated from formula 19

are Eq. 2, Schoklitsch(1932); Eq. 3, Hartung(1959); Eq. 4, Mason & Arumugam(1985), and Eq.10, Bormann(1988). Of these equations Bormann's is the only one which is physically based.

I have compared these equations to the scour depth measurements recorded by Bormann during his extensive model experiments. This data set has discharge ranging from 3.12 cfs/ft to 26.40 cfs/ft, and drop heights ranging from 0.50 ft to 1.25 feet. The following figures are plots of these prediction equations against the measured scour depth. The data used for these graphs is included in appendix III.

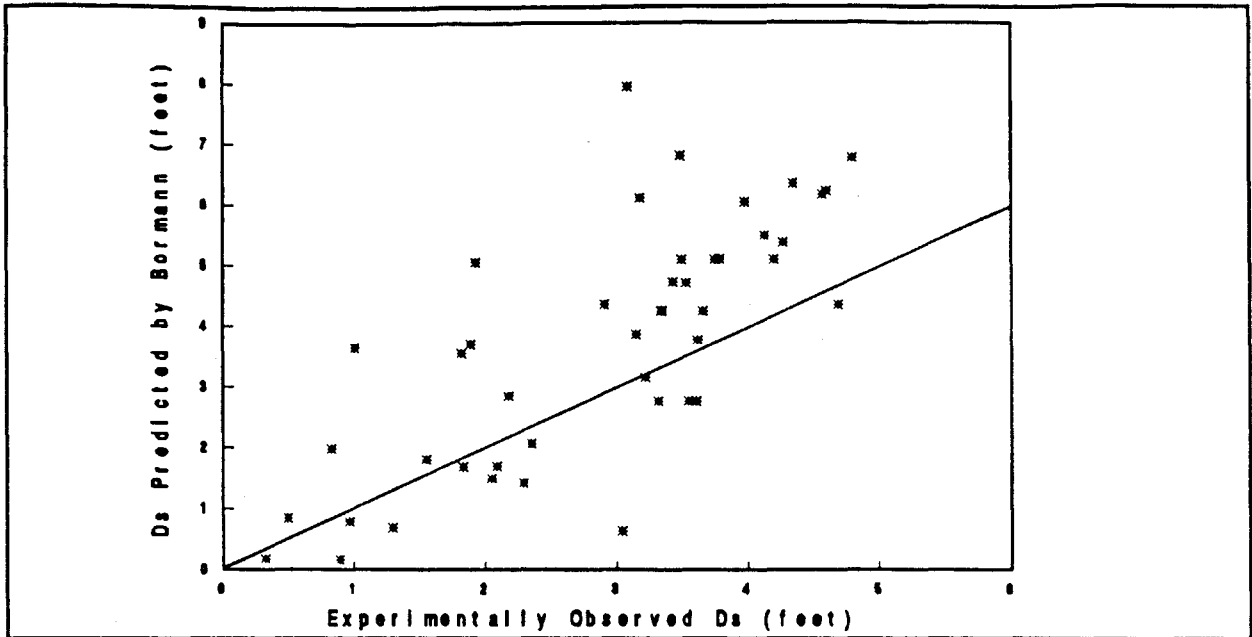


Figure 8 Bormann (1988)

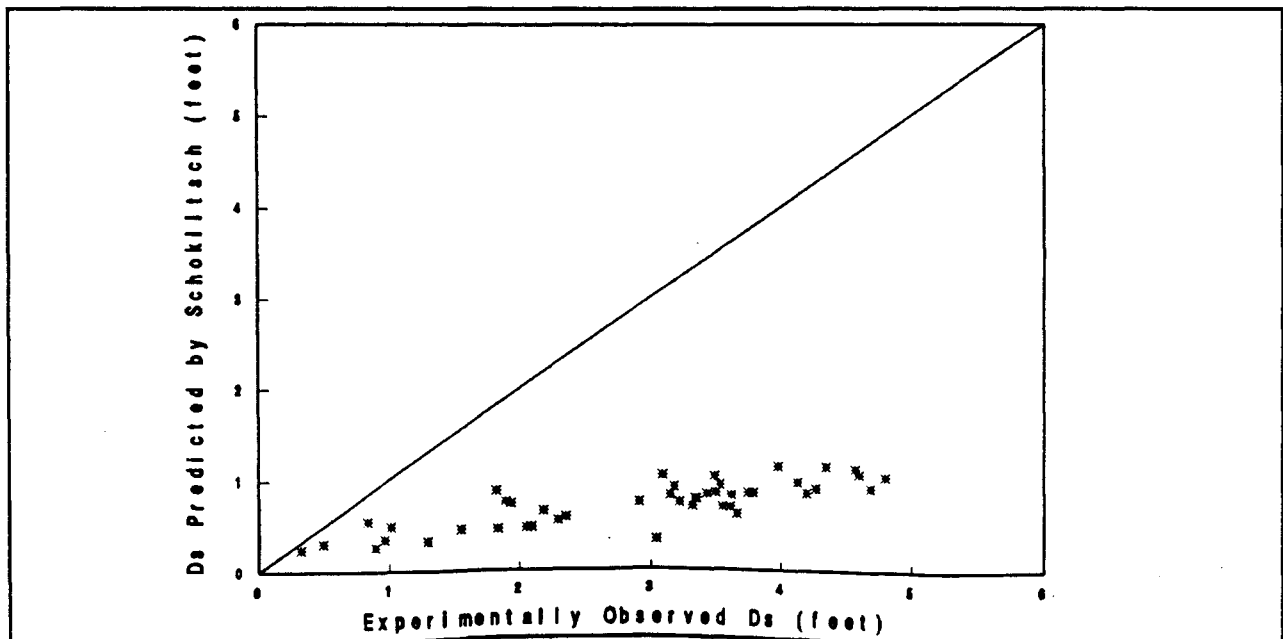


Figure 9 Schoklitsch (1932)

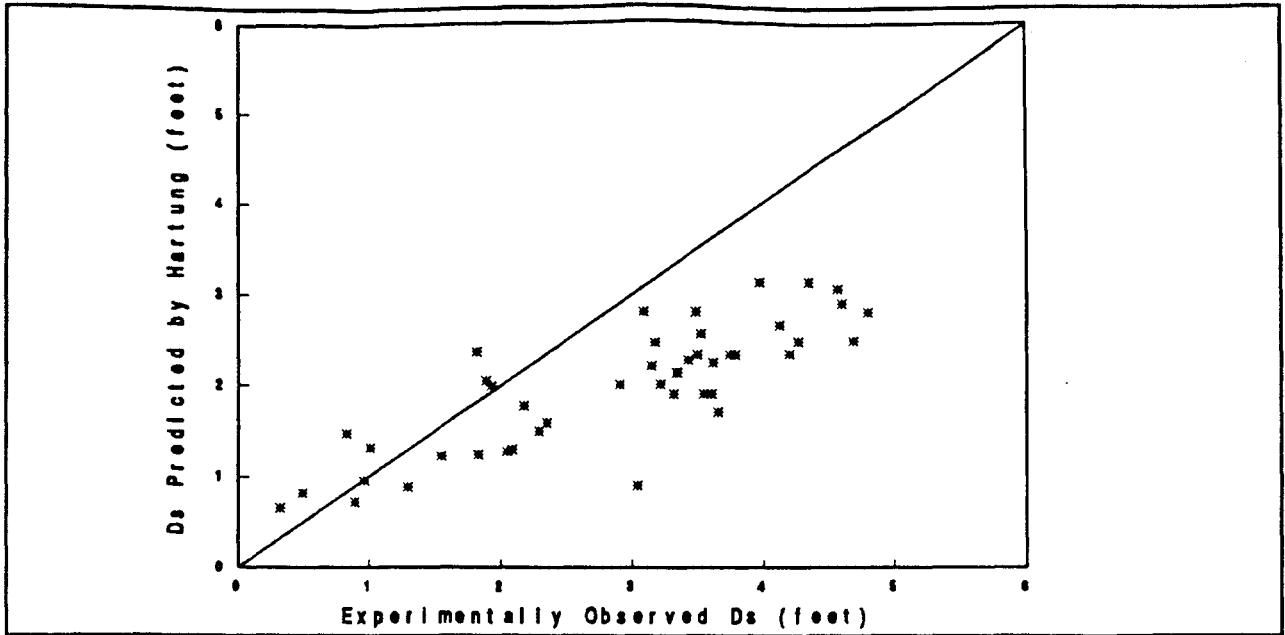


Figure 10 Hartung (1959)

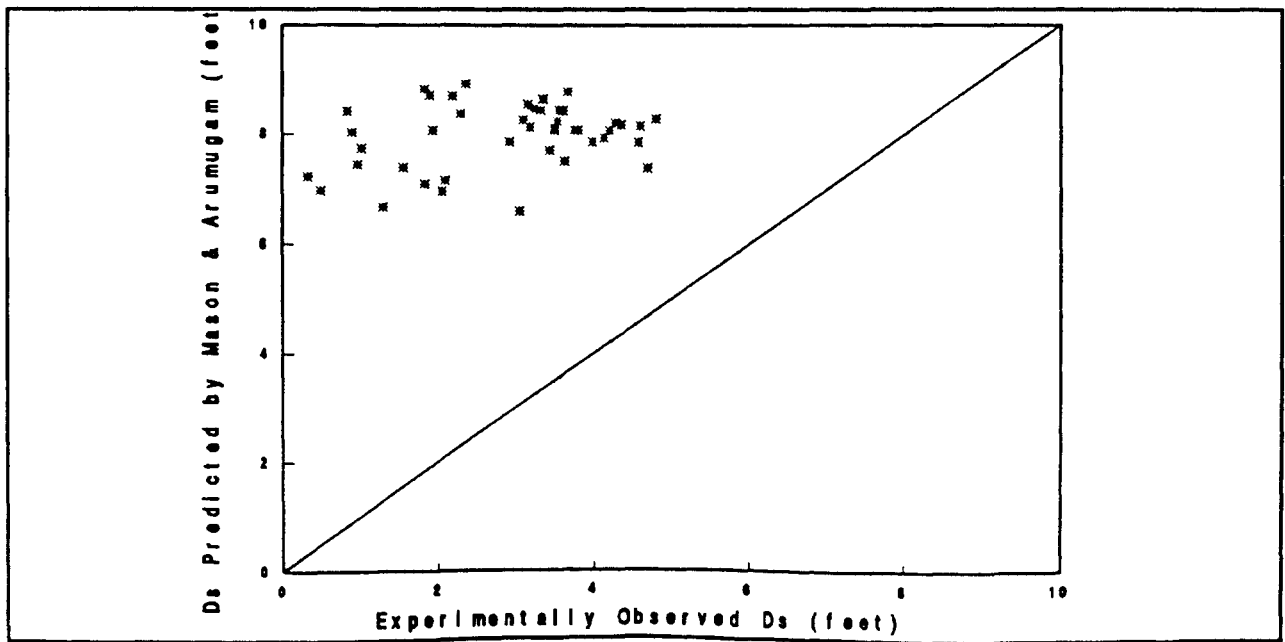


Figure 11 Mason & Arumugam (1985)

Conclusion

From the results shown in the previous section it appears that each equation computes widely different predicted scour depths. It must be noted that each equation may not be in error, but rather each equation was developed under a certain set of criteria where it works quite well. Many of the model runs performed by Bormann were for low drop heights and partial submergence. Schoklitsch, Hartung, and Mason's prediction equations were generally developed for large drop heights where you would not expect to encounter submergence effects. Mason's equation predicted values that are extremely high compared to the measured values. This could be due to their assumption of the free jet condition, but that shouldn't account for this large of a discrepancy. Generally, the further you get from the initial criteria that the equations were developed for, the greater the chance of error in your analysis. That is why an equation based on physical parameters and not a regression analysis of the results of a model study is so sorely needed. As can be seen by the results of Bormann's predicted results, this physically based equation which was not based on empirical data gives the best consistency under these varying conditions. Although to make further verification of the applicability of Bormann's equation comparisons should be made to data of measured scour depths from a high head structure where the previous three equations would be expected to give better results.

Appendix I. References

- Ahmad, Nazir, "Mechanism of Erosion Below Hydraulic Works," Proceedings Minnesota International Hydraulics Convention, International Association for Hydraulic Research, Minneapolis, Minnesota, August 1953.
- Barfuss, Steven L., "Design of Ripraped Scour Holes For Flip Bucket and Overfall Spillways", Proceedings of the National Hydraulic Engineering Conference, American Society of Civil Engineers, 1988.
- Bogardi, J., "Sediment Transport in Alluvial Streams", Akademiai Kiado, Budapest, Hungary, 1974.
- Bormann, Noel E., "Equilibrium Local Scour Depth Downstream of Grade Control Structures", Dissertation, Colorado State University, Fort Collins Colorado, August 1988.
- Breusers, H.N.C., "Computation of Velocity Profiles in Scour Holes", XVI th. IAHR Congress Sao Paulo Brazil, Delft Hydraulics Laboratory Publication No. 152, November 1975.
- Chow, Ven Te, "Open Channel Hydraulics," Page 512, McGraw-Hill Book Company, Inc, New York, 1959.
- Garde, R.J., "Mechanics of Sediment Transport and Alluvial Stream Problems", John Wiley & Sons, New Delhi, India, 1985.
- Laursen, Emmett M., "Observations on the Nature of Scour", Proceedings of the Fifth Hydraulics Conference, Iowa Institute of Hydraulic Research, State University of Iowa, June 1952.
- Mason, P., and Arumugam, K., "Free Jet Scour Below Dams and Flip Buckets", Journal of Hydraulic Engineering, American Society of Civil Engineers, Vol 111, No. 2, February 1985.
- Rouse, H, "Engineering Hydraulics", Proceedings of the Forth Hydraulics Conference, Iowa Institute of Hydraulic Research, John Wiley & Sons, 1949.
- "Sedimentation Engineering", ASCE Manuals and Reports on Engineering Practice No. 54,

American Society of Civil Engineers, 1975.

Shixia, Wang, "Scour of Riverbeds below Sluices and Dams", Proceedings of the International Symposium on Design of Hydraulic Structures, Colorado State University, Fort Collins Colorado, August 1987.

Simons, D.B., "Sediment Transport Technology", Water Resources Publications, Littleton, CO.

Uyumaz, Ali, "Scour Downstream of a Vertical Gate", Journal of Hydraulic Engineering, American Society of Civil Engineers, Vol 114, No. 7, July 1988.

Appendix II. Notation

The following symbols are used in this paper:

- y_1 = Supercritical Conjugate Depth [M]
- y_2 = Sub Critical Conjugate Depth [M]
- F_1 = Froude Number corresponding to Supercritical Flow
- F_2 = Froude Number corresponding to Subcritical Flow
- D_s = Maximum Scour depth [M]
- H_t = Head Difference Upstream and Downstream of the structure [M]
- q = Unit Discharge over the structure [M]
- d_{90} = The sediment size fraction of which 90% is smaller [mm]
- d_s = Effective sediment diameter [Ft.]
- Y_t = The Tailwater Depth [M]
- g = The Gravitational Constant [M/s^2]
- D_p = The Distance from the Jet outlet to the bed [M]
- ϕ = The Angle of repose of the bed material
- β = The angle the jet makes with the scour hole bottom
- C_d = Coefficient of diffusion
- U_o = Velocity of jet entering the tailwater [Ft./s]
- Y_o = Thickness of the jet [Ft.]

Appendix III. Tabulated Data

T e s t N o	Jet Thickness	Jet Velocity	Drop Height	Head water Elev.	Tail water Elev.			Unit Discharge	Measured data	Computed Maximum Scour Depth			
	Y_o	U_o	D_p	H_w	T_w	d_{90}	d_{50}	q	D_s	D_s	D_s	D_s	D_s
	(Feet)	(Ft/s)	(Feet)	(Feet)	(Feet)	(mm)	(mm)	(cfs)	(Feet)	(Feet)	(Feet)	(Feet)	(Feet)
1	3.100	7.80	0.50	4.5447	4.40	0.0052	0.0009	24.18	3.66	4.26	0.6368	1.7112	8.7769
2	3.100	7.80	0.50	4.5447	4.10	0.0052	0.0009	24.18	3.34	4.26	0.7971	2.1420	8.6455
3	3.100	7.80	0.50	4.5447	4.10	0.0052	0.0009	24.18	3.35	4.26	0.7971	2.1420	8.6455
4	1.860	12.86	0.50	4.9280	3.20	0.0052	0.0009	23.92	4.80	6.78	1.0393	2.7928	8.2773

1.860	12.86	0.50	4.9280	3.20	0.0052	0.0009	23.92	4.80	6.78	1.0393	2.7928	8.2773
1.860	12.86	0.50	4.9280	2.90	0.0052	0.0009	23.92	4.60	6.24	1.0731	2.8837	8.1493
2.900	6.40	0.50	4.0360	3.50	0.0052	0.0009	18.56	3.32	2.77	0.7116	1.9123	8.4352
2.900	6.40	0.50	4.0360	3.50	0.0052	0.0009	18.56	3.61	2.77	0.7116	1.9123	8.4352
2.900	6.40	0.50	4.0360	3.50	0.0052	0.0009	18.56	3.55	2.77	0.7116	1.9123	8.4352
1.566	11.75	0.50	4.2098	2.70	0.0052	0.0009	18.40	3.79	5.12	0.8711	2.3408	8.0726
1.566	11.75	0.50	4.2098	2.70	0.0052	0.0009	18.40	3.50	5.11	0.8711	2.3408	8.0726
1.566	11.75	0.50	4.2098	2.70	0.0052	0.0009	18.40	3.75	5.11	0.8711	2.3408	8.0726
1.566	11.75	0.50	4.2098	2.70	0.0052	0.0009	18.40	4.20	5.11	0.8711	2.3408	8.0726
3.900	5.00	0.83	5.1181	4.93	0.0052	0.0009	19.50	2.35	2.06	0.5937	1.5954	8.9188
2.450	7.80	0.83	4.2247	3.58	0.0052	0.0009	19.11	3.22	3.16	0.7508	2.0176	8.4568
1.518	12.59	0.83	4.8093	3.03	0.0052	0.0009	19.11	4.27	5.39	0.9198	2.4718	8.2066
3.800	6.80	0.83	5.3480	4.73	0.0052	0.0009	25.84	1.82	3.55	0.8842	2.3760	8.8204
1.800	13.89	0.83	5.6258	2.98	0.0052	0.0009	25.00	4.35	6.36	1.1606	3.1188	8.1719
3.850	5.40	0.17	4.4727	4.20	0.0052	0.0009	20.79	2.18	2.85	0.6632	1.7823	8.6942
2.600	9.40	0.17	4.1420	3.07	0.0052	0.0009	24.44	3.53	4.72	0.9563	2.5698	8.2455
1.785	13.99	0.17	4.9950	2.32	0.0052	0.0009	24.99	3.98	6.06	1.1629	3.1249	7.8703
1.710	12.24	0.17	4.2063	2.82	0.0052	0.0009	20.93	3.18	6.12	0.9216	2.4766	8.1299
1.730	12.35	0.17	4.2683	2.42	0.0052	0.0009	21.38	4.13	5.51	0.9881	2.6552	7.9339
3.700	7.20	0.75	5.2549	4.80	0.0056	0.0014	26.64	3.15	3.87	0.8264	2.2207	8.5416
1.920	13.04	0.75	5.3103	3.55	0.0056	0.0014	25.00	3.49	6.82	1.0447	2.8073	8.1122
1.800	13.88	0.75	5.5415	2.90	0.0056	0.0014	25.00	4.57	6.18	1.1330	3.0447	7.8535
3.400	4.50	0.75	4.4644	4.15	0.0056	0.0014	15.30	2.29	1.42	0.5595	1.5035	8.3692
1.410	11.16	0.75	4.0939	2.85	0.0056	0.0014	15.73	2.91	4.36	0.7484	2.0111	7.8600
1.290	12.15	0.75	4.3322	2.15	0.0056	0.0014	15.75	3.62	3.78	0.8380	2.2520	7.5116
2.250	2.90	0.75	3.1305	3.04	0.0056	0.0014	6.52	0.89	0.16	0.2682	0.7209	8.0256
1.113	5.60	0.75	2.3503	1.92	0.0056	0.0014	6.24	0.96	0.79	0.3573	0.9602	7.4436
0.655	9.83	0.75	2.9058	1.46	0.0056	0.0014	6.44	1.83	1.68	0.4636	1.2457	7.0985
0.624	10.21	0.75	2.9933	1.29	0.0056	0.0014	6.38	2.05	1.49	0.4765	1.2804	6.9607
0.806	4.47	0.75	1.8669	1.56	0.0056	0.0014	3.61	0.32	0.18	0.2444	0.6569	7.2255
0.444	8.11	0.75	2.2153	1.27	0.0056	0.0014	3.61	0.49	0.85	0.3061	0.8227	6.9663
0.387	9.19	0.75	2.4484	0.97	0.0056	0.0014	3.56	1.29	0.69	0.3321	0.8925	6.6717
0.379	9.40	0.75	2.5010	0.91	0.0056	0.0014	3.56	3.04	0.63	0.3370	0.9057	6.6048
3.850	6.60	1.25	5.7763	5.42	0.0056	0.0014	25.41	1.89	3.70	0.7661	2.0586	8.7075
1.910	13.04	1.25	5.8003	4.00	0.0056	0.0014	24.99	3.09	7.95	1.0492	2.8193	8.2578
2.800	5.60	1.25	4.5369	4.27	0.0056	0.0014	15.68	0.83	1.98	0.5491	1.4756	8.4108
1.400	11.18	1.25	4.5908	3.38	0.0056	0.0014	15.75	1.93	5.05	0.7449	2.0017	8.0648
1.270	12.38	1.25	4.8998	2.56	0.0056	0.0014	15.75	3.43	4.74	0.8498	2.2836	7.7077
1.149	13.86	1.25	5.3819	1.96	0.0056	0.0014	15.92	4.69	4.36	0.9226	2.4791	7.3883
0.525	12.80	1.25	4.3190	2.60	0.0056	0.0014	6.72	1.01	3.65	0.4917	1.3213	7.7323

DISTORTED PHYSICAL HYDRAULIC MODELS THEORY AND PRACTICE

by
Fred L. Ogden

Abstract

The applicability of distortion in physical hydraulic models is examined, and changes in philosophy regarding their use over time are discussed. Distortion in physical models has been identified as an additional factor preventing the achievement of dynamic similarity. The degree to which this affects the results of a physical model can be significant. Early writers tend to list limits on distortion ratios, while theories from more recent experimenters enumerate distortion effects and applicability.

Historical Introduction

The history of hydraulic models and the laws of similarity in their present form date back to Sir Isaac Newton, who enumerated his Law of Similarity in 1687. In his "Principia Mathematica" (originally in Latin) Newton published his theory of similarity in a single paragraph as follows:

"Suppose two similar systems of bodies consisting of an equal number of particles, and let the correspondent particles be similar and proportional, each in one system to each in the other, and have a like situation among themselves, and the same given ratio of density to each other; and let them begin to move among themselves in proportional times, and with like motions (that is, those in one system among one another, and those in the other system among one another). And if the particles that are in the same system do not touch one another, except in the moments of reflection; nor attract nor repel each other, except with accelerative forces, that are as the diameters of the correspondent particles inversely, and the squares of the velocities directly, I say that the particles of those systems will continue to move among themselves with like motions and in proportional times."

The term "accelerative force" means that the intensity of a force per unit mass acted upon by the force. The most common example is the acceleration of gravity, g , which is the acceleration of a freely falling body at the earth's surface. If this is multiplied by the measure of the mass acted upon, the result is the total force acting upon the mass. Hence, Newton's Law of Similarity supplies the fundamental equation of similitude, namely,

$$g = \frac{V^2}{D}$$

in which the symbols in the above equation relate to ratios of homologues.

It was not until 1850 that Stokes noticed certain important mathematical relations involved in the theory of similarity and models. Stokes paper entitled "On the Effect of Internal Friction of Fluids on the Motion of Pendulums" touched on the topic of viscosity, which Newton wisely did not mention in his theorem, or it would have been much larger than one paragraph. Newton's theorem does not, however, exclude any force which can be made to conform to it. Stokes essayed to study the laws of similarity in viscous fluids, since it was necessary to determine the effect of changing the sizes, shapes, and conditions of bodies moving in a viscous fluid, such as air. He showed that the sizes of bodies did not change the mathematical treatment. In other words, the same differential equations would represent each of two, or more, similar linear systems.

From his analysis of the works of Stokes, based upon the earlier work of Newton, Groat concludes that as of 1930 the present usage of models is not wholly consistent with sound theory. The Buckingham pi-theorem (1915) introduced a technique by which modeling could be described solely in terms of dimensionless quantities, which isolated the laws of modeling from the mathematical description of the phenomenon, which was Stoke's approach.

Theoretical Introduction

A physical model is defined by Yalin (1989) as a precision device used to predict the behavior of a physical phenomenon at a different scale. A model is reliable only if it is designed and constructed with strict accordance to scaling laws. If the design is not correct the model is wrong in principle, and the most sophisticated instrumentation and measuring techniques will only improve the accuracy of predictions based on the wrong observed phenomena.

A small scale reproduction of a physical situation can be a valid model of the larger scale process if the particular forces observed can be theoretically related to both scales involved, namely the model and the prototype. Constant proportions of the observed forces in both scales are commonly used to relate model and prototype behavior. These constant proportions are referred to as scales, while similarity is defined as the equality of certain forces seen at different scales. The criteria for similarity are derived from mathematical relations (usually differential equations) describing the nature of the phenomenon under investigation.

The contemporary approach to physical modeling rests on the dimensional analysis technique (Bridgman, 1922). This method supplies criteria of similarity from the dimensionless study of the pertinent characteristics themselves, and not from the mathematical descriptions of the phenomenon. Accordingly, the criteria of similarity are obtained without undergoing any interpretations of the mathematical formulations of the physical processes. Models based on the theory of dimensions are the state of the art in current physical modeling.

Theory of Dimensions

Dimensional and Dimensionless Quantities

All physical quantities of space and matter can be expressed in terms of three fundamental properties. These properties are mass, length, and time. These are the only entities in the universe which cannot be physically defined in more basic terms. All other physical properties of the universe may be defined as different combinations of mass, length, and time. Let L, T, and M be the units for length, time, and mass. Since a physical quantity a can be considered as a composition of length, time, and mass, the unit of a, defined by [a] must be a certain function of the fundamental units:

$$a = f(L, T, M)$$

The ratio of two different numerical values of a quantity a cannot depend on the choice of the fundamental units. One can prove that this physical requirement can be satisfied only if the function f has the form of a power series.

$$a = L^{\alpha} T^{\beta} M^{\gamma}$$

1.

where the physical nature of the quantity a is given by the numerical values of the exponents α , β , and γ . The right hand side of the above equation therefore represents the "dimension" of the quantity a. The quantity a is said to possess a dimension or to be a dimensional quantity if at least one of the exponents alpha, beta, or gamma is non-zero. Any dimensional quantity which is not one of the fundamental quantities is usually referred to as a "derived quantity". A dimensional quantity found in mechanics is said to be:

a geometric quantity if	$\alpha <> 0$;	$\beta = 0$;	$\gamma = 0$
a kinematic quantity if	$\alpha <> 0$;	$\beta <> 0$;	$\gamma = 0$
a dynamic quantity if	$\alpha <> 0$;	$\beta <> 0$;	$\gamma <> 0$.

If all the exponents in equation (1) are 0, then the unit of the quantity a cannot depend on the fundamental units L, T, and M, and the quantity is referred to as "dimensionless".

Therefore, the unit and also the numerical value of a dimensional quantity is dependent on the choice of fundamental units; the unit and thus the numerical value of a dimensionless quantity is independent of the choice of the fundamental units. Accordingly, dimensionless quantities maintain the same numerical values in all systems of fundamental units. If it is possible to determine the exponents x, y, and z so that this power product becomes dimensionless, then it is said that the dimensions of the quantities are independent. If it is not possible to make the power product in equation (2) dimensionless, then the dimension of the a terms are dependent.

Dimensionless Expression of a Natural Law

The dimensionless equivalent of a dimensional relation such as that shown above is given by the procedure which is usually referred to as the π theorem, and which can be described as follows:

Among n characteristic parameters

$$\alpha_1, \alpha_2, \dots, \alpha_n$$

2.

any three parameters are selected which possess independent dimensions. These three parameters will be referred to as basic quantities. Let the basic quantities chosen for the set above be the first three, α_1, α_2 and α_3 . These three basic quantities are combined with the remaining $N-3$ parameters in the following set of $N-3$ power products

$$\begin{aligned} X_1 &= \alpha_1^{x_1} \alpha_2^{y_1} \alpha_3^{z_1} \alpha_4^{m_1} \\ X_2 &= \alpha_1^{x_2} \alpha_2^{y_2} \alpha_3^{z_2} \alpha_5^{m_2} \\ &\vdots \\ X_N &= \alpha_1^{x_N} \alpha_2^{y_N} \alpha_3^{z_N} \alpha_n^{m_N} \end{aligned}$$

3.

where $N=n-3$

It is clear that $N=n-3$ power products X_1, X_2, \dots, X_N are independent for none of them can be expressed in terms of the remaining $N-1$ products. Each of them contains one characteristic parameter $\alpha_4, \alpha_5, \dots, \alpha_n$ which does not appear in the remaining $N-1$ power products. The power products are the dimensionless variables of the phenomenon. The exponents m_1, m_2, \dots, m_N the exponents x_j, y_j , and z_j ($j=1, 2, \dots, N$) must be determined so that each of the power products X_j becomes dimensionless. In order to determine three unknown exponents x_j, y_j , and z_j , we have the following three equations:

$$\begin{aligned} \alpha_1 x_j + \alpha_2 y_j + \alpha_3 z_j &= -\alpha_{j+3} m_j \\ \alpha_1 x_j + \alpha_2 y_j + \alpha_3 z_j &= -\alpha_{j+3} m_j \\ \gamma_1 x_j + \gamma_2 y_j + \gamma_3 z_j &= -\gamma_{j+3} m_j \end{aligned}$$

where α_i, β_i , and γ_i are known from the dimensional equation:

$$\alpha_i = L^{\alpha_i} T^{\beta_i} M^{\gamma_i}$$

4.

of the parameters α_i . The system of three linear equations for x_j, y_j , and z_j can certainly be solved, for its coefficient determinant is different from zero because the basic quantities α_1, α_2 and α_3 are linearly independent.

Principles of the Theory of Similarity

Models

Since the numerical values of the dimensionless quantities remain the same in all systems of fundamental units, the numerical values of the dimensionless quantities X_j will not change if the system of fundamental units $L', T',$ and M' , is replaced by another system of fundamental units called $L'', T'',$ and M'' . It follows that the dimensionless quantities in general, and the X_j terms in particular, remain invariant with respect to the transformation from one fundamental system of units to another.

Dynamic Similarity

If two systems are related to each other by the proportionality constant λ_L then they are referred to as geometrically similar systems. If two systems are related to each other by the two proportionality constants λ_L and λ_T then they are kinematically similar systems, and if two systems are related by all three proportionality constants λ_L , λ_T and λ_M they are dynamically similar systems. It follows that the model and prototype are dynamically similar systems.

Since the dynamic similarity implies that all dimensionless quantities are linearly independent, dynamic similarity can be defined as the validity of:

$$\lambda_{\pi_i} = 1$$

It is important to note that kinematic similarity is necessary for dynamic similarity while geometric similarity is required for kinematic similarity. Hence, the statement "two systems are dynamically but not geometrically similar" is meaningless.

Scales of Dynamically Similar Models

It is assumed (necessarily) that the model and prototype are geometrically similar. If so, dynamic similarity can be achieved if:

$$\lambda_{X_j} = 1$$

(for all $j=1,2, \dots, N$)

Substituting for all X_j their values, and replacing α^n by $\lambda_{\alpha_i}^n$ the result is:

$$\begin{aligned}\lambda_{X_1} &= \lambda_{\alpha_1}^{x_1} \lambda_{\alpha_2}^{y_1} \lambda_{\alpha_3}^{z_1} \lambda_{\alpha_4}^{m_1} = 1 \\ \lambda_{X_2} &= \lambda_{\alpha_1}^{x_2} \lambda_{\alpha_2}^{y_2} \lambda_{\alpha_3}^{z_2} \lambda_{\alpha_4}^{m_2} = 1 \\ \lambda_{X_N} &= \lambda_{\alpha_1}^{x_N} \lambda_{\alpha_2}^{y_N} \lambda_{\alpha_3}^{z_N} \lambda_{\alpha_4}^{m_N} = 1\end{aligned}$$

therefore:

$$\lambda_A = \lambda_{\alpha_1}^{-x_A} \lambda_{\alpha_2}^{-y_A} \lambda_{\alpha_3}^{-z_A}$$

The $N=n-3$ equations involving n scales λ_{α_i} are the criteria of similarity for that phenomenon. Using these criteria one can design the dynamically similar model as follows:

1. Out of n characteristic parameters α_i of the phenomenon under investigation, select (theoretically at random) three dimensionally independent parameters, say α_1 , α_2 and α_3 and their scales λ_{α_1} , λ_{α_2} and λ_{α_3}
2. Using the selected values λ_{α_1} , λ_{α_2} and λ_{α_3} determine from the above N equations the values of the remaining scales, λ_{α_4} , λ_{α_5} and λ_{α_n}
3. Knowing, thus, the scales λ_{α_i} of all n characteristic parameters α_i and knowing the prototype values α'_i of these characteristic parameters, determine the values of n model parameters α''_i as

$$\alpha''_i = \lambda_{\alpha_i} \alpha'_i$$

($i=1,2, \dots, n$)

Any property A' of the prototype can be predicted from the dynamically similar model defined in this fashion. Measuring the model value A'' and dividing it by the scale λ_A will give the prototype value.

Distortion of Scales

Distortion is an additional factor preventing the achievement of dynamic similarity. The utilization of different horizontal and vertical length scales undermines the geometric similarity, and hence, the dynamic similarity of a model. Consider Figure 1, the width to depth ratio for the model cross section is twice smaller than the prototype and the bank inclination is twice as steep. This affects the similarity of the mechanical character of the

flow. The velocity distribution in the model cross section can no longer be similar. Even the relative location of the maximum velocity may not be the same. This is because the larger the width-depth ratio, the closer to the surface are the maximum velocities. Similarly the structure of secondary currents can be substantially altered. As is well known, the structure of the cells of the secondary current is a stability phenomenon, and therefore, the slightest change in the geometry of the cross section can produce a totally different configuration. Note, for example in Figure 2, that the variation of flow depth from $h=0.494$ to 0.562 in the same flume (i.e. a distortion factor of 1.14) can cause a marked difference in the secondary flow pattern.

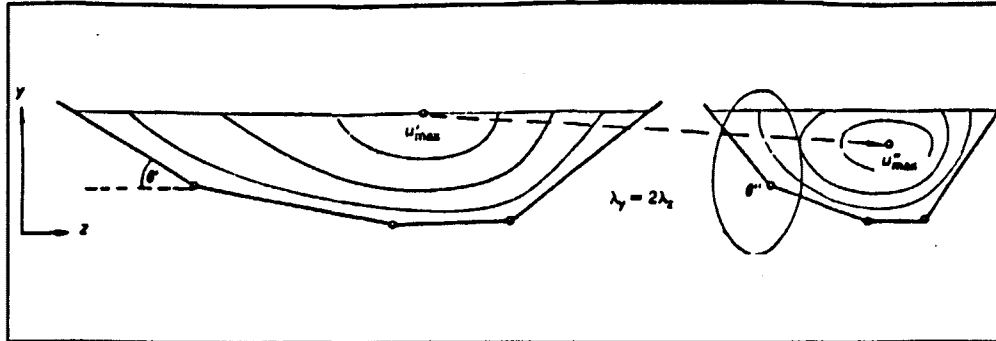


Figure 1. Effect of Distortion on Velocity Field

The distortion is often justified on the grounds that the relevant part of the flow subjected to model studies is not at the banks but in the central region of the flow cross section. And since the flow in the central region can be considered as two dimensional, and hence independent of the width to depth ratio, the distortion cannot undermine the similarity of the flow in the central region. This reasoning is correct, providing that there is a substantial central region in the model. Fortunately, the majority of natural rivers have rather large values of the width to depth ratio, and therefore, if the distortion ratio is not too large, a substantial central region will exist in the model. It is advisable to be cautious on this matter. A model distortion of 4, for instance, reduces a prototype river with a width depth ratio of 32 with about 84% of the width under two dimensional flow to a model with about 35% two dimensional flow across the width. This represents quite a reduction in the amount of cross section in which dynamically similar flow may be claimed. Clearly the representative length of the flow in the central region is the flow depth, h , and therefore any property of the flow (and its consequences) that is dependent on h will be scaled in the flow depth scale λ_y .

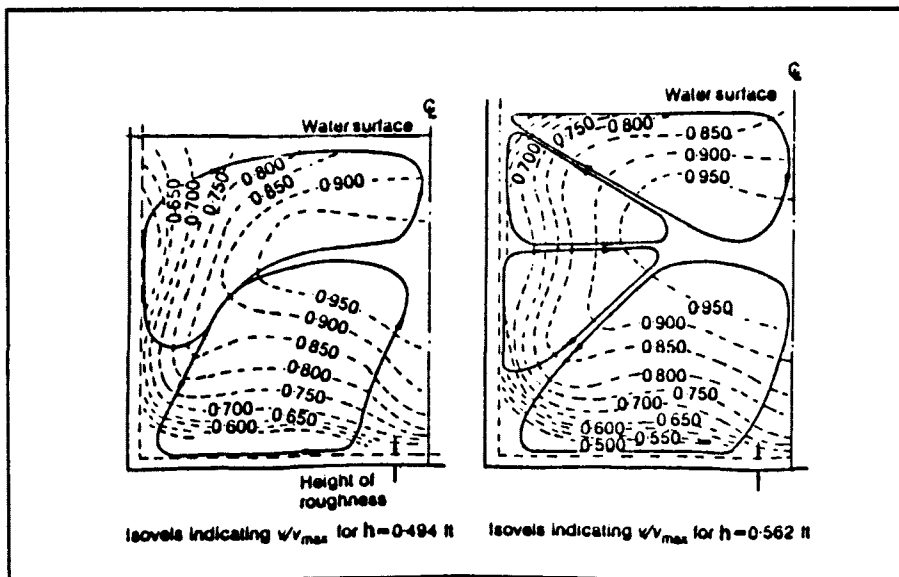


Figure 2. Effect of Small Depth Change on Velocity Field

Strictly speaking, there is no such thing as "permissible distortion". The permissible value of distortion depends upon the topic under investigation, as well as upon the magnitude of the model scales. The Wallingford practice limits distortion in the vertical scale as:

$$\lambda_x = \lambda_y^{\frac{3}{2}}$$

5.

Historical Interpretation of the Applicability of Distortion

Model Studies, 1937

In his short report on the state of the art in modeling in 1937, G. E. Barnes discusses current philosophies with regard to distortion. He writes that complete similarity is not essential as long as observations on the model can be related within proper limits of precision to the performance of the prototype. Geometric similarity may be sacrificed in certain types of studies, where better results may be achieved than by other methods. Barnes goes on to state that the subject of distortion is approached with caution by most experimenters, since it can be shown that results may be misleading or erroneous in selected cases, particularly those involving backwater, drawdown, transition, or hydraulic jump curves. He notes that wherever friction effects are dominant, as in river models where the flow is shallow, and where turbulent flow has to be maintained on a small scale, the model may be built with exaggerated vertical scale or longitudinal slope, or both.

Hydraulic Models, 1942, ASCE.

The ASCE Manual of Engineering Practice number 25, entitled "Hydraulic Models", which was first published in 1942, discusses the applicability of scale distortion in brief. It states that the departure from strict geometric similarity which is caused by the distortion of the vertical scale is warranted in two cases.

- (1) The areas necessary to reproduce in a model for proper simulation of the prototype may be so large that, for practical and economic reasons, the horizontal scale of the model must be made small. If the vertical scale were made the same, vertical measurements, such as water surface elevations, would be concerned with quantities of such small magnitude that accuracy would be lost. Hence, it is desirable to increase the size of the vertical scale of the model.
- (2) In the case of a movable bed model, in which the water in the model must be made to move bed material in a manner similar to that in which water in the full-sized stream moves its bed material the slopes and velocities resulting from use of an undistorted model are usually too small to move any of the materials which have been developed for use as bed materials in models. Here again, the solution is the adoption of a vertical scale which is larger than the horizontal scale.

As implied by the preceding paragraph, it is only in models of open channels or harbors that such geometric distortion is used normally. Distorted models should be designed so that the velocity scale is equal to the square root of the vertical linear scale, and the time scale is equal to the horizontal scale divided by the square root of the vertical scale. In practice, many distorted scale models depart somewhat from these requirements.

This manual also discusses maximum allowable distortion. Movable bed models should never be so distorted as to affect, appreciably, the accuracy of the reproduction of the velocity distribution. The simulation of bed movement is directly dependent upon an accurate reproduction of the velocity distribution. It has been found that a distortion of about six is the permissible maximum for movable bed models, although it is desirable to keep the distortion to a value of four or less. The amount of distortion depends largely upon the shape of the stream which the model represents. If the stream is wide and shallow, the distortion can be relatively great. If the stream is narrow and deep, the distortion should be less.

Engineering Hydraulics, 1949

Fixed Bed Models

In the volume "Engineering Hydraulics, H. Rouse, ed., 1949", J. E. Warnock of the USBR Hydraulic Laboratory discusses the necessity of model distortion in certain instances. In modeling long reaches of either a canal or a river where actual changes in bed configuration are not critical, fixed bed models are used. In fixed bed models, unless an unusually large river is involved, distortion of the slope of the model is required. There are three reasons given by Warnock for this:

1. to offset the disproportionately high resistance to flow due to additional viscosity created when $\lambda \geq 1.0$
2. to obtain a sufficiently high value of the Reynolds number which will insure turbulent flow
3. to accommodate the model in the available laboratory space.

The required distortion of slope can be computed with sufficient precision using the Manning equation. Doing so produces the following result:

$$\frac{\lambda_y}{\lambda_L} = \frac{\lambda_n^2 \lambda_y}{\lambda_R^{\frac{4}{3}}}$$

6.

where:

y=depth
L=length
n=Manning's n
R=hydraulic radius

If n is known in both the model and the prototype, then λ_n is also known, and the exaggeration $\frac{\lambda_y}{\lambda_L}$ can be computed for a given depth y and hydraulic radius R. In models for which the slope distortion is dictated by other considerations, an adjustment of model roughness is required to duplicate prototype conditions. If the distortion and the value of n for the prototype are known, the required value of n for the model can be computed from the above equation.

Movable Bed Models

Despite the limitations on similitude created by distortion, distorted scale movable bed hydraulic models have proved invaluable aids in the solving of complex problems involving the transport of bed material. Instead of arranging the various hydraulic forces involved to meet definite requirements laid down in any law of similitude, the successful prosecution of a movable bed model study requires that the combined action of the hydraulic forces bring about similitude with respect to the all important phenomenon of bed motion, which is the essence of this type of model study.

Generally, in this type of model, the distortion as well as the size and specific gravity of the bed material are selected as to provide similarity with respect to bed forms in both model and prototype. There are two prerequisites for such a model design. First, a thorough knowledge of the characteristics of the prototype based upon the collection and study of hydraulic and hydrographic data, and second, experience in the field of movable bed hydraulic models.

Einstein and Chien's Approach

Einstein and Chien (1956) derived from theoretical and empirical equations the similarity conditions for distorted river models with movable beds. Consideration was given to both the hydraulics and sediment transport in such rivers. The derivation of the relationships for distorted modeling by Einstein and Chien is based on a form of the Manning equation. This equation is of the form:

$$V = \frac{C\sqrt{g}}{D^m} S^{\frac{1}{2}} h^{\left(\frac{1}{2} + m\right)}$$

7.

where:

V= flow velocity
C= constant factor involving roughness
g= gravitational acceleration
h= hydraulic radius
m= unknown exponent

The above equation is identical to the Manning equation when $m=1/6$ and if one uses the relationship $n \sim D^{\frac{1}{6}}$, in which n is the Manning roughness coefficient. It is assumed that the exponent m can be used to describe both the prototype and the model relationships, at least for the most important discharges.

The Froude law may be written in ratios as:

$$\lambda_V \lambda_h^{-\frac{1}{2}} = \Delta_f$$

8.

The sediment transport similarity conditions depend that the intensity of the sediment transport Φ and the intensity of shear Ψ for the individual grain sizes be equal in model and prototype as these two quantities are not connected by a power-type equation. Only if the transport rates are restricted to a very narrow range of values is it possible to combine the two conditions. The equality of the values,

$$\Phi_s = \frac{i_B q_B}{i_b g(\rho_s - \rho)} \left(\frac{\rho}{\rho_s - \rho} \right)^{\frac{1}{2}} \left(\frac{1}{g D^3} \right)^{\frac{1}{2}} \quad 9.$$

is possible for all fractions of a mixture only if the two mixtures are similar so that the ratios of the i -values become equal to unity. For water in both the model and prototype, the equation of equal Φ values is:

$$\lambda_{q_B} \lambda_{(\rho_s - \rho)}^{-\frac{3}{2}} \lambda_D^{-\frac{3}{2}} = 1 \quad 10.$$

To meet the zero sediment load criterion, in ratios, equality of corresponding Ψ values is expressed by:

$$\lambda_{(\rho_s - \rho)} \lambda_D \lambda_\eta^{-1} \lambda_h^{-1} \lambda_s^{-1} = 1 \quad 11.$$

where η is the ratio of the hydraulic radius R'_b referred to the surface drag to the entire radius R_T . This correction must be introduced as λ_{R_T} is equal to λ_h but $\lambda_{R'_b}$ does not equal λ_h .

To meet the laminar sublayer criterion, λ_δ must equal λ_D . This can be written in ratios as:

$$\lambda_D \lambda_\eta^{\frac{1}{2}} \lambda_h^{\frac{1}{2}} \lambda_s^{\frac{1}{2}} = \Delta_\delta \quad 12.$$

By computing some characteristic flows in model and prototype the ratio of q_T and q_B the average ratio of these ratios $\frac{\lambda_{q_T}}{\lambda_{q_B}}$ can be determined and is called B . This value can be used to give a general relationship between the two load ratios:

$$\lambda_{q_B} \lambda_{q_T}^{-1} B = 1 \quad 13.$$

Hydraulic time t_1 may be defined as the time which a water article takes to move with velocity V through a distance L .

$$\lambda_V \lambda_{t_1} \lambda_L^{-1} = 1 \quad 14.$$

The time t_2 may indicate the duration of individual flows. Ratios of this time must be such that corresponding time intervals are required by corresponding sediment rates q_T to fill corresponding volumes. Expressed in ratios this equation can be written for a unit width as

$$\lambda_{q_T} \lambda_{t_2} \lambda_h^{-1} \lambda_{(\rho_s - \rho)}^{-1} = 1 \quad 15.$$

assuming the porosity of the deposits to be equal in model and prototype; the sediment rates q_T are measured in weight under water. The time λ_{t_2} is the time scale at which the prototype hydrographs must be repeated in the model.

A tilt is applied to the model during construction and because it is assumed to be proportional to the prototype slope, it can be applied only to flows which have, at all points, water surface slopes and energy grade line slopes which are constant with time. This condition is not fulfilled when the flow reverses direction, such as under the influence of a tide or in most overbank flows. In all such cases no additional tilt can be permitted and:

$$\lambda_s \lambda_L \lambda_h^{-1} = \Delta_N$$

16.

in which Δ_N is equal to unity when there is zero tilt. A small tilt is represented by a small deviation of this quantity from unity.

Table 1. Exponents for Model Laws for River Models with Sed. Transport

λ_L	λ_h	λ_V	λ_S	λ_D	$\lambda_{(\rho_s - \rho)}$	λ_{q_B}	λ_{q_T}	λ_{t_1}	λ_{t_2}	B	λ_C	λ_n	Δ_V	Δ_F	Δ_δ	Δ_N
	-1- 2m	2	-1	2m							-2		-1			=1
	-1	2												-2		=1
				-3	-3	2										=1
	-1		-1	1	1							-1				=1
	1		1	2								1			-2	=1
						1	-1			1						=1
-1		1						1								=1
-1	-1				-1		1		1							=1
-1	-1		1													-1 =1

Table 1 contains the exponents from the nine independent equations above. The nine equations can be solved in several ways. Einstein and Chien solved them for first λ_h chosen freely, second, λ_L the horizontal scale chosen freely and thirdly, the density of the model sediment chosen.

In conclusion, Einstein and Chien point out that a distorted river model is, at best, an acceptable compromise permitting the solution of certain problems which otherwise cannot be solved except by experimentation in the prototype, which under all conditions is more expensive. Their method of designing a distorted hydraulic model has the inherent advantage allowing the prediction of the theoretical model behavior in a qualitative way, with respect to the Δ values it gives quantitative values, something heretofore impossible.

The Einstein Chien approach also reveals several reasons for the loss of similarity. The values of the exponent m will be different in the model and prototype over a wide range of discharges. Multi-channel flows complicate the determination of the exponent m. A different time scale is necessary for each independent flow channel. Wash load and overbank sedimentation are not included in the formulation.

Novak and Cabelka

In their widely acclaimed volume on Hydraulic Modeling (1981), Novak and Cabelka discuss the application of distortion. They point out that fixed bed models with distortion can only achieve similarity at one unique depth or at a constant ratio of $\frac{h}{\delta}$. In wide channels, $\frac{h}{\delta}$ will change only within small limits and approximate similarity may therefore be assumed to be valid. If this is not the case, it is necessary to compute the model scales for a mean depth (and thus a mean value of $\frac{h}{\delta}$) from the range of depths and take into account the scale effect introduced in the case of other depths. More importantly, they point out that dynamic similarity cannot be achieved in movable bed distorted models.

Sample Calculations of Model Distortion

The following table contains the results of the calculations for the design of a model at different scales, both distorted and undistorted (Bennett, 1988). The calculations are based on dimensional theory and are included to give the reader an idea of the effects of distortion on model behavior.

Table 2. Effects of Distortion on Flow Variables

Scale		Depth (ft)	Velocity (fps)	Reynolds number
Prototype		20	2	1.13×10^7
Undistorted	1:150 H & V	0.13	.16	5900
Distorted-				
1:150 H	1:75 V	.27	.23	18000
1:150 H	1:50 V	.40	.28	32000
1:150 H	1:37.5 V	.53	.33	50000
1:150 H	1:30 V	.67	.37	70000

In particular, notice how the distortion affects the Reynolds number. The increase in R with increasing distortion is what makes distortion valuable in modeling of sediment transport phenomena.

An Example of the Application of the Π Theorem

Consider the simple case of sediment transport "en masse": steady and uniform two-dimensional flow, cohesionless sediment. This transport phenomenon can be defined by the following $n=6$ characteristic parameters

- ρ fluid density
- ν kinematic viscosity
- γ_s specific gravity of sediment
- v_* shear velocity
- D typical grain size
- h flow depth

The parameters ρ , D and v_* have independent dimensions. Selecting them as basic quantities (i.e. as α_1 , α_2 , and α_3) one obtains the following $N=n-3=3$ dimensionless variables:

$$X_1 = \rho^0 D^1 v_*^{-1} \nu^{-1} = \frac{\nu_* D}{\nu} = X \quad (\text{Grain Reynolds number})$$

$$X_2 = \rho^1 D^{-1} v_*^2 \gamma_s^{-1} = \frac{\rho v_*^2}{\gamma_s D} = Y \quad (\text{Mobility number})$$

$$X_3 = \rho^0 D^{-1} v_*^0 h = \frac{h}{D} = Z \quad (\text{Relative flow depth})$$

where X_1 , X_2 and X_3 represent the influences of ν , γ_s and h respectively.

Suppose that during experiments, one will vary h , S , and D only. In this case, the above set of equations, though physically meaningful, is disadvantageous, because the basic quantities D and $v_* = \sqrt{g S h}$ do not remain constant. To remedy this situation, form new dimensionless by adopting as fundamental quantities ρ , γ_s and ν which will not vary during the experiments. The result is then:

$$\bar{X}_1 = \frac{\gamma_s D^3}{\rho \nu^2} = \frac{X_1^2}{X_2}$$

$$\bar{X}_2 = \frac{\gamma_s h^3}{\rho \nu^2} = \frac{X_3^3 X_1^2}{X_2}$$

$$\bar{X}_3 = \frac{\rho g S}{\gamma_s} = \frac{X_2}{X_3}$$

in this case, the variations of D , h and S induce variations only in \bar{X}_1 , \bar{X}_2 and \bar{X}_3 respectively. Note also that \bar{X}_1 , \bar{X}_2 and \bar{X}_3 are not really new variables, just independent combinations of the original variables X_1 , X_2 and X_3 . Knowing (from experimental measurements) the values of \bar{X}_1 , \bar{X}_2 and \bar{X}_3 , the corresponding values for X_1 , X_2 and X_3 can be determined by solving the above system of equations.

Distorted Model Design from Einstein and Chien Theory

In their original derivation of the equations for the design of a distorted model, Einstein and Chien allowed for three different design conditions. These three are; known depth scale ratio λ_y , known length scale λ_b and known sediment density ratio $\lambda_{(\rho_s - \rho)}$. The most common desire in the design of a distorted hydraulic model is to find the vertical scale permissible for a given horizontal scale. This is because the horizontal scale often determines the economic cost of the model in terms of required laboratory space and material outlay.

To determine the rest of the dependent values, λ_y , λ_b and λ_D the values of the independent variables C_p , C_m and the exponent in the Manning friction equation m must be determined. This is done by performing a best fit of the prototype behavior and expected model behavior using the Manning equation.

For example, if a prototype with $S=0.00105$ and $D_{65} = K_s = 0.00115$ ft, and with $C_r = 0.827$ and $m=0.186$, assuming λ_η and all of the Δ values = 1.0,

$$\lambda_y = \lambda_L^{\frac{(m+1)}{(4m+1)}} \lambda_C^{\frac{-2}{(4m+1)}} \lambda_\eta^{\frac{-m}{(4m+1)}}$$

which = $150^{0.68} 0.827^{-1.147} = 37.3$

$$\lambda_S = \lambda_L^{\frac{(-3m)}{(4m+1)}} \lambda_C^{\frac{-2}{(4m+1)}} \lambda_\eta^{\frac{-m}{(4m+1)}}$$

which = $150^{-0.32} 0.827^{-1.147} = 0.25$

$$\lambda_D = \lambda_L^{\frac{(2m-1)}{(2(4m+1))}} \lambda_C^{\frac{2}{(4m+1)}} \lambda_\eta^{\frac{-(2m+1)}{(2(4m+1))}}$$

which = $150^{-0.18} 0.827^{1.147} = 0.326$

from these values, the remaining unknowns can be determined:

$$\lambda_{(\rho_s - \rho)} = \lambda_D^{-3} = 28.6$$

$$S_m = \frac{0.00105}{0.25} = 0.0042$$

$$\rho_{sm} = 1.059 \frac{g}{cm^3}$$

$$D_{35m} = 0.00288 \text{ ft}$$

$$D_{65m} = K_{sm} = 0.00352 \text{ ft}$$

If the channel is not wide, and hence wall shear is significant, a different process must be followed. For an illustration of this process, as well as tabulated values for the exponents of model ratios, the reader is referred to the original paper by Einstein and Chien.

Summary.

Throughout this report, I have outlined the changes in techniques and philosophy regarding the application of distortion of the vertical scale in physical hydraulic models. From Newtons original insights into the physical possibilities of similitude, to Einstein and Chiens' theoretical analysis of the problems associated with distortion, the philosophy regarding the application of distortion in physical hydraulic modeling has passed through several important phases.

The original incompatibility between Froude and Reynolds criteria determined from the analysis of works by Stokes and others has persisted. Attempts to reconcile the fundamental differences in the two phenomenon were realized to be futile in the early twentieth century. From that point on efforts by researchers and theoreticians alike focused on mitigation of so called "scale effects". The use of the term scale effects is broad, while any deviation from strict similarity is lumped into the term. The vagueness in the term lets it be ambiguous and explains why it was not used in this text.

The inherent problems associated with distortion must be recognized by anyone contemplating its use, and the proper realization of the errors which may be present in data obtained on a distorted model must be made. As authors of papers on the topic have repeatedly pointed out, the application of distortion requires a knowledge of the phenomenon being modeled and above all, experience with this type of modeling.

References

- American Society of Civil Engineering "Hydraulic Models", Manual of Engineering Practice No. 25, 1942
- Barnes, G. E. "Model Studies", From the private collection of E. W. Lane, Unpublished, (1937)
- Bennett, B. M. "A look at Physical Hydraulic Modeling", Masters Degree Paper, Colorado State University, Unpublished, 1988
- Bridgman, P. W. "Dimensional Analysis", Yale University Press (1931)
- Buckingham, E. "Model Experiments and the Forms of Empirical Equations", Trans. ASME, Vol. 37, p. 263, 1915
- Einstein, H. A. and Chien, N. "Similarity of Distorted River Models with Movable Beds", Trans. ASCE, Vol. 121, 1956, pp. 440-457
- Groat, B. F. "Theory of Similarity and Models", Trans. ASCE, Vol. 96, 1932, pp.273-303
- Newton, Sir Issac "Principia Mathematica" Book II, Proposition XXXII, Theorem XXVI, (1687)
- Novak, P. and J. Cabelka, "Models in Hydraulic Engineering", Pittman Publishing Company, London, (1981)
- Stokes, G. "On the effect of Internal Friction of Fluids on the Motion of Pendulums," Trans. Cambridge Philosophical Soc., (1850), p. 19, Sec. 5.
- Warnock, J. E., "Hydraulic Similitude", from Engineering Hydraulics, Proc. 4th Hydraulics Conference, H. Rouse, ed., 1949, pp. 136-176
- Watkins R. D. and A. Brebner "Model-Scale Relations for Open Channels with Non-uniform Flow", Proc. ICE, 3, pp. 183-215
- Yalin, M. S. "Fundamentals of Hydraulic Physical Modeling", Proc. NATO ASI, Kluwer Academic Publishers, Dordrecht, The Netherlands, 1989, pp. 1-40

LIFE EXPECTANCY OF RESERVOIR

with special reference to

TRAP EFFICIENCY OF SEDIMENT.

(By T.G. ANTONY BALAN)

Abstract

Premature sedimentation of reservoirs have serious economic consequences. Existing methods of predicting life expectancy of reservoirs include estimation of trap efficiency of sediment in the reservoir. Defined as a ratio of the deposited sediment to the total sediment inflow, the trap efficiency primarily depends on the sediment load characteristics, the detention time of the inflow, the operation and the age of the reservoir.

Starting with Brune and Allen (1941) a number of empirical and mathematical models are developed for calculation of expected trap efficiencies. These are Brune and Allen (1941), Churchill (1948), Brune (1953), Brown (1958), Shen (1975), Borland (1971), and Karaushev (1966).

These were applied to some Indian reservoirs where reservoir surveys were carried out recently to calculate the trapping efficiencies of these reservoirs by various methods and compare the efficacy, usefulness or applicability of these methods to these particular reservoirs.

RESERVOIR SEDIMENTATION PLANNING

INTRODUCTION: All reservoirs formed by dams on natural rivers and streams are subjected to some degree of sedimentation. The problems confronting the project planner is to estimate the rate of sedimentation and the period of time before the sediment will interfere with the useful functions of the reservoir. Provision is normally made for sufficient sediment storage in the reservoirs at the time of design so as not to impair the reservoir functions during the designed life of the project.

RESERVOIR SEDIMENTATION : When a stream flow enters a natural lake or reservoir, its velocity and transportation capacity is suddenly retarded causing it to drop a part of the sediment load. The entire sediment load is deposited in the case of natural lakes, but in the case of artificial lakes or reservoirs with outlets, the amount deposited depends on the detention time, shape of the reservoir, operating schedule etc. As much as 90 percent of the sediment load is trapped in some reservoirs.

TRAP EFFICIENCY : Defined as the ratio of the deposited sediment to the total sediment inflow, the trap efficiency primarily depends on the sediment load characteristics and the detention time of the inflow and the age of the reservoir. The detention time depends upon the: type of reservoir ratio between the storage capacity and inflow; shape of the reservoir basin; type of operation of the dam.

METHODS: A number of analytical methods are now available for estimating the trap efficiency of reservoirs, many of which are based primarily on a function of the ratio of reservoir volume to inflow rates. Some recent ones includes an analysis of sediment characteristics. For large reservoirs empirical relationships have been developed by Brune and Allen (1941), Churchill (1948), Brown (1958), Borland (1971) and Shen (1975).

BRUNE: Brune (1953) presented an empirical relationship based on the records of 44 normally ponded reservoirs [1]. His curves, relating trap efficiency and the ratio between reservoir capacity and mean annual water inflow, both in acre-feet, are shown in Fig.4. Brune's model relates the percentage of deposited sediment with the capacity inflow ratio, which is nothing else than the detention time. The semi-logarithmic curvilinear relation between trap efficiency and the capacity-inflow ratio in resulted from his study.

CHURCHILL: Churchill (1948) presented a relationship based on Tennessee Valley Authority reservoirs. His methods relates the percentage of incoming sediment passing through the reservoir and the sediment index of the reservoir, i.e., the period of retention (capacity, in cubic feet per second) divided by velocity

(mean velocity, in feet per second, obtained by dividing average cross-sectional area, in square feet, into the inflow). The average cross-sectional area in this case is computed by dividing capacity, in cubic feet, by length, in feet. Churchill's curve is shown in fig.5. In brief, Churchill correlated trap efficiency with a sediment index equal to the ratio of the retention period to the mean velocity of flow through the reservoir. This method resulted in a logarithmic relationship between the percent of incoming sediment passing through a reservoir and the sedimentation index of the reservoir.

BORLAND: Borland (1971) verified Churchill's method with reasonable accuracy by applying known data from number of sources, including reservoirs with a capacity of several hundred thousand acre-feet, and concluded that Churchill's method gave better results than the Brune curves.

The following description of terms will be helpful in applying the Churchill curve:

1. Capacity:- Reservoir capacity at mean operating pool elevation for the period considered.
2. Inflow:- Average daily inflow rate during the study period.
3. Period of retention:- Capacity (in cubic feet) divided by inflow rate (in cubic feet per second).
4. Length:- Reservoir length in feet at mean operating pool level.
5. Velocity:- Mean velocity in feet per second obtained by dividing the average cross-sectional area is computed by dividing capacity by length.
6. Sedimentation index:- Equals period of retention divided by velocity.

BROWN: Brown related the relationship of sediment trapped (in percent) to the ratio of the original storage capacity to the watershed area. Brown (1944) proposed the curves of Fig. 6 for the computation of T_E

$$T_E = 100 \left(1 - \frac{1}{1 - \frac{K C}{W}} \right)$$

where K = numerical coefficient equal to 0.046 for the lower curve and $K = 1.0$ for the upper curve. A value of $K = 0.1$ is suggested for the design curve; C = original reservoir storage capacity (acre feet); W = watershed area for preliminary investigations.

SHEN: Shen (1975) presented a series of curves for various particle sizes, in mm, relating the trap efficiency to the ratio of the basin area A , in m^2 , to the outflow ratio Q_o , in cm. This is shown in Figure.7. He compared Brune and Churchill's methods and reported that the two well known methods tend to under-estimate trap efficiency for coarser material, but overestimate for finer material, the average size diameter, however, is well represented.

BORLAND: In 1971, Borland introduced a new approach showing the relation between the fraction of material deposited and the setting velocity of the suspended material:

$$TE = 1 - \exp [-1.055 L\omega/vd]$$

where TE = fraction of sediment deposited in the reservoir; L = total length of the reservoir; ω = fall velocity of the sediment; v = mean velocity of the flow in the reservoir and d = flow depth.

His procedure for computing the trap efficiency of a settling basin was developed by applying the results obtained by Einstein (1965). Two basic equations in Einstein's study were used by him.

KARAUSHEV: Karaushev (1966) developed a similar theory for the trap efficiency of small reservoirs:

$$T_e = 1 - \left[1 - \left(\frac{C}{I} \right) \right] e^{\left[\frac{-\phi (C/I)}{1 - (C/I)} \right]}, \quad \phi = \bar{\omega} T_s / h$$

where:

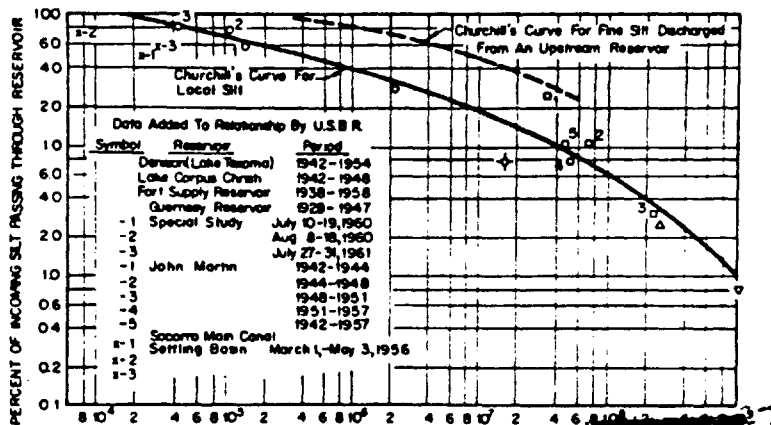
$\bar{\omega}$ = mean fall velocity of the transported sediment, T_s = duration of spill over period (second), h = mean depth of the reservoir, C/I = capacity-inflow ratio.

These equation can be used in mathematical models related to reservoir sedimentation, since they both take into consideration the major parameters involved in the processes of silting

SINGH 1989: Singh et. al. reports that a new method has been developed for estimating future reservoir storage capacities, allowing for sediment deposition and compaction. Reservoir sedimentation surveys for 117 reservoirs, conducted by the Illinois State Water Survey over the past 60 years, were used to determine regional constants (K) to represent the severity of sediment deposition in the reservoirs.

BUBE 1986: It has been reportedly Bube et. al. [6] that the method of smoothing splines was employed by them to revise Churchill's curves for predicting reservoir trap efficiency which have not been revised since 1948, even though more data are now available. The revised curve for local sediment mostly is reported to be slightly below the original curve in that reservoirs with small sedimentation efficiencies have positive local trap efficiencies

HEINEMANN 1984: The process occurring in agricultural reservoirs during an inflow was described by Heinemann using flow diagrams, and the various parameters that influence sediment trap efficiency are discussed. The mechanics of reservoir silting were also reviewed by him. He has quoted 44 methods and authors on the topic, starting from Hazen (1904).



Trap efficiency curve for reservoirs, Churchill (1948).

Source [1]



Chen's trap efficiency curve from "Design of Sediment Retention Curve" at Hydrology and Sediment Control Symposium, Lexington, USA, 1975. (Graf,

Source [10]

CASE STUDY DATA

CASE STUDY: A large number (19) of existing reservoirs in India are taken for case study and their trap efficiencies have been worked out by six different methods available.

THE DATA: The following data were available :-

1. Catchment area
2. Reservoir capacity (original)
3. Capacity/inflow ratio
4. Assumed sedimentation rates at the time of design
5. Observed sedimentation rates (after reservoir surveys)

Since these were inadequate to evaluate the trap efficiencies by different methods, additional data on these reservoirs from the World Register of Dams (1973). The data so collected were :-

1. Height of Dam
2. Length of Dam

AVERAGE ANNUAL INFLOW : From capacity and C/I ratio, the average annual inflow was calculated. Since the C/I ratios were originally worked out from inflow figures, this data is reliable.

THE LENGTH OF RESERVOIR : Churchill curves were based on use of the data of length of the reservoir. This information was not readily available. Therefore the length of reservoir was indirectly calculated from the three parameters reservoir capacity, height of the dam and the length of the dam. There is considerable approximation involved on the above procedure of finding the length of reservoir. However, the procedure will be useful as the first approximation in the absence of reliable data.

SIZE DISTRIBUTION OF THE DEPOSITED SEDIMENT : The Shen, Borland and Karashev formulae are dependent on gradation curve of the deposited material. As such, it was not possible to make assumption on the gradation curve and base any conclusions on the results thus obtained. The results are therefore compared on each size fractions separately.

RESERVOIRS:

Name of project	River	Year of - impounding
Aliyar	Aliyar	1962
Bhakra (Gobindsagar)	Sutlej	1963
Gandhisagar	Chambal	1960
Hirakud	Mahandi	1956
Koyna (Sivajisagar)	Karad	1964
Kunda	Dudhinala	1962
Lower Bhawani	Bhawani	1955
Maithon	Barakar	1957
Matatila	Betwa	1963
Mettur Stanley Dam	Cavery	1934
Nizamsagar	Manjera	1932
Panchet hill	Damodar	1959
Peechi	Manali	1957
Pegumbahalla Dam	Pegumbahalla	1965
Pothundy	-	1968
Sathanur	Ponnar	1958
Tungabhadra	Tungabhadra	1957
Ukai	Tapi	-
Vaigai	Vaigai	1959

STUDIES

STUDIES CARRIED OUT: An elaborate spread-sheet computer program on LOTUS 123 was prepared which given the necessary data would work out the trap efficiencies by six different methods given below:

NAME	PARAMETER USED	DATA REGD.
1. Brown	C / W ratio	C, W, Std curve
2. Churchill	S I ratio	C, L, V, Std curve
3. Brune	C / I ratio	C, I, Std curve
4. Shen	A / Qo ratio	W, I, Std curve Gradation curve
5. Borland	(LW / Vd) ratio	C,L,V,Grad.curve
6. Karaushav	(wT / L), C/I ratio	Gradation curve duration spill (outflow) C, I,

The work-sheet is so made out that as when each piece of reliable information is received, the approximate method used to calculate that information gets replaced by field data.

INPUT DATA: The reservoir data is given in table 1 and consists:

PARTICULARS:

1. Serial Number
2. Name of Reservoir
3. Year of Completion
4. Name of River

DATA AS PER WORLD REGISTER OF DAMS:

5. Height above the lowest foundation (in meters)
6. Length of Crest (in meters)
7. Gross capacity of reservoir (in 1000 cubic meter)
8. Maximum discharge capacity of spillway (in cu. m. per sec)

DATA AS PER CBI&P RESERVOIR CAPACITY RESURVEY REPORTS:

9. Catchment area (in Sq. km.)
10. Reservoir (Gross) capacity at the time of impounding
11. Year of impounding
12. Capacity / Inflow ratio
13. Rate of sedimentation (in Ha. m/100 Sq.km/yr.)
 - (a) Assumed at the time of design
 - (b) Observed as per the resurveys

COMPUTATION: The reservoir-wise computation of trap efficiency by each method is enclosed. In the Shen, Borland and Karaushev methods, the trap efficiency of each of the six sediment sizes (0.001 mm, 0.004 mm, 0.016 mm, 0.062 mm, 0.250 mm and 2.0 mm) have been calculated. Depending on the predominant grade of the inflowing sediment, the percentage of trapping will change from very low to near 100%.

RESULTS: The trap efficiencies obtained for the individual reservoirs by the BRUNE, CHURCHILL and BROWN methods are tabulated in table 2. The reservoirs are mostly large reservoirs and very high percentage of sediment is trapped by these reservoirs. However in terms of actual numbers the three

methods give widely varying results.

In view of the fact that most of the reservoirs chosen fall within the flat-limb portion of the respective curves, in order to afford comparison between the above three methods the trap efficiencies obtained by two methods are plotted on the third curve. This way the agreement of results by different methods were tested.

Figures 1, 2, 3 are trap efficiencies calculated by the Brown and Churchill methods plotted in the standard Brune curve .

Figures 2, 3, 4 are trap efficiencies calculated by the Brune and Churchill methods plotted on the standard Brown curve.

Figure 3 gives trap efficiencies by Brown and Brune method on log-log plotting with standard Churchill curve as a standard for measurement. (not enclosed)

Due to the sensitivity of the particle diameter to the settling characteristics, it was not possible to compare the Borland, Shen and Karashev methods directly with the other three methods without sufficient data on the insitu-gradation curve or bed-gradation curve.

For the Shen and Borland methods for the given index of measurement (e.g. the A/Q_0 ratio, the L_w/vd ratio) there appears to be one dividing sediment diameter above which nearly all the sediment drops on the reservoir. As regards the Karashev method, the formula though containing a major variable in the sediment size, appears not to have pronounced effect on the trap efficiency. Also the trap efficiencies obtained are widely varying and very different from results obtained from other methods.

APPLICABILITY OF DIFFERENT METHODS (as per literature): According to various researchers, the different methods have been developed under different conditions. The Brunes curve have been developed for normal- ponded reservoirs. Borland observed that Churchill curve is more applicable estimating trap efficiencies for desilting and semidry reservoirs. Borland's method for computing trap efficiency of a settling basin has been developed by results obtained by Einstein(1965) over gravel bed flume system. Karashev has also developed his theory for small reservoirs.

DIRECT OBSERVATION : The direct observation of trap efficiencies are at best possible only in small test-plots. It is practically impossible to have any direct measurement of trap efficiencies for large reservoirs as being analyzed in the case studies. One of the indirect method which could give some clues is the results of re-surveys of existing very old reservoirs. Even in this case, there are various factors (such as rate of incoming sediment, variation of sediment transport capacity with changes in temperature, the operating rules of the reservoir) which have more predominant effect in the sediment deposition than trap efficiency.

The Shen method invariably gave 100% trap efficiency to all the sediment fractions considered (0.001mm and above) in all the reservoirs except in "P". This was a reservoir on a comparatively small catchment compared to others (55 sq Km). (Table 4 c)

The Brown and Brune methods showed more closeness of fit as compared to Churchill method.

The Borland method shows 100% entrapment of sediment sizes above 0.016 mm for all the reservoirs except 3. The Borland method showed better agreement with Brune, Brown and Churchill compared to the Shen or Karashev methods.

Conclusions:

1. The method to be used for calculation of Trap Efficiency primarily depends on the amount of reliable data that is available for analysis.
2. With only 3 parameters available Brune and Brown methods are best suited.
3. Where the data on gradation-curve of the deposit is available, Borland method seems to be better for application.

REFERENCE

- 1 Borland, W.M., (1971)
River Mechanics
Reservoir Sedimentation, Chap.29, Fort Collins, USA.
- 2 Borland, W.M., (1975)
Sedimentation Engineering, ASCE,
Manual No.54, pp. 587-605
- 3 Borland, W.M. & Miller, C. (1962)
"Stabilization of Five Mile and Muddy Creek,"
May 1962 ASCE Meeting at Omaha, Neb.
- 4 Brown, C.B., (1958)
Sediment Transportation, Engineering Hydraulics, Wiley
New York, USA
- 5 Brune, G.M., (1953)
Trap Efficiency of Reservoirs, Trans. AGU
Vol.34, No.3, pp.407-418
- 6 Bube, K.P and Tribble S.W (1986)
Water Resources Bulletin, WARBAQ
Vol.22, No.2, pp.305-309
- 7 Chen, (1975)
Design of Sediment Retention Curve, Urban Hydrology
and Sediment Control Symposium, Lexington, USA
- 8 Churchill, M.A., (1948)
Analysis and Use of Reservoir Sedimentation Data
L.C.Gottschalk: Proc. Federal Inter-Agency
Sedimentation Conf. Denver, Colorado, pp.139-140
- 9 Graf, W.H., (1971)
Hydraulic of Sediment Transport, McGraw Hill, New York
- 10 M.Frenette and P.Y.Julien (1986)
Advances in Predicting Reservoir Sedimentation
Third International Symposium on River Sedimentation
The University of Mississippi
- 11 Graf, W.H., (1984)
Hydraulics of Reservoir Sedimentation,
1981 EPFL, Lausanne, 40p.
- 12 Karashev, A., (1965)
*A Method of Calculating Sedimentation in
Reservoirs," Soviet Hydrology AGU, No.3.*
- 13 Gottschalk LC (1975)
Sedimentation Engineering, ASCE, Manual no. 54, pp.1
- 14 Heinemann HG (1984)
Reservoir Trap Efficiency
IN: Erosion and Sediment Yield: Some Methods of
Measurement and Modelling. Geo Books, Regency House
Norwich, England. p. 201-218
- 15 Simons, Li and Ass. (1982)
Engineering Analysis of Fluvial System
Fort Collins, Colorado
- 16 K.P.Singh, and A. Durguno (1989)
Water Resources Bulletin WARBAQ
Vol.25, No.2, p.263-274
- 16 Miller, C.R., (1953)
Determination of the Unit Weight of Sediment
for Use in sediment Volume Computations
USBR
17. Ramarao, K. (1984)
Report of Reservoir Sedimentation Committee
Ministry of Water Resources, New Delhi (unpublished)

LIST OF SYMBOLS:

- C Trap Efficiency
- C/I Ratio of Capacity by Inflow
- d Flow Depth
- h Mean Depth of the Reservoir
- K Numerical Coefficient
- l Total Length of Reservoir
- T_E Trap Efficiency (ratio, Percentage)
- V Mean Velocity of the Flow in The Reservoir
- W Watershed Area
- w Fall Velocity of Sediment

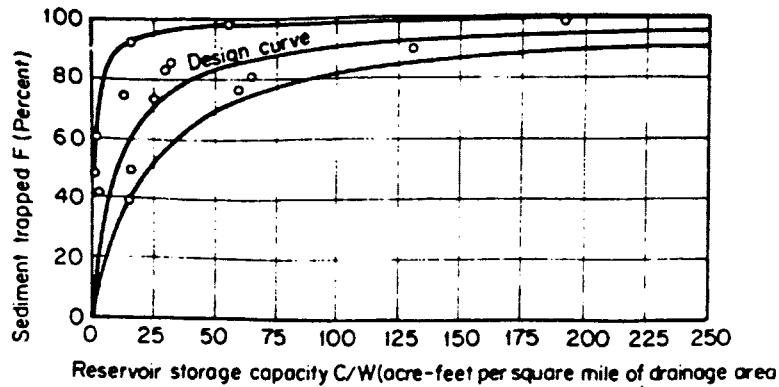


Fig. 4 Trap efficiency curves due to Brown.

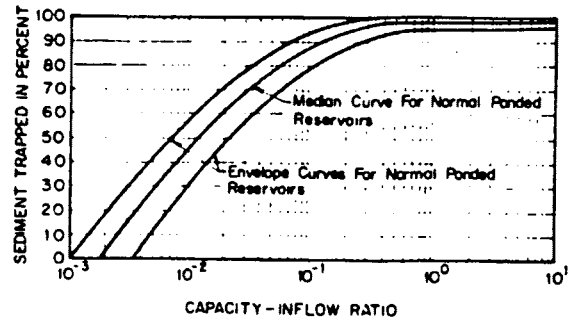


Fig. 5 Trap efficiency curves due to Brune.

Table 2.

RISON OF BRUNE, BROWN & CHURCHILL METHODS:

Name of project	Year	Catchment area (sq. km.)	Brune			Churchill	
			4	5	6	7	
"A"	1959	56980	99	98	90		
"B"	1956	10966	98	97	62		
"C"	1955	5206	99	99	58		
"D"	1953	28179	95	96	95		
"E"	1956	20720	88	90	97		
"F"	1931	21694	87	85	98		
"G"	1961	891	99	100	69		
"H"	1956	83395	91	94	95		
"I"	1960	23025	99	100	-		
"J"	1953	4200	99	99	42		
"K"	1972	66220	99	95	75		
"L"	1957	107	99	100	66		
"M"	1971	31	99	100	22		
"N"	1958	2255	93	93	60		
"O"	1957	5398	98	89	67		
"P"	1962	55	45	100	100		
"Q"	1960	114	60	75	80		
"R"	1934	42200	94	92	97		
"S"	1966	41	45	80	99		

Borland Method

Trap Efficiency by Size Fractions

Table 4 a.

Particle Diameter	0.001 mm	0.004 mm	0.016 mm	0.062 mm	0.25 mm	2 mm
ProjectName						
1 "A"	5	66	100	100	100	100
2 "B"	15	97	100	100	100	100
3 "C"	15	97	100	100	100	100
4 "D"	11	92	100	100	100	100
5 "E"	6	75	100	100	100	100
6 "F"	4	58	100	100	100	100
7 "G"	16	98	100	100	100	100
8 "H"	0.61	12	98	100	100	100
9 "I"	40	100	100	100	100	100
10 "J"	12	94	100	100	100	100
11 "K"	16	98	100	100	100	100
12 "L"	23	100	100	100	100	100
13 "M"	31	100	100	100	100	100
14 "N"	13	95	100	100	100	100
15 "O"	16	97	100	100	100	100
16 "P"	1	11	97	100	100	100
17 "Q"	2	38	100	100	100	100
18 "R"	7	80	100	100	100	100
19 "S"	0.3	8	92	100	100	100

Shen method

Trap Efficiency by Size Fractions

Table 4 b.

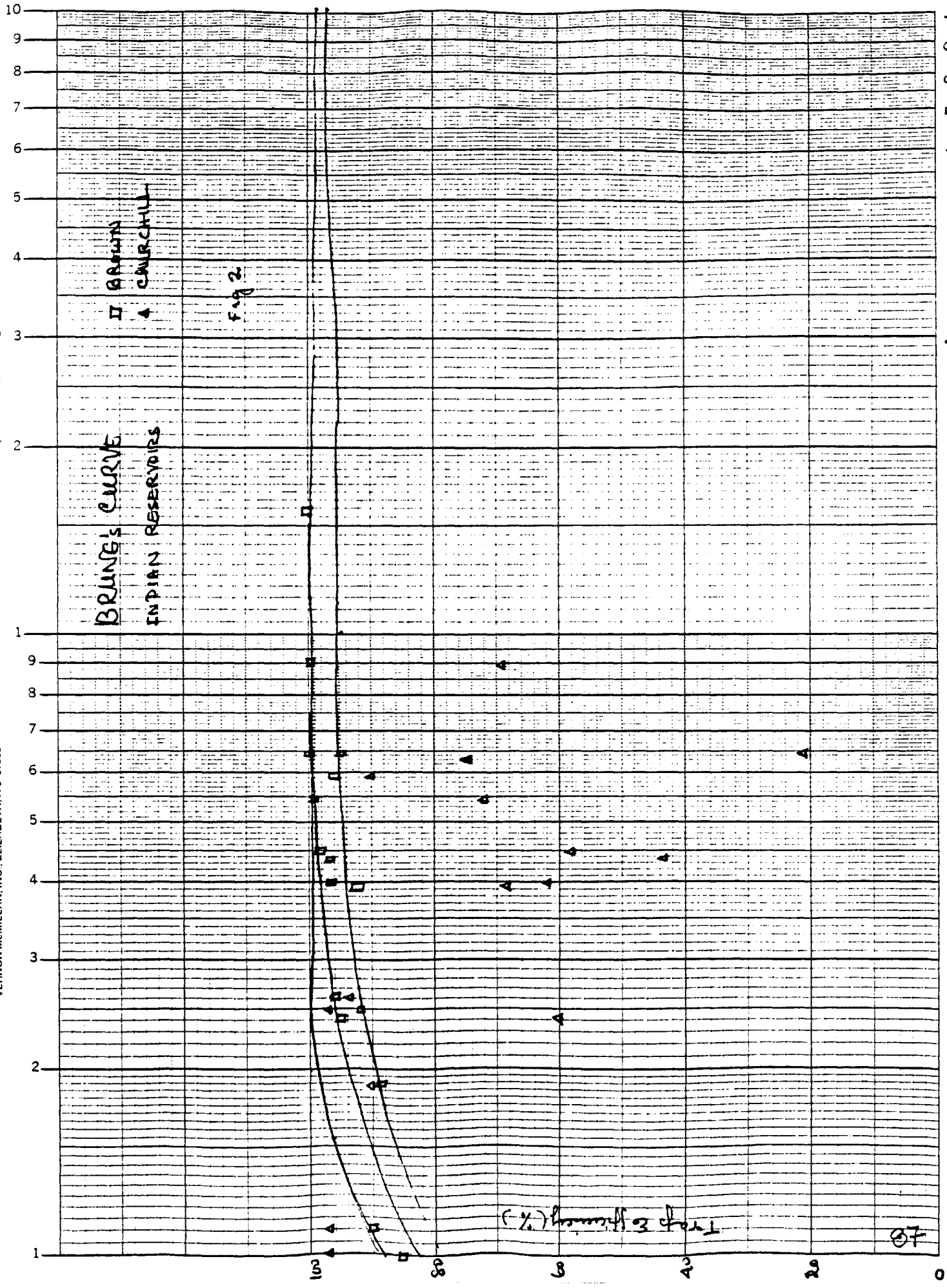
Particle Diameter	0.001 mm	0.004 mm	0.016 mm	0.062 mm	0.25 mm	2 mm
Project						
1 "A"	100	100	100	100	100	100
2 "B"	100	100	100	100	100	100
3 "C"	100	100	100	100	100	100
4 "D"	100	100	100	100	100	100
5 "E"	100	100	100	100	100	100
6 "F"	100	100	100	100	100	100
7 "G"	100	100	100	100	100	100
8 "H"	100	100	100	100	100	100
9 "I"	100	100	100	100	100	100
10 "J"	100	100	100	100	100	100
11 "K"	100	100	100	100	100	100
12 "L"	100	100	100	100	100	100
13 "M"	100	100	100	100	100	100
14 "N"	100	100	100	100	100	100
15 "O"	100	100	100	100	100	100
16 "P"	10	75	100	100	100	100
17 "Q"	100	100	100	100	100	100
18 "R"	100	100	100	100	100	100
19 "S"	100	100	100	100	100	100

Karashev Method

Trap Efficiency by Size Fractions

Table 4c.

Particle Diameter	0.001 mm	0.004 mm	0.016 mm	0.062 mm	0.25 mm	2 mm
ProjectName						
1 "A"	58	58	58	58	59	62
2 "B"	40	40	40	40	42	53
3 "C"	45	45	45	45	46	57
4 "D"	29	29	29	29	30	38
5 "E"	10	10	10	10	10	14
6 "F"	10	10	10	10	10	13
7 "G"	90	90	90	90	91	97
8 "H"	18	18	18	18	18	19
9 "I"	60	60	60	61	67	30
10 "J"	44	44	44	44	46	55
11 "K"	64	64	64	64	66	77
12 "L"	54	54	54	54	57	73
13 "M"	63	63	64	64	68	86
14 "N"	24	24	24	24	26	36
15 "O"	39	39	39	39	41	53
16 "P"	1	1	1	1	1	2
17 "Q"	2	2	2	2	2	4
18 "R"	25	25	25	25	26	32
19 "S"	1	1	1	1	1	1



10
9
8
7
6
5
4
3
2
1
9
8
7
6
5
4
3
2
1
0
100
80
60
40
20
0

87

